NTNU
Innovation and Creativity

Biomass gasification integration in recuperative gas turbine cycles and recuperative fuel cell integrated gas turbine cycles
-

Kristian Aase Løver

Norwegian University of Science and Technology
Department of Energy and Process Engineering

Problem Description

A biomass gasifier will be integrated in both a gas turbine cycle and a gas turbine/fuel cell cycle in the Aspen Plus simulation software.

The gasifier will perform steam gasification and tar cracking of solid biomass fuel, providing gaseous fuel in the form of light hydrocarbons, hydrogen, and carbon monoxide after fuel gas cleaning.

Both cycles are recuperative, recycling waste turbine exhaust heat back to the cycle. Steam feed and heat for the gasification process will be provided by recuperation, as far as possible.

Aspen Plus simulations will be based on steady-state, zero dimensional unit models. For common units like heat exchangers, turbines, compressors, and combustors, Aspen Plus built-in models will be used. For other units, like the fuel cell, gasifier, and gasifier-related units, models must be made for this specific use and incorporated in Aspen Plus.

The gasifier model will be based on empirical data on biomass gasification, with gaseous yield and composition a function of temperature and biomass type. Reaction kinetics and heat and mass – transfer inside the gasifier will not be considered. Methods for ensuring sufficient heat and mass-transfer will however be discussed to support the assumptions used, as will limiting factors of reaction kinetics.

The fuel cell model used in the simulations will be based on models developed and published by other authors, with any adjustments deemed necessary.

Cycle exergy flow will be made based on simulation results. Integration of both cycles will be assessed through exergy flow and central concepts for efficient integration will be developed.

Assignment given: 15. May 2007
Supervisor: Ivar Ståle Ertesvåg, EPT

Abstract

A multi-reactor, multi-temperature, waste-heat driven biomass thermochemical converter is proposed and simulated in the process simulation tool Aspen Plus™. The thermochemical converter is in Aspen Plus™ integrated with a gas turbine power cycle and a combined fuel cell/gas turbine power cycle. Both power cycles are recuperative, and supply the thermochemical converter with waste heat. For result comparison, the power cycles are also integrated with a reference conventional single-reactor thermochemical converter, utilizing partial oxidation to drive the conversion process. Exergy analysis is used for assessment of the simulation results.

In stand-alone simulation, the proposed thermochemical shows high performance. Cold gas efficiency is 108.0% and syngas HHV is 14.5 MJ/kg on dry basis.

When integrated with the gas turbine power cycle, the proposed converter fails to improve thermal efficiency of the integrated cycle significantly, compared to reference converter. Thermal efficiency is 41.8% and 40.7%, on a biomass HHV basis, with the proposed and the reference converter respectively. This is despite superior cold gas efficiency for the proposed converter, and the gas turbine cycle is found not to be able to properly take advantage of the high chemical energy in the syngas of the proposed converter.

When integrated with the combined fuel cell/gas turbine power cycle, the proposed converter significantly improves the thermal efficiency of the integrated cycle, compared to the reference converter. Thermal efficiency is 56.0% and 51.2%, on a biomass HHV basis, with the proposed and the reference converter respectively. The fuel cell is found to be able to take advantage of the high chemical energy in the syngas of the proposed converter, which is the main cause of increase in thermal efficiency.

Operation of the proposed thermochemical converter is found to be feasible at a wide range of operating conditions, although low operating temperatures in the converter may cause problems at very high carbon conversion ratios.

Sammendrag

En termokjemisk biomasse-konverter, bestående av flere interne reaktorer som opererer ved forskjellige temperaturer, er foreslått og simulert i prosess-simuleringsvektøyet Aspen Plus™. Konverteren er drevet av overskuddsvarme. I Aspen Plus™ blir konverteren integrert med en gassturbin-syklus og en kombinert brenselscelle/gassturbin-syklus. Begge disse syklusene er rekuperative og forsyner den termokjemiske konverteren med overskuddsvarme. Som sammenligningsgrunnlag er også syklusene integrert med en referanse-konverter. Denne er en konvensjonell en-reaktor konverter som bruker partiell oksidasjon til å drive konverteringsreaksjonene. Eksergi-analyse er brukt i analyserings-arbeidet av simuleringsresultatene.

Simulert som enkeltstående enhet har den foreslåtte konverteren høy ytelse. Cold gas efficiency er 108.0% og tørr syngass HHV er 14.5 MJ/h.

Gassturbinsyklusen integrert med den foreslåtte konverteren har ikke vesentlig høyere virkningsgrad enn hva som oppnåes ved integrering med referanse-konverteren. Virkningsgradene er henholdsvis 41.8% og 40.7% (på biomasse HHV basis) for den forslåtte konverteren og referanse-konverteren. Dette er til tross for betydelig høyere cold gas efficiency for den foreslåtte konverteren. Det er funnet at gassturbinsyklusen ikke i tilstrekkelig grad kan nyttegjøre seg av økningen i kjemisk syngass-energi besørget av den foreslåtte konverteren .

Den kombinerte brenselscelle/gassturbin syklus integrert med den foreslåtte konverteren har vesentlig høyere virkningsgrad enn hva som oppnåes ved integrering med referanse-konverteren. Virkningsgradene er henholdsvis 56.0% og 51.2% (på biomasse HHV basis) for den foreslåtte konverteren og referanse-konverteren. Det er funnet at brenselscellens evne til å nyttegjøre seg av økningen i kjemisk syngass-energi besørget av den foreslåtte konverteren er hovedårsaken til høyere virkningsgrad.

Drift av den foreslåtte konverteren ansees å være mulig med store variasjoner i operasjonsparametre. Ved svært høy konverteringsgrad av karbon kan imidlertid lave reaktor-temperaturer i konverteren forårsake problemer.

Acknowledgement

Index

1 Thermochemical conversion

Through history biomass has been an important source of energy, then primarily for heating purposes. For power production, fossil fuels have been and are preferred because of their high energy density, homogenous make-up, and availability. With growing concern for global warming and diminishing fossil fuel supply, interests for biomass as an energy-source for power production are increasing.

Even though biomass may replace fossil fuel power production in steam turbine cycles, its natural form precludes it from use in other important power producing processes such as the gas turbine cycle, the internal combustion engine, and in future years the fuel cell. An important step on the road to biomass utilization is therefore to develop and mature processes for converting biomass from its natural form into gaseous or liquid homogeneous fuel.

There are two main routes for biomass conversion; through biochemical and thermochemical processes. Biochemical processes are the controlled decomposition or fermentation of biological matter, similar to the processes occurring in nature, at ambient or close to ambient temperatures. Thermochemical processes are processes occurring spontaneously as a result of heating to elevated temperatures. Of these routes, the latter has significantly higher conversion rate and efficiency.

Since well-known processes like combustion and tar- and charcoal manufacture depend on, at least partial, thermochemical conversion of biomass, the principal reactions and sub-processes are well understood. This knowledge is used to optimize the conversion process for production of particular products. However, the huge number of intermediate reaction-steps and chemical components participating make it difficult to describe the complete process in detail.

Thermochemical conversion may include one or more of the sub-process mentioned below. The sub-processes may occur simultaneously or sequentially both in time and space.

- Pyrolysis
- Tar cracking
- Gasification
- Reform/Shift reaction

In this paper, the complete conversion of biomass to gaseous fuel and a small fraction of residual char will be termed thermochemical conversion, or conversion in short. The gaseous product of the complete conversion process will be termed syngas.

1.1 Pyrolysis

Pyrolysis is the first step of thermochemical conversion, and occurs as biomass is heated from ambient temperatures. Pyrolysis is defined as chemical reactions and physical processes run without addition of external reactive materials [1], i.e. air, oxygen, or steam. As no mixing of reactants is required, pyrolysis is kinetically controlled by heat transfer processes, and fast when the required temperature is reached.

The products of pyrolysis are put in three lumped categories; gas, tar, and char. At pyrolysis temperature, gas and tar are in the gaseous phase, while char is the solid remains of the biomass. Gas is the non-condensable part of the gaseous phase, a mixture of CO_2, CO, H_2, and light hydrocarbons. Tar is the condensable part of the gaseous phase, including water, and is a mixture of a huge number of organic components such as phenols, acids and aromatics. The solid remain is carbon-rich char, with small amounts of elemental hydrogen and oxygen, along with any ash present in the biomass.

Thermogravimetric analyses of lignin and cellulose pyrolysis conducted by Fushimi et al. [2] at 1 K s^{-1}, so that temperature lag in the biomass is of little significance, show that pyrolysis starts at approximately 250 ºC (indicated by reduction of biomass mass). Biomass used in the experiment was pre-dried at 110 ºC, for moist biomass mass-reduction (and yield of gaseous products) will therefore start earlier as water is evaporated, this is however not defined as pyrolysis. As temperature is increased gradually up to 700 ºC there is a continuous reduction of solid. From approximately 450-500 ºC however, the reduction rate is significantly reduced, indicating that the main pyrolysis reactions are completed at temperatures below 500 ºC.

Pyrolysis also occurs in the presence of reactive external components, any reactions with such external components are then defined as simultaneously occurring processes other than pyrolysis. A distinction must therefore be made between controlled pyrolysis, deliberately separated from external reactants to optimize the production of particular products, and pyrolysis as a spontaneous occurring part of another process like combustion.

The process of pyrolysis is a very complex one, and its behavior is highly dependent on operating conditions and biomass type. Pyrolysis reactions may be organized in lumped reaction groups such as primary and secondary reactions, where primary reactions are the actual release of gaseous matter from solid biomass, and secondary reactions are the reactions between gaseous components. Significant operating conditions such as temperature and heating rate influence the kinetics and selectivity of these sub-processes, and hence the yield of products. As pyrolysis is a heat transfer controlled process, biomass particle size and properties are also important. Biomass is a collective term for a huge number of organic materials. The amount of different chemical components, i.e. cellulose, varies both between type and species of biomass, and is also significant to the pyrolysis process.

The effort of describing pyrolysis reactions with mathematical models has only been partly successful. Few or none of these models have predicting power for any other pyrolysis process than the processes for which it has been derived because of the sensitivity to operating conditions. Most such models follow the approach of lumped reactions with experimentally determined kinetic coefficients, either in a single arrhenius-expression or in a set of arrhenius-expressions with intermediate pseudo-components. The experimental determination of these coefficients causes the model to lack functional relationship between several, in practice, significant parameters, and hence the lack of predicting power for processes with other types of biomass or operating conditions. Some models use the principle components of biomass (wood), lignin, cellulose, and hemicellulose as input parameters in the kinetic model to improve accuracy for a variety of wood types.

Experiments in literature on pyrolysis are almost exclusively conducted at ambient pressure. An exception to this is an article by W.S.L. Mok and M.J. Antal [21], reporting a tendency toward higher char content as pressure increase, accompanied by a increase in the pyrolysis reaction duty.

1.2 Tar cracking

Tar is a major product of pyrolysis. It is a lumped category of hundreds of chemical components, along with water, that is condensable at ambient temperatures and pressure. Tar cracking is the break-down of heavy molecular tars to light molecular, non-condensable, gases, a processes occurring spontaneously as soon as the tar is released from biomass through pyrolysis. Complete conversion of tar to non-condensable gases however, requires higher temperatures and in most practical applications also some kind of catalyst.

The object of some biomass thermochemical processes is to manufacture tar, such processes are designed to avoid extensive tar cracking. Other processes, utilizing the thermochemical conversion products in the gas phase, requires close to complete conversion of tar to avoid condensation and carbon depositioning downstream of the converter. Fouling caused by these phenomena is a serious threat to the reliability of gas turbines, heat exchanger etc.

The need to perform tar cracking at feasible temperatures and time scales necessitates the use of catalytic materials. Common catalytic materials are nickel and dolomite, both inexpensive, especially in the latter case. As tar is cracked, solid carbon is formed which covers and fouls the active surface of the catalyst. This requires the catalyst to undergo a re-activation process, usually by oxidation of the carbon layer. Consequently, high demands are put on the catalyst to be able to sustain this cyclic operation for long periods of time. Temperature requirements for tar cracking are highly dependent on the catalyst used, for commercially available nickel-catalysts temperatures in the range of 850 ℃ seems to be required [3][4].

1.3 Reform/shift reactions

Reform and shift reactions are well-defined gas-phase reactions, responsible for conversion of hydrocarbons and steam to a mixture of CO and H_2. The principle reforming reaction is given below:

$$C_xH_y + x \cdot H_2O \rightleftarrows x \cdot CO + (x + 0.5y) \cdot H_2 \qquad (1.1)$$
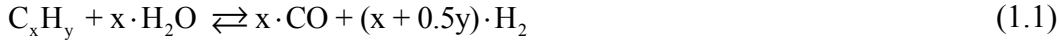
The shift reaction, also called the water-gas shift reaction, is

$$CO + H_2O \rightleftarrows CO_2 + H_2 \qquad (1.2)$$

1.4 Gasification

Gasification is the sub-process of thermochemical conversion that deals with gas phase to solid carbon reactions. In this paper, gasification implies the use of steam as a reactive atmosphere. The main reaction responsible for consummation of solid is then:

$$C(s) + H_2O \rightleftarrows CO + H_2 \qquad (1.3)$$

although the boduard reaction, also known as dry reforming, may also consume carbon:

$$C(s)+CO_2 \rightleftarrows 2CO \qquad (1.4)$$

Solid carbon is normally in the form of char from pyrolysis, which may also contain other elements such as hydrogen and oxygen. Release of these elements (partially or completely), simultaneously with the above reactions, must be regarded as an extension of the pyrolysis reactions, e.g. without the aid of a reactive atmosphere.

Kinetics and final conversion ratio of gasification is heavily dependent on the characteristics of the char, represented by the parameter char activity. Fushimi et al. [2] and Mermoud et al. [5] have shown that the heating rate of biomass has a significant effect on char activity. Chaudhari et al.[6] have conducted laboratory-scale gasification experiments on char derived from biomass pyrolysis. They found that, depending on steam flow, at gasification temperature 650 ºC between 29% and ca. 50% char is converted. At gasification temperature 800 ºC conversion ratio is between 87% and ca. 95%, which corresponds to carbon conversion ratios between 2.6% and 13.4% (of char carbon, fraction of biomass carbon will be lower). In this experiment, gasification is conducted for 30 min. after desired temperature is reached, which is as least as long as the time assumed available for gasification reactions in this paper. This suggests that gasification temperature should be no less and preferably more than 650 ºC.

In the experiments conducted by Fushimi et al., steam gasification conversion ratio for bagasse at 1 K s^{-1} (and 10 1 K s^{-1}) is 94%. This corresponds to a carbon conversion ratio (of biomass) of 12.8%.

2 Aspen Plus™ simulation software

All system simulations are performed with the Aspen Plus™ simulation software (AP). AP is a powerful simulation tool allowing for a wide range of simulation types in most industrial applications. This chapter aims to explain central aspects of AP simulations. For further details, see appendix 4 and AP documentation [7]

2.1 Structure

Properties of the system in question are given to AP in a flowsheet, through three central entities; units representing common processes, streams representing mass or energy flow, and calculation scripts defining additional processes or altering existing ones. The chemical components present in the system must also be defined, along with the equation of state used in calculation.

AP contains several built-in units for processes like compression, expansion, heat exchange, and chemical reactions. Other more complex processes are also built-in in AP. Processes not built-in in AP may be represented by combining built-in units and/or calculation scripts, or defined altogether in external Fortran scripts.

AP contains thermodynamic libraries for a huge number of chemical components. Additional components may be added by supplying the necessary data.

2.2 Solver methods

AP offers the possibility of solving the equations given in the units, streams, and calculator blocks either sequentially or simultaneously. For sequential solution the equations are iterated, for simultaneous solution the equations are solved as an equation-set. AP offers a choice of several iteration methods and iteration parameters.

2.3 Stream classes

Streams represent mass- or energy flow. Energy streams may be defined as either work or heat streams, of which the latter also contain temperature information to avoid infeasible heat transfer. Mass streams are divided by AP in three categories; Mixed, Solid, and non-conventional. Mixed may contain mixtures of components of gaseous, liquid and solid phase. Solid contain only solid phase components. Only chemical components included in the AP libraries, for which all thermodynamic properties are defined, may be present in the mixed and solid stream classes (the conventional classes). Components present in the mixed and solid stream classes may participate in phase and chemical equilibrium, and are automatically flashed by AP at stream temperature and pressure.

Components used for simulations in AP not included in the libraries are placed in the non-conventional stream class, with the significant difference from the mixed and solid classes that they are only partially thermodynamically defined, unable to participate in phase or chemical equilibrium. Non-conventional components do not have a defined phase and may not undergo phase-change.

Non-conventional components are defined in AP by supplying standard enthalpy of formation and coefficients for heat capacity and density versus temperature polynomials. The elementary composition (ultimate and proximate analysis) of the components may also be defined.

2.4 Result output

Properties of the streams and process units, along with calculation results, are available after simulation for viewing in AP or export to other programs. Special or custom result properties may also be defined. Although AP calculates enthalpy and entropy (for conventional components only), and ambient temperature and pressure are defined, exergy is not readily available in the result output. A property termed availability by AP *is* calculated for conventional components, this is however not included chemical availability/exergy, and streams are not flashed for ambient conditions, making it fall short of the complete exergy definition.

3 Recuperative thermochemical conversion

The process of thermochemical conversion requires heat. The global reaction is endothermic, and heat is also needed to heat biomass and other reactants to reaction temperature. The reaction heat demand is usually met by supplying air or oxygen to the conversion process for partial oxidation. As air or oxygen is used, biomass chemical energy is partly consumed, and consequently the heating value and energy density of the product gas is decreased. If air is used as oxidizer, further reductions are caused by nitrogen dilution. The result is a product gas with far lower chemical energy content per mass unit than solid biomass.

An alternative way of supplying heat to the conversion process is to utilize waste heat from a power production cycle, preferably the power production cycle run by the product gas of the thermochemical conversion, e.g. integrating the thermochemical conversion with a power cycle. Heat is a byproduct of power production, available in large quantities. By means of energy recuperation the need for partial oxidation in the conversion process can be eliminated.

While huge quantities of energy are available, only a fraction of this energy is available for heat transfer at thermochemical conversion temperature, 700-800 ºC. This imposes severe restrictions on the operating conditions and design of the power cycle if the energy. Furthermore, design options which in them self decreases cycle efficiency, may be required. This topic has been investigated by Kuchonthara [8], who in his doctoral dissertation calculated the energy balance of recuperative thermochemical conversion and discussed central modifications to standard gas turbine cycles to provide sufficient high-temperature heat for conversion.

3.1 Proposed system

If thermochemical conversion is conducted in a single reactor, the reactor must be supplied with heat satisfying the temperature requirements of even the most high temperature reaction. There is however a number of reactions and processes occurring at lower temperatures, among them the heating of incoming reactants. A natural solution to the problem is therefore to split the thermochemical conversion process into multiple processes at different temperatures, allowing for heat transfer from the waste heat stream in a wider range of temperatures. A principle representation of the process is given in figure 3.1.
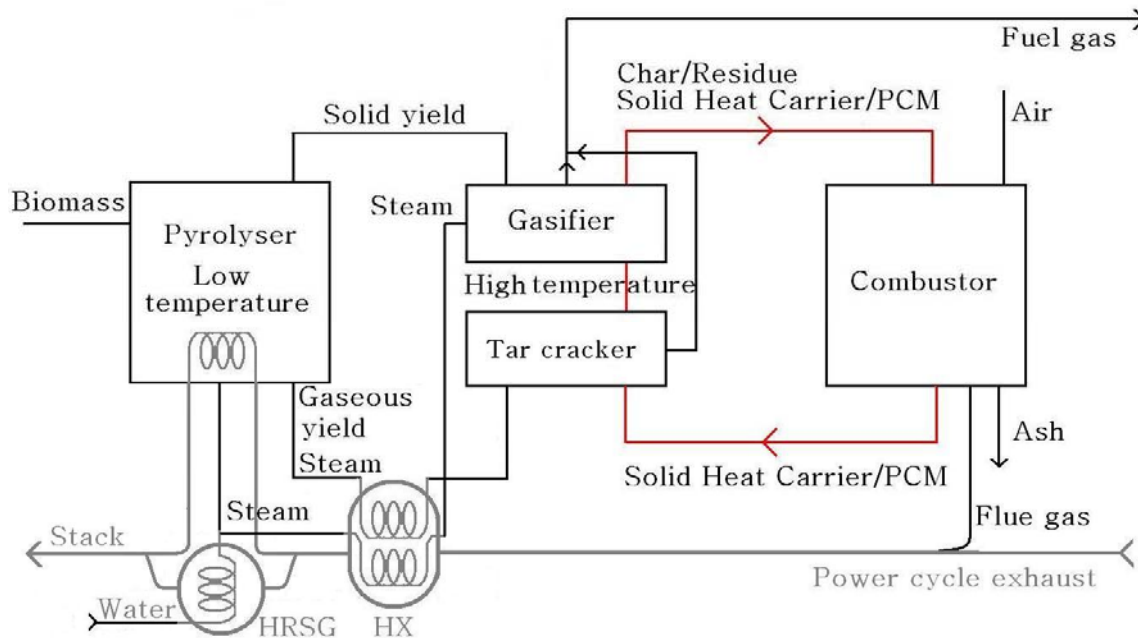
figure 3.1

The principle is an extension of a dual bed gasifier. Biomass is fed into a pyrolyser, operating at low temperature (~500 ºC), where it is heated up and pyrolysis occurs. The pyrolyser contains sand as bed material to improve heat transfer. Steam, generated by waste heat, is injected into the pyrolyser to fluidize the reactor and to carry the gaseous products out of the reactor. Additional pyrolysis heat is provided by heating coils, facilitating heat transfer from the waste heat stream. Even though reactions between steam and biomass or biomass derived products might occur, pyrolysis will be the major and significant process.

Gaseous products from pyrolysis is extracted with steam and heated further to high temperature, again by heat transfer from the waste heat stream, and introduced to the tar cracker. In the tar cracker, tar is broken down to light molecular gases, while at the same time reforming and shift reactions are occurring. After subsequent gas cleaning the product gas, or syngas, is available for the power production cycle.

Solid pyrolysis product is extracted from the pyrolyser with the gaseous products and steam, and separated from them in a cyclone before entering the gasifier. Steam at gasification temperature is supplied to the gasifier to react with the char. The light molecular product gas, syngas, is then extracted from the gasifier and mixed with the product of the tar cracking.

The gasifier and tar cracker is joined with a combustor, combusting char not successfully converted by steam gasification, through a circulating stream of sand acting as bed material and heat carrier. Hot bed material from the combustor is first led to the tar cracker, then to the steam gasifier where char is introduced, before it goes back to the combustor for combustion of unreacted char.

Hence heat is transferred from the waste heat stream at four different points; generation of low temperature steam for pyrolysis bed fluidization, convection heat transfer with the pyrolyser bed material, high temperature steam and gaseous pyrolysis products heating, and generation of high temperature steam for steam gasification. Additional heat for tar cracking and steam gasification is provided by combustion of residual char.

3.2 Assumptions for the proposed system

The aim of the present paper is the conceptual analysis of biomass thermochemical conversion. The design of a biomass thermochemical converter is in itself a huge engineering task, clearly out of the scope of this paper, or indeed any single paper, and several assumptions and simplifications must be made to facilitate modeling.

3.2.1 Pyrolyser

The pyrolyser is a fluidized bed with non-circulating bed material, e.g. pyrolysis products must be extracted from the reactor with neglible loss of bed material. This is unproblematic as far as the gaseous products are concerned. The solid products, on the other hand, can only be separated from the bed material if particle size and density is sufficiently different to let the former be carried by the gaseous stream and the latter not, and such is the assumption.

Heat transfer in the pyrolyser is assumed sufficient, that is, heat transfer between biomass and bed material and bed material and heating coils is assumed sufficient at reasonable reactor-size and volume.

Steam injected to the pyrolyser is assumed inert at the temperatures in question, and does not participate in any reactions.

3.2.2 Tar cracker

The tar cracker is assumed to contain a renewable catalytic material carried in the circulating bed material, as described in chapter 1. Char formation and deposition is assumed neglible regarding energy and mass balance. Heat transfer between the bed material and gas phase components in the reactor is assumed to bring both to the same temperature, the reactor temperature.

The product syngas stream exiting the reactor is assumed free of tar.

3.2.3 Steam gasifier

Char at pyrolysis temperature is assumed to reach gasification temperature as it makes contact with the bed material and steam. Characteristic conversion time and residence time are not defined parameters; the fraction of conversion is however. This fraction is chosen to match feasible conversion and residence time by estimate. As with the tar cracker, heat transfer in the steam gasifier is assumed to bring all components to the same temperature, the reactor temperature.

Although char from the pyrolyser is made up of other elements besides carbon, residual char from the steam gasifier is assumed to be pure carbon, both regarding thermodynamic calculations and mass and energy balance.

3.2.4 Combustor

Combustion is done at close to stochiometric conditions, and assumed complete. Again heat transfer is assumed to bring all components to the same temperature.

3.2.5 Other

Biomass is assumed to be ash-free and only made up of the elements carbon, hydrogen, and oxygen.

4 Pyrolysis modeling

As detailed in chapter 1, no general, accurate, mathematical model is available for the pyrolysis process. The kinetic models available are only applicable for certain operating conditions, and require good knowledge of the process at hand. In this paper the pyrolyser is modeled as a zero-dimensional, steady state unit, not detailing internal processes such as heat transfer, crucial for the use of kinetic models. Any calculations of such data would be time consuming and inaccurate, as well as redundant for any other purpose than use in the kinetic models. A different approach is therefore chosen. Pyrolysis will be modeled by empirical correlations, curve fitted from experimental data available in literature, giving the data of interest directly without describing the physical and chemical processes responsible for them.

The pyrolyser model must calculate the solid and gaseous yield (gas and tar), the enthalpies of these streams, and the energy balance of the reactor itself.

To calculate the enthalpy of a component, or stream, its composition must be known to some extent. While composition may not be given explicitly for all components in any one article in literature, the problem can be side-stepped by applying an element mass balance as shown in equation 4.1. The equation serves two purposes; as a check and balancing tool for the mass balance and for acquiring the element make-up for undescribed product groups.

$$
m_{biomass}\begin{bmatrix} C \\ H \\ O \end{bmatrix}^{wt.\%}_{biomass} = m_{gas}\begin{bmatrix} C \\ H \\ O \end{bmatrix}^{wt.\%}_{gas} + m_{tar}\begin{bmatrix} C \\ H \\ O \end{bmatrix}^{wt.\%}_{tar} + m_{char}\begin{bmatrix} C \\ H \\ O \end{bmatrix}^{wt.\%}_{char} \qquad (4.1)
$$

A number of articles are available describing experimental results of small scale pyrolysis. These articles span a wide range of operating conditions and biomass types. The application of these data in the element mass balance is however not straight forward, as the articles rarely contain complete and unequivocal datasets. Direct use of the data will not satisfy mass balance as the mass closure, e.g. the mass of measured product divided by the mass of biomass, usually is significantly below unity, and element composition may be lacking or incomplete for too many products to solve the equation. Data from two or more articles or data sets may therefore be combined to create a synthesized complete data set.

Data from an article by Di Blasi et al [9] on the fixed bed pyrolysation of wood is used as the primary data source to the complete data set. Yields of gas, tar and char are given at several temperatures, along with molar fractions of non-condensable (CO, H_2, CO_2, etc.) main components in the gas mixture. The element composition of the gas mixture can then be calculated, element composition of the tar is however lacking, and element composition of the char is given at only one temperature.

Tar element composition must consequently be derived from elsewhere. The issue of tar element composition is however complicated by the fact that water is also a part of the condensable tar product group. Articles detailing tar properties, among them element composition, are often on the subject of tar applications as an energy source, and hence the tar in question may have been treated and upgraded by partly removing water. It follows that such tars, or bio-oils, are of different quality and composition than untreated pyrolytic condensables, and will produce infeasible results applied in the element mass balance.
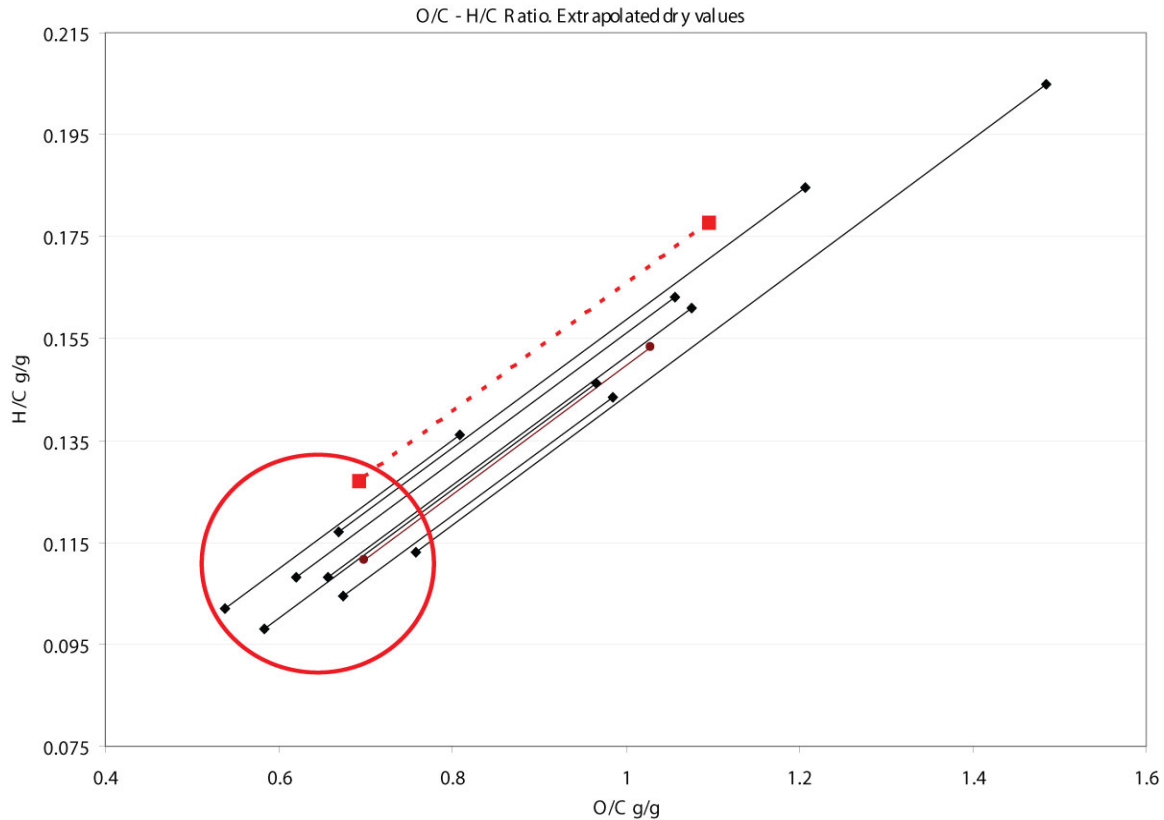
figure 4.1

The problem is approached by gathering tar composition data from several articles in literature, where element composition and water content is known. Dry tar element composition can then be extrapolated. The extrapolation is represented graphically in figure 4.1.

Lines are in the direction of increasing water content, from left to right. The rightmost dot of every line is at the composition given for wet tar in the respective articles. As can be seen, tar composition is more unison for dry tar, suggesting that differences in water content are a significant factor for the difference in composition given in literature.

The tar used in the synthesized data set is given by the red dotted line, and taken from flash pyrolysis as described in the works of D. Meier and O. Faix [10]. The dry tar has

average oxygen/carbon ratio, while the hydrogen/carbon ratio is above average, making it a less than perfect candidate for representing tar composition. Calculations show however that feasible results from the element mass balance are only attainable with high hydrogen content of the dry tar. The choice is therefore a reasonable compromise between deviations from average and reasonable values for tar and char (as char element composition is calculated by difference).

As dry tar composition is established, the water content of the pyrolytic tar must be decided to produce the final tar composition. The element mass balance can then be applied to calculate element composition of remaining products. An overview of the inputs and outputs of the element balance is given below, table 4.1.

Biomass composition	Model biomass
Gas yield	Primary data source [9]
Gas element composition	Primary data source [9]
Tar yield	By difference
Dry tar element composition	Suppl. data source [10]
Tar water content	Assumed
Wet tar element composition	Calculated
Char yield	Primary data source [9]
Char element composition	By difference

table 4.1

The synthesized data set is in the form of continuous functions with product yields and product compositions a function of temperature. Because of discrepancies in the measured data, deriving these functions is a compromise between not deviating too much from measured data and obtaining feasible element compositions. Figure 4.2 shows the functions for product yields (red lines), while the red dots are measured data from the primary data source. Black lines represent measured data from similar experiments in literature. It is worth noting that the measurements from the primary data source are given at moisture free (biomass, 8% moisture) basis, as opposed to the functional values and other measured values, which are not. Even though there are deviations between the

figure 4.2

13
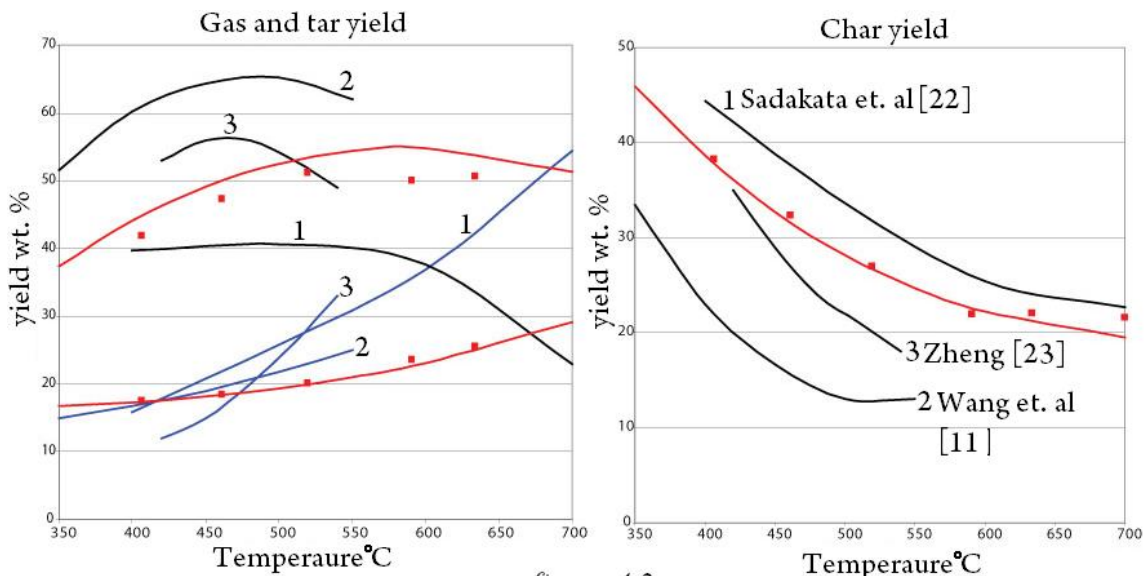
functional values and the primary data source, these are small compared to general differences in pyrolytic product yields. Tar yield is by difference, e.g. calculated by summing the mass balance to zero, which accounts for some of the difference, as mass closure in primary data source is less than unity.

The same technique of curve fitting is used with the gas element composition, figure 4.3. Biomass composition is presented in table 4.2, with typical values for softwood. The biomass is sulfur-, ash-, and nitrogen-free for modeling convenience. Tar water content is set to 40%, as opposed to 20% which is given in the article for the tar in use. It is however not elucidated whether 20% is an optimized minimum through some sort of selective condensation process, or if care is taken to condense and collect all water from pyrolysis. Water content of 40% is reported elsewhere in literature, by Wang et al. [11], although corrected by the authors to approximately 35% due to the liquid collection method used. The primary data source makes no mention of tar water content.

With biomass, gas, and tar element composition established, char element composition is given by the element mass balance by difference. Figure 4.4 shows char O/C and H/C weight ratio as a function of tar water content along comparisons from other experiment in literature.

As can be seen, the results are in reasonable accordance with the single char element composition given in the primary data set at high tar water content. Accordance is also reached with other experimental results.

Char O/C - H/C Ratio
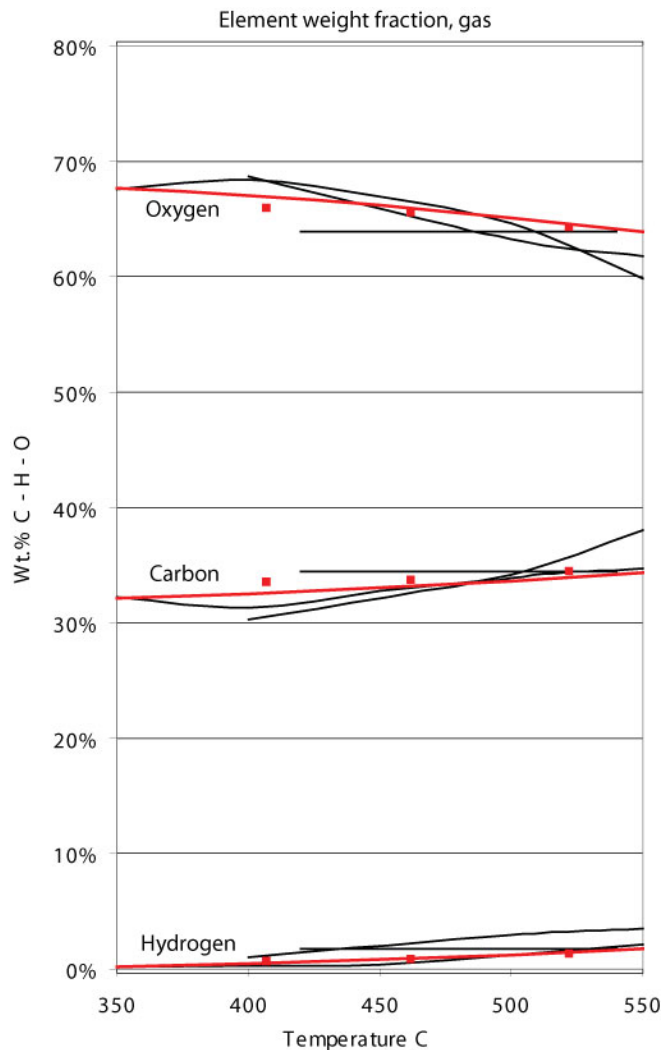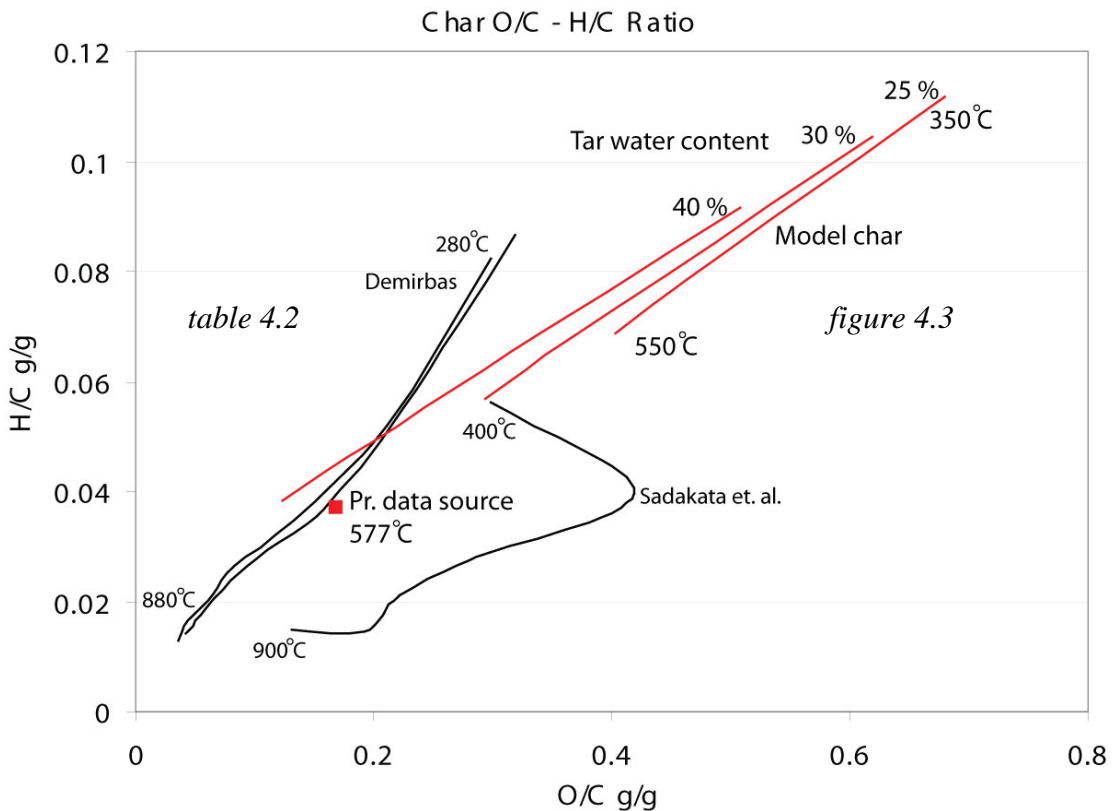
figure 4.3

The energy balance of the pyrolyser can now be derived by calculating the enthalpies of the

figure 4.4

products and reactant. As the composition of the gas mixture is given in the primary data source, enthalpies of formation can be calculated directly with table data of the well defined gas species. The enthalpies are calculated at the composition given at the various temperatures given in the primary data source, curve fitting is then used to produce a continuous function of gas enthalpy versus temperature.

The biomass, tar, and char remain lumped and not well defined product groups, which precludes the use of table data. However, as element composition is known for all three, empirical correlations can be used to estimate their heating value at 25 ºC, and consequently their standard enthalpy of formation. Several such empirical correlations exist for estimating the heating value of compounds defined by their elemental composition, some are for general applications while others are for more specialized purposes. To calculate the energy balance of the pyrolyser in simulations where the reaction and exit of products occurs at other temperatures than the defined standard temperature, heating values of the reactants and products must be known. For calculation convenience, these are assumed to be constant regardless of changes in product composition. Table 4.3 summarizes the literature sources for calculation of enthalpies.

Carbon wt.% dry basis	50
Hydrogen wt% dry basis	5.5
Oxygen wt.% dry basis	44.5
Moisture %	7.4

15

The effect of pressure on pyrolysis, as described in chapter 1, is not included in the pyrolysis model as little or no data is available to produce reliable correlations with pressure as is done with temperature. Figure 4.5 shows the cold product efficiency of the pyrolyser, defined in equation 4.2, as a function of several empirical correlations [12] for heating value.

Data type	Method/Source
Biomass, Char HHV	Boie correlation Sheng, Azevedo[12]
Tar HHV	Suppl. data source [10]
Gas HHV	Primary data source [9]
Heat capacity, all components	Grønli, Melaaen [13]

table 4.3

$$\eta_{\text{cold product}} = \frac{\sum HHV_{prod}}{HHV_{biomass}} \qquad (4.2)$$
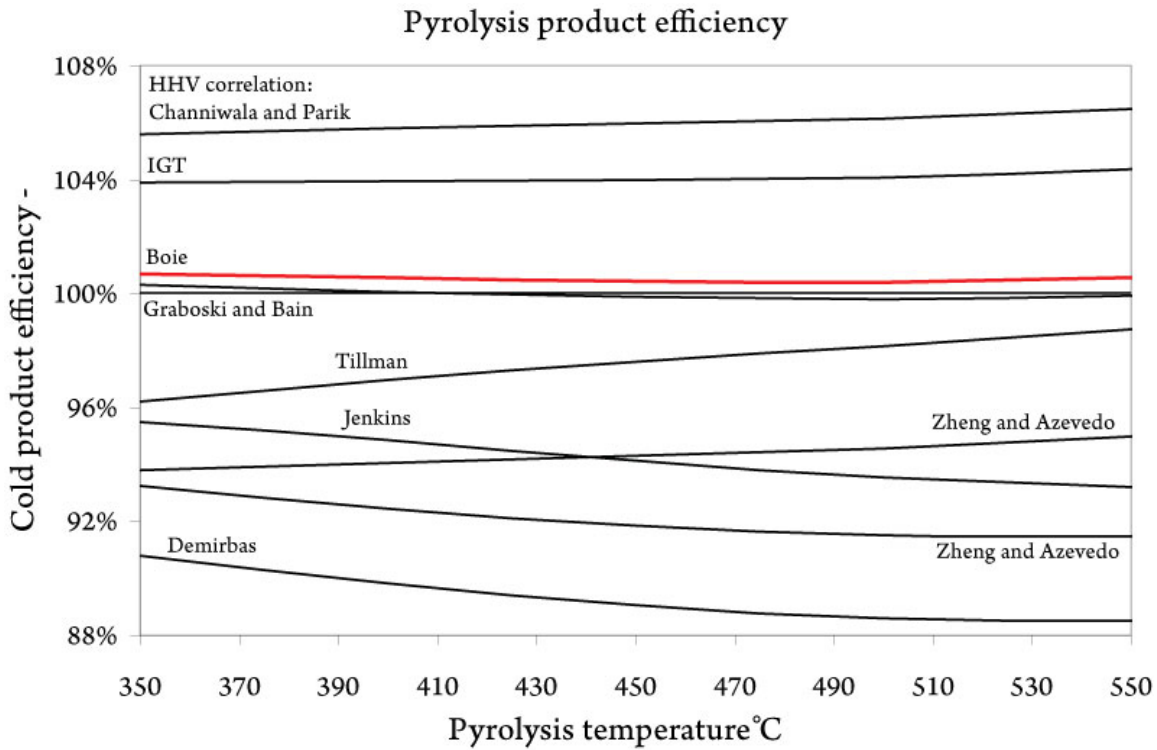
figure 4.5

Cold product efficiency (analogues to cold gas efficiency) above 100% implies that product higher heating value is higher than biomass higher heating value. Difference in higher heating value is however not equivalent to the reaction duty of pyrolysis, as steam consumed/released in the reaction also contributes to higher heating value. Boie's empirical correlation is used for biomass and char, and gives pyrolytic cold product

efficiency close to zero for all temperatures. The majority of other correlations is within (100 ± 6)%. Few articles are available on experimental values, in one of the few available Daugaard and Brown [14] estimate the reaction heat to approximately 1.5 MJ/kg of the biomass heating value, which below 10% of most biomass HHV.

5 Modeling of the thermochemical converter

A complete flowsheet of the thermochemical converter is given in figure 5.1, and as with the principle overview, four reactors make up the fundamentals of the converter.
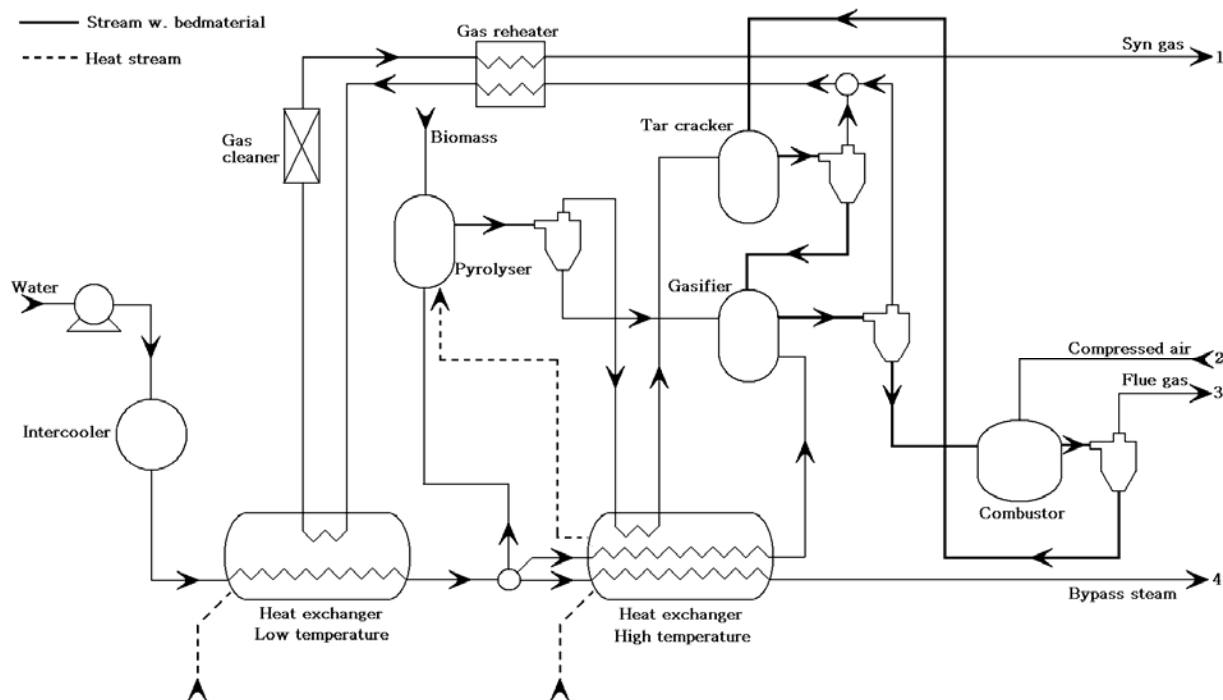
figure 5.1

Heat transfer is here elucidated with two counter-current heat-exchangers detailing heat transfer between the waste heat stream and the reactors. Note that the waste heat stream is not depicted, heat transfers from this stream are denoted by a dashed heat stream line. Steam is generated and superheated to pyrolysis temperature in a low temperature heat exchanger. A part of the steam-flow is used to fluidize the pyrolyser, while the rest is sent to the high temperature heat-exchanger for further heating to steam gasifier/tar cracker temperature. Gaseous pyrolysis products are also heated in the high temperature heat exchanger. Counter current heat exchange is not possible for heat transfer with the pyrolyser bed material; heat must be transferred from the waste heat stream at temperatures above pyrolysis temperature, e.g. from the high temperature heat exchanger. This heat transfer is represented by the dashed line from the heat exchanger to the pyrolysis reactor.

Downstream of all reactors, a cyclone separates solid from gaseous stream components. A gas cleaner is incorporated in the flowsheet, representing the thermodynamically significant processes of gas cooling; reheating and pressure loss. As the whole converter including all reactors is pressurized, pressurized air for combustion of residual char is obtained from the power cycle.

An additional steam splitter is provided for the option of bypassing steam from the converter directly to the power cycle, thus making the total amount of steam admitted to the complete integrated cycle partly independent of the amount of steam used for biomass conversion (the former must be at least as much as the latter).

5.1 Mathematical models

The flowsheet of figure 5.1 is used in Aspen Plus™ (AP) for analysis. An introduction to AP is given in chapter 2. While AP contains several built-in flowsheet units, several units of the thermochemical converter can not be directly represented. Combinations of built-in units and calculator scripts are therefore used to represent certain physical units.

5.1.1 Pyrolyser

The pyrolyser is represented in AP as a stochiometric reactor, with stochiometric coefficients of the reactions taking place as input values. The mathematical model of pyrolysation as detailed in chapter 4 is introduced in AP as a calculator script, taking reactor temperature as input and returning product yields, element compositions, and enthalpies of formation. The calculated product yields are used as stochiometric coefficients in the reactor, e.g. incoming biomass is converted to given fractions of pyrolytic gas, tar, and char, while element compositions and calculated enthalpies of formation are used to define the lumped product groups as AP non-conventional components.

AP uses the element composition of biomass and the lumped product groups to check the mass balance across the reactor. Enthalpies of formation along with supplied data for heat capacities (these are not supplied by the pyrolysis model and constant regardless of pyrolysis conditions) are used to calculate the energy balance of the reactor. The lumped product groups are now sufficiently defined to have a temperature dependent enthalpy, and are consequently capable of participating in downstream heat exchange calculations.

5.1.2 Tar cracker

Along with cracking of tar in a catalytic environment, reform and shift reactions are also spontaneously occurring. These reactions are assumed to approach equilibrium, and as tar is assumed completely cracked, only non-condensable gases participate in the equilibrium mixture. Consequently, the lumped product group tar can be avoided in

calculation. The benefit of equilibrium calculations is that the initial composition of the mixture (which includes tar and pyrolytic gas) is irrelevant as long as the element composition of the feed as a whole is known.

Tar and pyrolytic gas are parts of the AP non-conventional stream type, which cannot participate in equilibrium calculations. The calculations must therefore be conducted in two steps, by the use of two unit reactors in AP. In the first reactor tar and pyrolytic gas is stochiometrically converted to an arbitrary mixture of gases (with correct element balance) present in the AP libraries, and the heat of reaction calculated. This reactor serves the purpose of "translating" flow from the non-conventional to the mixed AP stream class. The gas mixture is then mixed with steam in a second reactor where it undergoes equilibrium calculations. The heat of reaction of the second reactor is set so that the sum of the first and second reactor is zero. The net result is an adiabatic equilibrium reaction.

The assumption that equilibrium represents the products of tar cracking and the reform/shift reactions only holds if the reactor residence time is sufficiently long and component mixing good enough. This is also the case for gasification. As pointed out by Jand et. al. [15], actual product composition of biomass steam gasification (equivalent to thermochemical conversion in this paper) deviates from equilibrium composition in a predictable way, e.g. certain components are always under-represented by equilibrium calculations. According to the authors, deviations are caused by the slow kinetics of the reforming reactions, accounting for under-representation of methane and other hydrocarbons, and failure of the heterogeneous gas-char reactions to completely gasify solid char within reasonable residence time, as predicted by the equilibrium calculations. The authors propose a solution to the problem by setting a fraction of the under-represented components as inert, excluded from the equilibrium calculations. Although the experimental values the article is based on is a single reactor thermochemical process, the same shortcomings of the equilibrium model are assumed to be present in a multi-reactor process too, and the solution is applied to the tar cracking reactor by setting a fraction of methane as inert.

5.1.3 Gasifier

From a computational point of view, the gasifier is exactly similar to the tar cracker. As the reactor represents the conversion of solid char from pyrolysis, a non-conventional component, the same approach with two unit reactors representing the gasifier as was the case with the tar cracker is used.

Reform and shift reaction are occurring simultaneously with the gasification reactions, and the mixture is assumed to approach a restricted equilibrium as detailed for the tar cracker, with inert methane. In the gasifier, a fraction of solid carbon is also set as inert. While char entering the steam gasifier is a non-conventional compound containing carbon, hydrogen, and oxygen, char exiting the gasifier is pure carbon as found in the AP libraries.

5.1.4 Other units

The reactors presented above are the only units requiring special treatment due to the use of non-conventional components and processes not built-in in AP. The rest of the flowsheet units are modeled with units made for the purpose in AP, e.g. heat exchangers are modeled with AP heat exchangers etc. A possible exception to this is the tar cleaner which is modeled as a throttle valve, as pressure drop is the only thermodynamic significant effect of gas cleaning (cooling and reheating is controlled by AP heat exchangers).

6 Recuperation

Recuperation is a central concept in the integrated cycle of thermochemical converter and power cycle. In the wide sense, recuperation might have many definitions both thermodynamical and not, in this paper recuperation is defined in its narrow sense, applicable to open-circuit heat engines such as gas turbine cycles. Such systems discharge energy in the form of sensible heat in a mass stream, also termed a waste heat stream. Recuperation is the transfer of heat energy from the waste heat stream to any intermediate form of energy directed back to the heat engine. Recuperation can be divided into sub-categories according to the type of intermediate energy-form they utilize for transportation of energy back to the heat engine (as opposed to the process of energy transfer they use, which is heat transfer in all cases).

Energy efficiency of recuperation is in most cases close to 100%, and not a suitable value for assessment of recuperation performance. 2.nd law efficiency (in this chapter referred to as efficiency) is therefore the preferred parameter for this task, measuring the irreversibility of the energy transfer. Consequently, exergy and not energy is the important flow parameter.

6.1 Heat recuperation

Heat recuperation transfers heat energy from the waste heat stream to heat energy in another stream. Efficiency is determined by the temperature difference between the streams exchanging heat energy. Proper control of mass-flow in one or both streams makes it possible to achieve comparatively small differences in temperature through the entire heat exchange, making heat recuperation a potentially very efficient recuperation type.

There are two major drawbacks to heat recuperation which both apply to gas turbine cycles. First is the availability of mass-flow at temperatures allowing for heat transfer from the waste heat stream. In the gas turbine cycle compressed air is the predominant source of this mass-flow. The compressed air is however already heated to some extent by compression, reducing the temperature down to which the waste heat stream can be cooled and supply heat energy.

Second is the decrease in specific output on a mass-flow basis caused by heat recuperation. As air and/or fuel entering the gas turbine is preheated by recuperation, less fuel is required to reach a given turbine inlet temperature. Conversely, with fixed fuel flow, mass-flow to the combustion chamber must be increased not to exceed the given turbine inlet temperature. In this way, power output is increased by heat recuperation. Increased mass-flow however also means that more energy is present in the waste heat stream at given temperature, increasing losses as it is discharged from the cycle. Losses are also caused by irreversibilities and energy losses in the cycle (compression, pressure loss, etc.), resulting in less than proportional relationship between mass-flow and cycle

thermal efficiency. Heat recuperation can therefore be summed up as beneficial to the cycle because of increased mass-flow for a given fuel input, however deteriorated by losses associated with mass-flow.

6.2 Steam recuperation

Steam recuperation transfers heat energy from the waste heat stream to vaporize pressurized water in another stream. Steam recuperation is exclusively concerned with the phase-change, preceding and subsequent heating of water and steam is regarded as heat recuperation. Pressurized steam is injected to the combustion chamber and contributes to higher mass-flow through the turbine, increasing power output.

Similarly to heat recuperation, steam recuperation increases power output by increased mass-flow through the turbine. While increased mass-flow requires more compression work in the case of heat recuperation, the increase in mass-flow by steam recuperation only requires neglible liquid-phase pump work. Power output is therefore increased more per mass-unit of additional flow, with the additional benefit of less irreversibilities and energy losses associated with mass-flow. Compressed water is at ambient temperature and vaporization normally occurs at temperatures below the temperature of the compressed air. Steam recuperation is therefore suitable for recuperation of low temperature waste heat stream energy, unavailable for heat recuperation.

Since vaporization is an isothermal process and transfer of heat energy from the waste heat stream is not, temperature difference in heat exchange are inherently greater than for heat recuperation. Consequently recuperation efficiency is lower. Furthermore, the vaporization heat of the created by steam recuperation, eventually ending up in the waste heat stream, is not recuperated back to the cycle and is discharged from the cycle. The energy content of the discharged stream is thus increased at a given temperature if steam recuperation is performed. As a result, steam recuperation is normally associated with more irreversibilities and energy loss than heat recuperation.

Steam recuperation is to sum up suitable in combination with heat recuperation, recuperating energy not available for heat recuperation.

6.3 Chemical recuperation

Chemical recuperation transfers heat energy from the waste heat stream to chemical energy through chemical reactions. This transfer of energy may use heat as an intermediate to transfer the energy to the reaction, e.g. direct heat transfer with the waste heat stream is not necessary.

If all chemical energy is combusted internally in the heat engine, as in the gas turbine cycle, chemical recuperation shares the characteristics of heat recuperation. For a fixed flow of primary fuel, if the chemical energy of the fuel combusted in the combustion

chamber is higher than the primary fuel due to chemical recuperation, mass-flow to the combustion chamber must be increased not to exceed the given turbine inlet temperature

In this paper, chemical recuperation is defined as change in lower heating value for a reaction or process. This corresponds to the heat requirement of a process where liquid water is not a part of either product or reactant. Alternatively, chemical recuperation may be defined as change in higher heating value for a reaction or process. This corresponds to the heat requirement of a process where liquid water is not a part of either or reactant *plus* the vaporization energy of steam consumed or produced in the process. If change in higher heating value is to be calculated for fuel being processed, the higher heating value of steam present in the product or reactant mixture must not be included, in which case the change in higher heating value will be equal to change in lower heating value. Any use of the higher heating value definition for chemical recuperation will be mentioned explicitly.

7 Integration

The thermochemical converter is integrated with two power cycles; a gas turbine cycle and a combined fuel cell/gas turbine cycle. Both these cycles are recuperative. High temperature syngas is supplied to the power cycle by the thermochemical converter, while the thermochemical converter receives heat from the power cycle. Conceptually, a third entity termed the recuperator is defined to facilitate the utilization and distribution of waste heat from the power cycle, both to the thermochemical converter and back to the power cycle. The principle is represented graphically in figure 7.1.
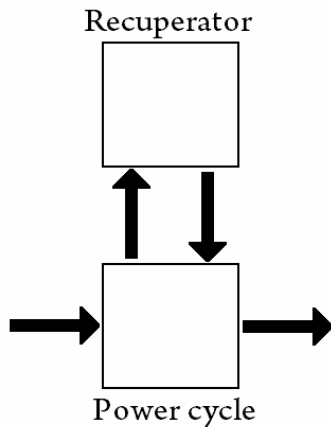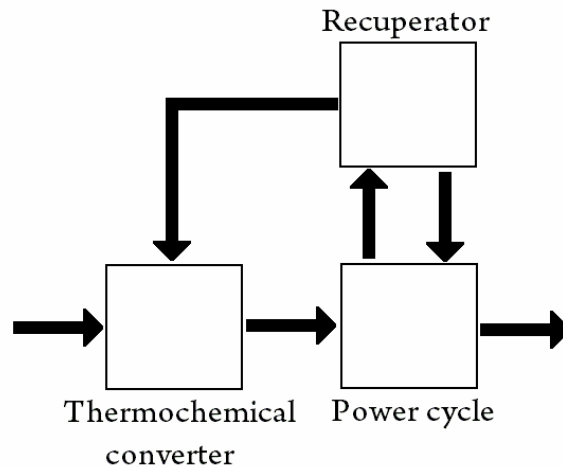
figure 7.1

Arrows represent the main flow of energy. The recuperator represents physical units such as heat exchangers and other heat transfer units. The principle presented in figure 1 has much in common with control theory representations of dynamic systems, and even though the systems dynamic behavior is irrelevant at this stage and regulators are lacking, it forms a feedback loop where all units are dependent on the performance of the other units. This acknowledgement is important for further analysis of system.

The complete system is calculated and analysed in Aspen Plus™ (AP) by introducing the models of the thermochemical converter, recuperator, and power cycle to the software. AP uses an iterative calculation process to deal with the feedback loops. The thermochemical converter is already described in chapters 3 through 5. The gas turbine and combined fuel cell/gas turbine power cycles will be defined and modeled for AP in chapters 10 and 11.

8 Thermochemical conversion results

The thermochemical converter is simulated in AP as a stand-alone unit. Inputs from what would normally be the power cycle can then be set as constants, isolating the responses of the converter itself. In the following treatment of the thermochemical converter, pyrolyser, gasifier, tar cracker and residual char combustor will be referred to as reactors. The thermochemical converter will be referred to as the thermochemical converter, or converter for short.

8.1 Input settings

The converter is modeled as described in chapter 5, with the following inputs:

Biomass feed	100 kg/h
Biomass moisture	7.4 %
Biomass C-H-O wt. %	46.4 – 5.9 – 47.7 wet b.
Biomass HHV (wet basis)	17.65 MJ/h
LHV (wet basis)	16.54 MJ/h
Biomass temperature	25 ºC
Steam feed (SC-ratio)	125.7 kg/h (2.5)
Pyrolyser temp	550 ºC
Steam to pyrolyser	550 ºC / 48.9 kg/h
Steam to tar cracker	800 ºC
Steam to steam gasifier	800 ºC / 76.8 kg/h
Pressure	12 bar
Inert solid carbon	10 % (of biomass C)
Inert methane	0 %
Circulating bed material	1000 kg/h

table 8.1

Integrated with a power cycle, the steam feed temperature to the converter is regulated by conditions of recuperation, and is thus a closed loop variable of the integral cycle. By setting the temperatures as constant, the number of variables affecting converter performance is decreased, to ease analysis. The reactors themselves, with the exception of the pyrolyser, are autothermal and cannot be directly temperature controlled. Energy needed for steam generation and heating, pyrolysis heat, and auxiliary processes are assumed to be available under all operating conditions.

The steam to carbon ratio SC is the molar amount of steam divided by the molar amount of carbon. Steam is defined as the steam injected *plus* biomass moisture *plus* the steam potentially produced by dry biomass if all its oxygen and hydrogen were to form water, leaving a surplus of either hydrogen or oxygen. In this way, the element composition of a reacting system can be more accurately described. Following this principle, steam to the tar cracker and gasifier is distributed to produce the exact same SC-ratio in both reactors. The globally calculated SC-ratio may differ from the SC-ratio calculated for a reactor, as

surplus hydrogen from one reactor might react with surplus oxygen from another. When referring to SC-ratio, reactor SC-ratio is implied unless stated otherwise.
The result section is in two parts; the pyrolysis reactor, and the complete converter (including the pyrolysis reactor).

8.2 Pyrolysis reactor results

Key results for the pyrolysis reactor are given in table 8.2. The mathematical model for pyrolysis presented in chapter 4 returns most of these values directly when given an input temperature, simulation in AP is however necessary to calculate pyrolysis reactor duty.

Tar HHV is given at dry basis, at wet basis (40% moisture) HHV is 15 MJ/kg. Note that the term gas in table 8.2 is the entire gas phase at the pyrolyser outlet, but the lumped product group gas (non-condensable pyrolysis products). The oxygen fraction in this group is very high, caused by high levels of CO and CO_2 (steam is not a part of this lumped product group). While CO, which is the main carrier of chemical energy in the mixture has a HHV of 10.1 MJ/kg, the gas mixture HHV is down to 7.0 MJ/kg due to its CO_2 content. Only 8.3 % of chemical energy from the pyrolysis products is carried by the non-condensable gases.

The amount of water produced by pyrolysis, 21.8 kg/h, is the sum of water introduced as moisture in the biomass and water produced in the pyrolysis reactions. Steam feed to the pyrolysis reactor is at reactor temperature, and has no net effect on the energy balance. Calculated energy demand is therefore the sum of energy required for heating of biomass (and any pyrolysis products produced below reactor temperature) and the energy required by the pyrolysis reactions. The total energy demand of the reactor is 194 MJ/h. Changes

Tar (dry basis)	
Yield	32.6 kg/h
Composition C-H-O	55.0 – 7.0 – 38.0 wt.%
HHV	25.0 MJ/kg
Gas	
Yield	21.0 kg/h
Composition C-H-O	34.4 – 1.8 – 63.9 wt. %
HHV	7.0 MJ/kg
Char	
Yield	24.7 kg/h
Composition C-H-O	86.1 – 3.3 – 10.6 wt.%
HHV	32.9 MJ/h
Pyrolysis water	21.8 kg/h
Reactor duty	194 MJ/h
Δ LHV	45 MJ/h
Δ HHV	10 MJ/h
Δ Chem. exergy	-74 MJ/h
Cold product eff.	100.6%

table 8.2

in lower heating value (LHV) and HHV are for the fuels only, e.g. liquid water with negative LHV accompanying biomass is not included, and steam has zero HHV. Larger difference in LHV than HHV suggests that elemental hydrogen is removed from the fuels in the pyrolysis products, confirmed by the production of water. Chemical energy is still increased, and remaining elemental hydrogen and carbon consequently form, on average, more energy–rich chemical components than those present in biomass.

8.3 Results, complete converter

As results for the pyrolysis reactor is established, the complete thermochemical converter including the pyrolysis reactor is analyzed. Figure 8.1 presents a flow diagram of the process. Both flow-energy and -exergy is specified, and temperatures are given in boldface letters.
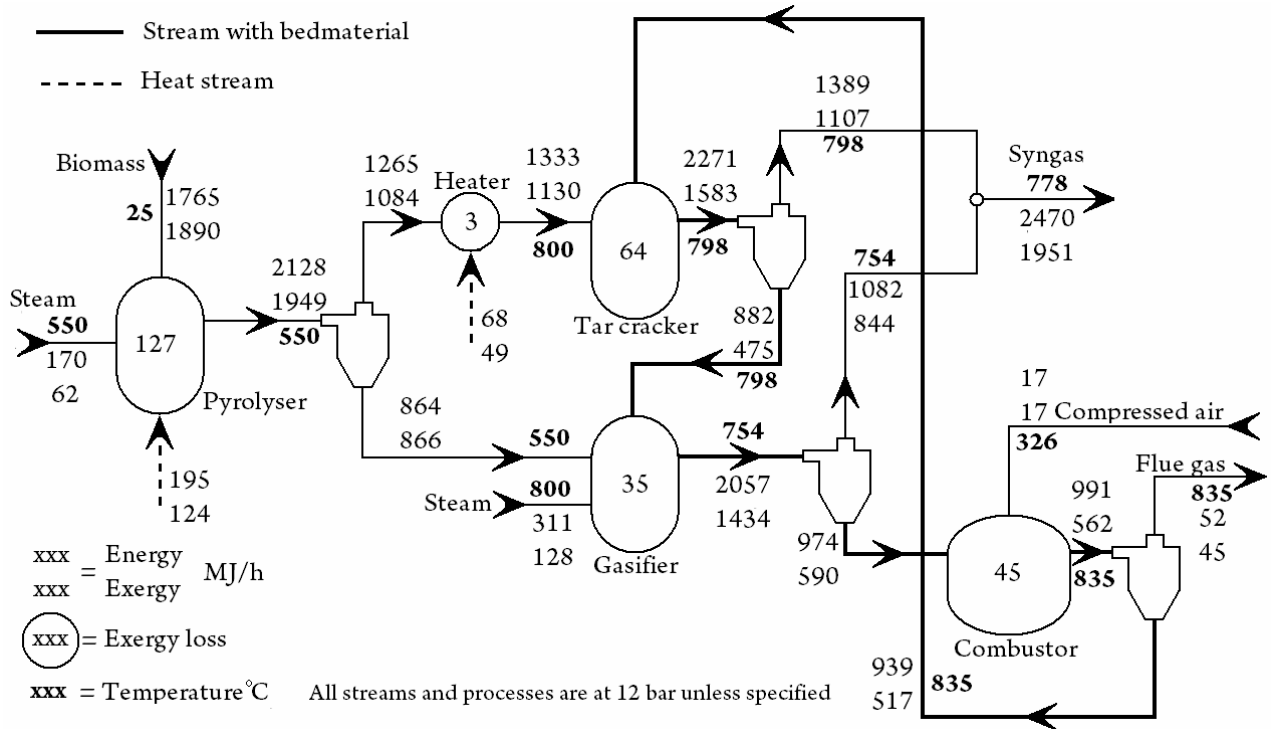
figure 8.1

Key results are summarized in table 8.3. Cold gas efficiency, e.g. the higher heating value of syngas exiting the converter divided by biomass higher heating value, is above unity, the mass flow of syngas is however higher than that of biomass, resulting in comparatively low specific HHV, approximately half that of the biomass. Clearly, high syngas water content reduces specific HHV. By removing water, which is the only condensable component in the syngas mixture, HHV is increased to a value in close proximity to biomass HHV.

Cold gas efficiency	108.0%
Cold gas exergetic efficiency	88.4%
Δ HHV	142 MJ/h
Δ LHV	34 MJ/h
Exergy loss (%biomass exergy)	14.5 %
Syngas mass flow	221 kg/h
Syngas HHV	8.7 MJ/h
HHV (dry basis)	14.5 MJ/h
Syngas water content	40.1% wt.
Tar cracker ΔHHV	120 MJ/h
Tar cracker Δ LHV	58 MJ/h
Tar cracker Δ Chem. exergy	-22.5 MJ/h
Gasifier ΔHHV	164 MJ/h
Gasifier ΔLHV	83 MJ/h
Gasifier Δ Chem. exergy	37 MJ/h
Combustor duty	-152 MJ/h

table 8.3

Fuel chemical energy is increased in the conversion process, 34 MJ/h measured by difference in lower heating value and 142 MJ/h measured by difference in higher heating value, both between the biomass inlet stream and the syngas outlet stream. Liquid water with negative LHV accompanying wet biomass is not included in the calculation, as vaporization of this water is no different to vaporization of water injected to the cycle (in the stand-alone converter simulation this enters as steam, as opposed to subsequent simulations), a process not regarded as changing chemical energy. Moisture in biomass may thus in this regard be considered as a separate stream entering the pyrolysis reactor. Similarly, HHV of steam which by definition is equal to vaporization energy, is not included in calculations. While chemical energy is increased in the conversion process 152 MJ/h of chemical energy in the form of unreacted char (pure carbon, LHV=HHV) is consumed by combustion. The actual chemical recuperation taking place in the converter, as the sum of chemical recuperation in all reactors, is therefore higher than the change in chemical energy from inlet to outlet of the converter, 272 MJ/h by HHV measurement and 186 MJ/h by LHV measurement.

The contribution to chemical recuperation differs greatly with the method of measurement used. In terms of LHV, the pyrolyser and tar cracker are approximately equal with somewhat higher chemical recuperation in the gasifier. In terms of HHV, chemical recuperation in the pyrolyser is very small, nearly all chemical recuperation is done in the tar cracker and gasifier, and again the gasifier has the highest contribution. This difference, which is especially pronounced in the pyrolyser, can be explained by the way chemical recuperation is done. While chemical recuperation in pyrolyser is done while removing elemental hydrogen in the production of water, the exact opposite is true for the tar cracker and gasifier, elemental hydrogen is added to the fuel mixture by consummation of water. Change in HHV thus includes the vaporization energy of the steam consumed (or produced and removed as in the case of the pyrolyser), otherwise not regarded as chemical energy.

It should be noted that exergy calculations involving the lumped product groups from pyrolysis (non-conventional components) are of higher uncertainty than exergy calculations involving conventional, well defined, gas components. This affects the exergy calculations of the pyrolyser, tar cracker, and gasifier. Exergy losses are greatest in the pyrolyser, partly caused by heating of biomass from ambient temperature and vaporization of biomass moisture, loss of chemical exergy is however also substantial. Chemical exergy is also reduced in the tar cracker, contributing to along with cooling of bed material (thermomechanical exergy loss in the gas phase is neglible) to exergy loss for the reactor. Again, best performance is found in the gasifier, increasing chemical exergy and counteracting thermomechanical exergy losses caused by cooling of the bed material. This is manifest in the comparatively low exergy loss for the gasifier reactor.

8.4 Sensitivity

With the thermochemical converter simulated in this protected environment, it is of interest to investigate its sensitivity to internal changes in operating conditions. Of particular interest are the sensitivity to the amount of char that is not converted in the gasifier reactor, and the response to variations in temperature in the different reactors. The tar cracker and steam gasifier are autothermal, their temperatures cannot be controlled directly, they are however sensitive to a number of other parameters. Pyrolysis reactor temperature can be controlled directly.

Figure 8.2 shows cold gas efficiency and different reactor temperatures as the pyrolysis reactor temperature is changed. The temperature of steam to pyrolysis is regulated too, so that it is equal to pyrolysis reactor temperature. By varying pyrolysis temperature, both product yield distribution and product composition from the pyrolysis reactor are altered, influencing the element distribution to the downstream reactors. The distribution of steam is however not regulated to compensate for this, resulting in deviating SC-ratios in the tar cracker and gasifier. These deviations are a secondary cause of change for the measured variables in figure 8.2, the effect is however assumed to be small. As figure 8.2 details, the effects of changes in pyrolysis reactor temperature are small, with only neglible increase in reactor temperatures and a small increase in cold gas efficiency. Keeping in mind the comparatively large error margins in the pyrolyser model, the effects can be said to be insignificant. Lowering the temperature might however have large consequences for reactor operation in practice, most significantly for required conversion time, aspects not covered by the model.
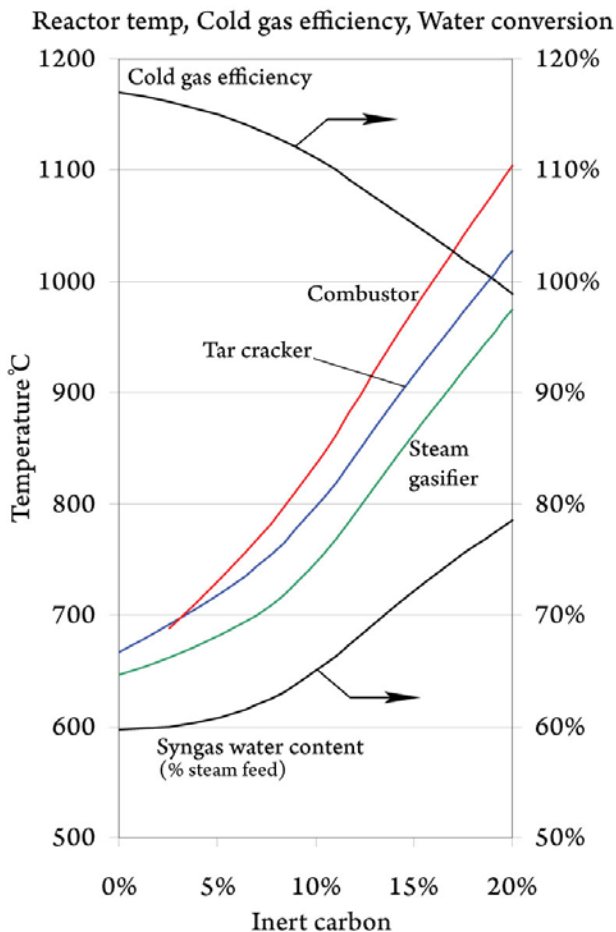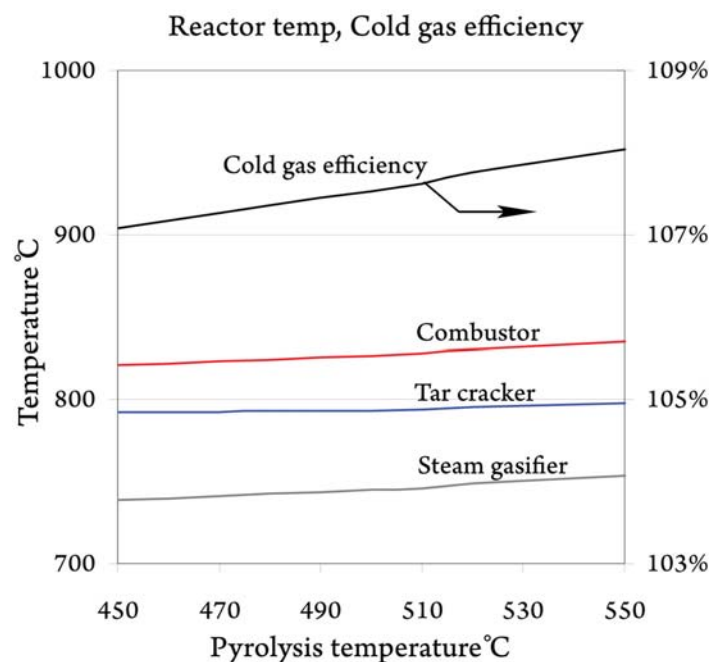

figure 8.2

figure 8.3

Pyrolysis is not simulated at higher temperatures than 550 ºC, as the assumption of inert steam will be less feasible when temperatures increase and the process will be closer to single-reactor thermochemical conversion with gasification.

In figure 8.3, the amount of carbon not converted in the gasifier is varied. This is done by varying the amount of inert carbon in the gasifier (ref. chapter 5.1.3). The amount of steam to the gasifier (and tar cracker) is constant, the elemental composition in the gasifier participating in equilibrium calculations is consequently changed as the amount of inert char is varied, so that SC-ratio deviates from 2.5 as stated in the input section. This is a secondary cause of change for the measured variables in figure 8.3, the effect is however assumed to be small. Performance and operating conditions of the converter is significantly affected by changes in the amount of inert carbon. Naturally, syngas energy and consequently cold gas efficiency decrease as larger proportions of biomass energy are inhibited from being converted to syngas. This effect should produce a linear relationship between cold gas efficiency and inert char. Chemical recuperation is however also significant for cold gas efficiency, through reforming. By decreasing the amount of carbon available for reforming in the gasifier, chemical recuperation is also decreased, giving raise to the non-linearity of figure 8.3. This effect must not be confused with the deviations in SC-ratio, which with increasing SC-ratios have the contrary effect of increasing reforming per unit of carbon.

Reactor temperatures are affected in the same way; more char is available to heat the bed material and less heat is required to drive endothermic reforming reactions. Syngas water content, as given in figure 8.3, is defined as the mass of steam in the product gas divided by the mass fed to the converter (excluding steam in the pyrolysis products and moisture in biomass). As can be seen, inert carbon can be varied between 0-5% before syngas water content is significantly affected. From 5%, increases in syngas water content, equivalent to decreases in steam consumption, causes and coincides with accelerating trends of the other measured values, confirming the role of reforming as a secondary and independent cause to decreasing cold gas efficiency.

Higher temperatures in the tar cracker and gasifier are thermodynamically beneficial, favoring reforming reactions. This effect is however smaller in magnitude than the effect of carbon decrease, and unable to compensate for the loss of carbon.

To achieve high cold gas efficiency from the conversion of biomass to syngas, it is certainly logical to maximize the amount of char that is converted, as this increases the amount (mass) of biomass converted to gas. The secondary effect of reforming and chemical recuperation is however not as obvious, but all the same a reason to convert as much char as possible. Thermodynamically speaking, conducting tar cracking and gasification at feasible temperatures is the only reasons for setting design targets at less than complete conversion of char, and as seen in figure 8.3, temperatures do approach critical values with small amounts of unreacted char. When integrated with a power cycle, this has to be compensated for by increasing steam feed temperatures, to which there are limits. Conversion of solid char is however an inherently stable process, as decreases in temperature will decrease reaction speed, and with constant gasifier reactor

time-space dimensions, the amount of unreacted char will increase. The coupling of reactor temperature and unreacted char seen in figure 8.3 is thus not present in practice, e.g. full conversion of solid char is not feasible at below 600 ºC in a practical reactor.

Attempting to completely convert the char in a real process might both be impossible due to chemical/physical consideration, and uneconomical due to reactor sizing. The use of 10% inert char in further simulation corresponds to empirical values for carbon conversion. See chapter 1 for details.

Removal of carbon from equilibrium calculations had the effect of decreasing reforming and chemical recuperation. Altering the steam feed will have an effect along the same lines. In figure 8.4, steam feed is varied between SC-ratio 2.0 and 3.0. The distribution of steam between the pyrolyser/tar cracker and gasifier is as described in the input section.
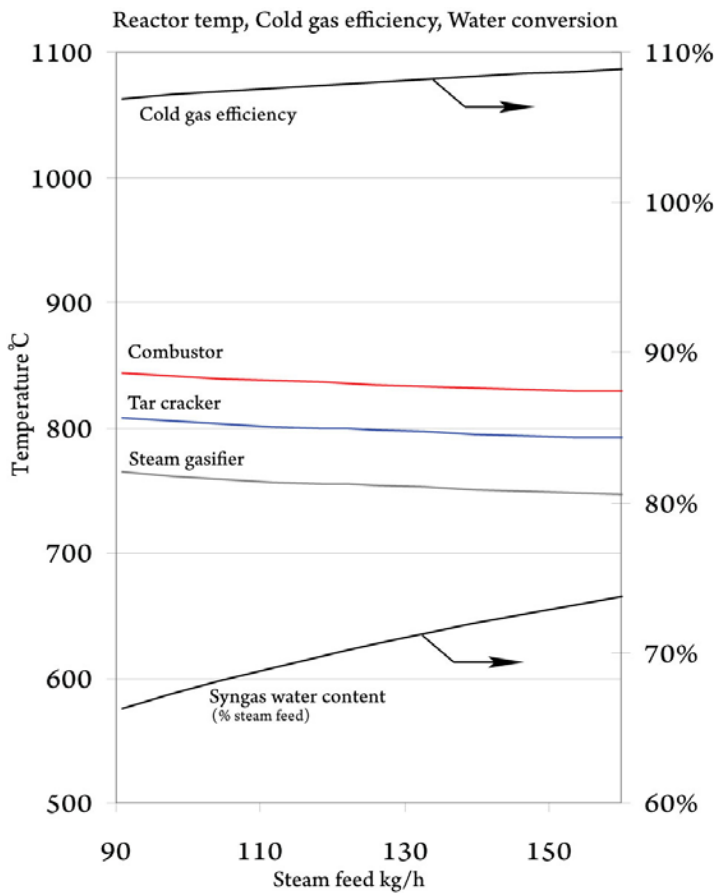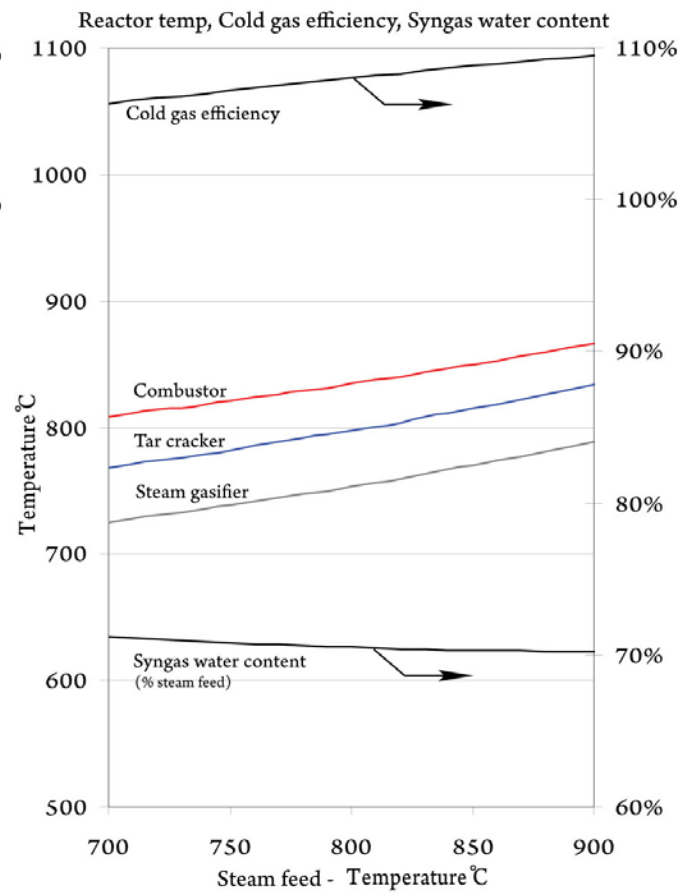
figure 8.4   figure 8.5

The result is an increase in cold gas efficiency along with decrease in reactor temperatures, both indicative of increases in reforming and chemical recuperation. Syngas water content is also increasing; increase in steam conversion is thus unable to keep up with the increase in steam flow. Even though reactor performance, regarding its capability as a chemical recuperator, increases with increased steam feed, high steam flow might have negative effects on downstream units and to an integrated power cycle.

First and foremost of these is the energy requirement for generating the steam, which might compete with other processes for waste heat. Second is the decrease in specific syngas HHV as the water content increases. The integrated cycle may therefore have another optimum than the stand-alone converter.

A last sensitivity analysis is conducted on what is strictly speaking an external variable; the steam feed temperature to the gasifier and tar cracker, represented in figure 8.5. Steam to the pyrolysis reactor is kept at 550 ºC. When integrated with a power cycle, steam feed temperature is determined by recuperation performance, and is the most influential coupling between power cycle performance and thermochemical converter performance, making it a looped feedback to the converter. This looped feedback makes it hard to isolate the effect of steam feed temperature, a de-coupling as used here is therefore necessary.

In figure 8.5, reactor temperatures are expectantly increasing with increasing steam feed temperature. Higher reactor temperatures are beneficial for reforming, and cold gas efficiency is consequently rising. The response of the cold gas efficiency is in the same order of magnitude as was the case with variable steam feed, while the syngas water content (and thus the steam conversion), changes very little. Regarding equilibrium calculations in the tar cracker and gasifier, both steam feed and carbon participating in equilibrium are constant through the sensitivity analysis, the only changing variable affecting equilibrium is the reactor temperatures. The increase in chemical recuperation as reactor temperatures are increased is done with very modest increases in steam conversion, suggesting that a more endothermic type of reforming is taking place, e.g. a more endothermic way of converting steam.

When investigating syngas composition at several steam feed temperatures, it is revealed that hydrogen makes up between 72.4 vol. % and 72.8vol. % of the fuels in the syngas (steam and CO2 excluded), while CO rises from 21.4 vol. % to 25.1 vol. % as temperatures increase. This suggests that the exothermic shift reaction (consumes CO, produces H_2) is less favored at higher temperatures compared to the endothermic reforming reactions (produces CO, H_2). This effect provides an alternative pathway to increased chemical recuperation, as opposed to the extensive, or even excessive, use of steam to meet the same goal.

9 Reference cycle model

As a mean to evaluate the performance of the proposed thermochemical converter with multiple reactors, a reference converter is modeled. The reference converter is a dual bed biomass steam gasifier with partial oxidation to provide reaction heat. Figure 9.1 shows the complete converter, paralleling the flowsheet of the proposed converter.

figure 9.1
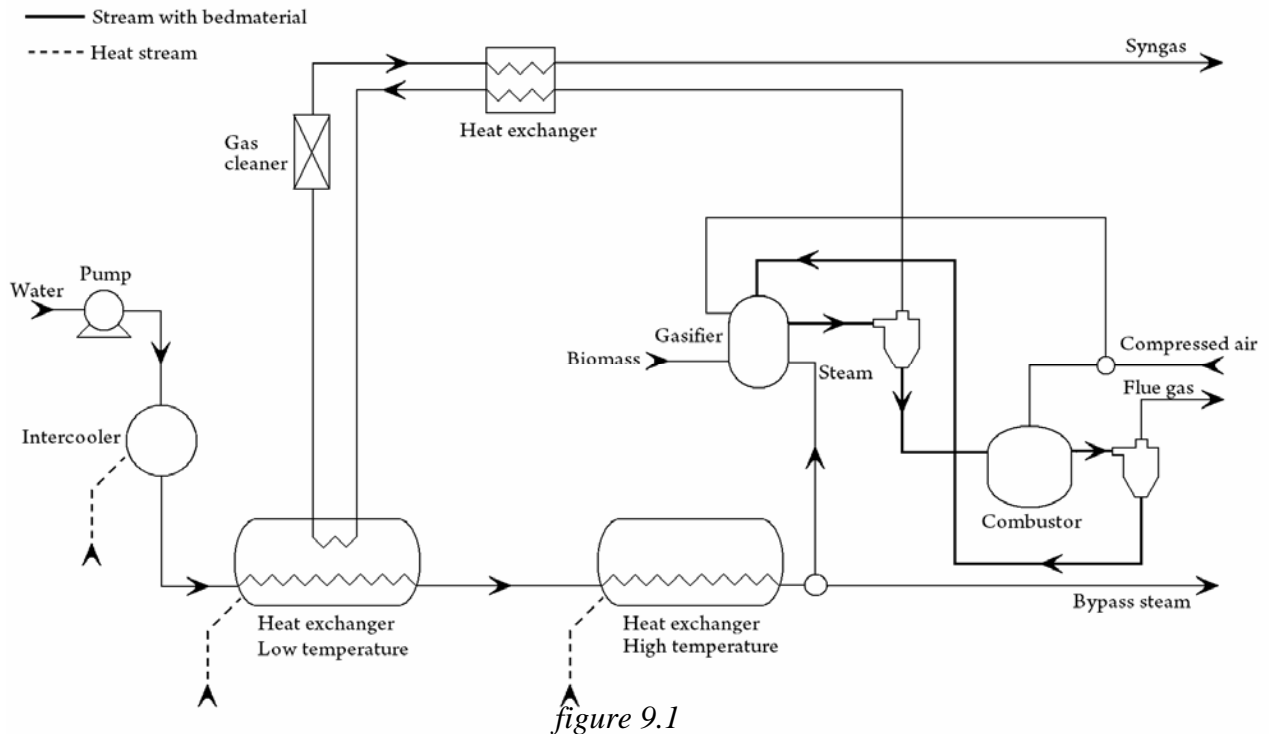
The three-reactor setup of the pyrolyser, tar cracker, and gasifier in the proposed converter is replaced by a single reactor, the gasifier. The gasifier is connected with a combustor combusting unreacted char through a circulating flow of bed material, as with the proposed converter. The gasifier receives compressed air from the power cycle for partial oxidation of biomass. Air flow is regulated to achieve a set temperature in the gasifier. Steam to the gasifier is provided by the recuperator, the temperature is controlled by recuperator conditions.

The gasifier is modeled as an equilibrium reactor, as with the tar cracker and gasifier of the proposed converter. A certain amount of carbon can be set inert, as detailed in the gasification modeling section.

All units in the reference converter also present in the proposed converter is as described for the proposed converter.

10 Gas turbine power cycle model

The gas turbine power cycle is a well known and matured system. This, and the fact that it is based on simple thermodynamic principles, makes for straight-forward modeling in AP with only built-in units.
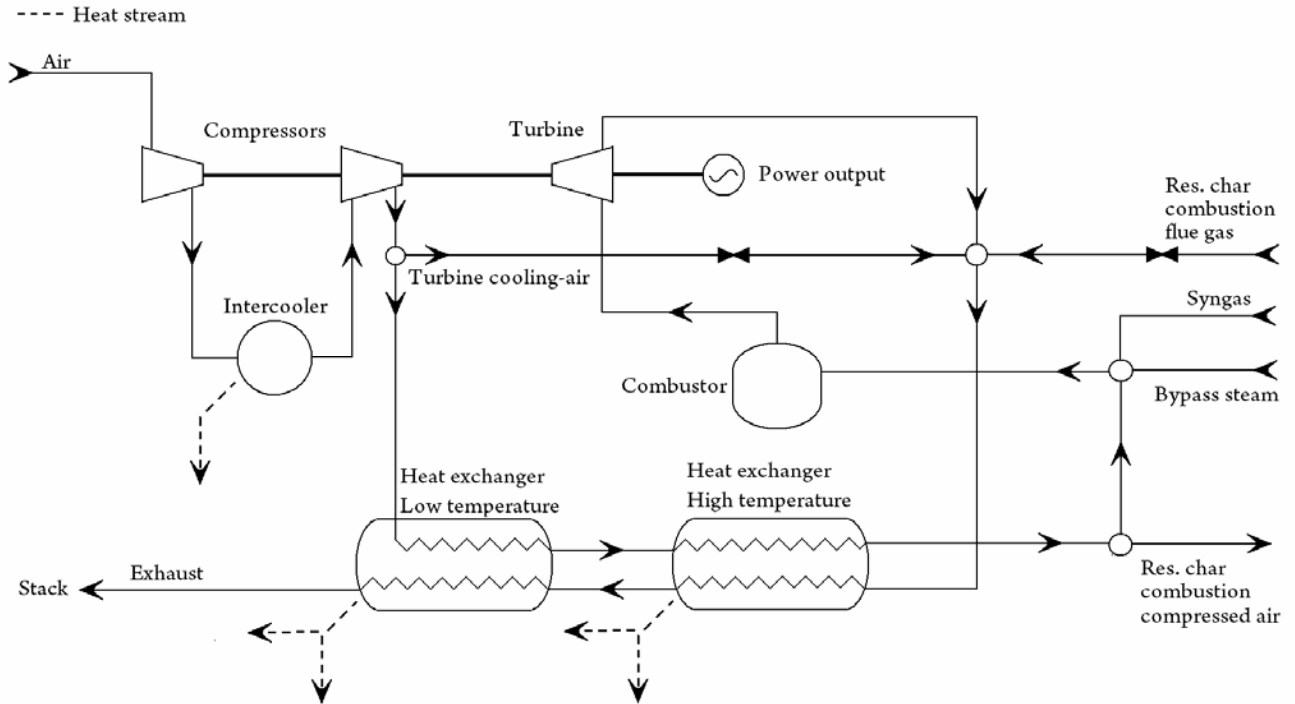
figure 10.1

The power cycle with the recuperator is given in figure 10.1. The recuperator includes both heat exchangers and the intercooler, units which are also depicted in the thermochemical converter model (chapter 5, page 17). Recuperator units are depicted in both models because they represent the interface between them. Dashed lines *from* the recuperator units in this model correspond with the dashed lines *to* the recuperator units in the thermochemical converter model, and represent the energy flow from the recuperator to the thermochemical converter. Energy flow from the recuperator units to the power cycle and energy flow from the power cycle to the recuperator units are given as a part of figure 1.10. Streams going in or out at the right-hand side of figure 10.1, represents mass flow between the power cycle and thermochemical converter.

The gas turbine cycle is a dual compressor cycle with intercooling and a single expansion stage. Compressed air from the compressors is preheated in the heat exchangers (recuperator) before it is mixed with syngas and combusted in a combustion chamber. Hot gases from combustion are expanded in the turbine. Expanded exhaust gas is then cooled down in the heat exchangers and discharged to the stack.

A fraction of compressed air is used for turbine blade cooling and separated from the main air stream prior to preheating. Air for combustion of residual or unconverted char in the thermochemical converter is supplied from the preheated air stream. Flue gas from this combustion is later mixed with turbine exhaust. The syngas stream entering figure 1.10 corresponds to the syngas stream exiting the thermochemical converter. There is also a choice of using steam straight from the recuperator to the power cycle, bypassing the reactors of the thermochemical converter. This stream is the bypass stream exiting the thermochemical converter model and entering the power cycle model at the right. Even though this is a recuperator - power cycle relation, the steam generation and heating is depicted in the thermochemical converter model for the practical purposes of collecting all steam processes in one figure.

Power output is calculated as electricity generated by the cycle.

In AP, compressors and turbine is modeled by built-in compression and expansion units. Both mechanical and isentropic efficiencies are considered in calculations. The heat exchangers are modeled as generic counter-current multi-stream heat exchangers, while the intercooler is modeled as a generic counter-current two-stream heat exchanger. For the heat exchangers, heat losses as a fraction of heat exchanger duty and pressure losses are considered. Turbine blade cooling is modeled by bleeding a given fraction of compressed air to the turbine exhaust without doing expansion work. Flue gas from residual char combustion is throttled and mixed with turbine exhaust in the same way after combustion at higher than ambient pressure.

The combustor is modeled as a stochiometric reactor. Complete combustion is assumed, without the generation of NO_X. Streams and units are, unless stated explicitly, adiabatic and without pressure loss.

11 Combined fuel cell/gas turbine power cycle model

The fuel cell converts the fuels chemical energy directly to electricity, heat is however a major byproduct. In many types of fuel cells, such as the PEM, this heat is discharged at low temperatures with little potential for work. Other types of fuel cells such as the SOFC produce heat at far higher temperatures. Although these in general are less effective than their low-temperature counterparts, they contain less expensive and pollutable materials and produce high-temperature heat with potential for work. In recent years, the integration of high temperature fuel cells with the gas turbine cycle has received much attention, as it provide a mean to utilize the heat generated by the fuel cell as well as any unconverted chemical energy in the fuel cell exhaust.

11.1 Combined fuel cell/gas turbine power cycle model

Figure 11.1 depicts the combined fuel cell/gas turbine cycle model, paralleling the approach used for the gas turbine cycle model.

Similarities with the gas turbine cycle are many, and intentional. The fuel cell is
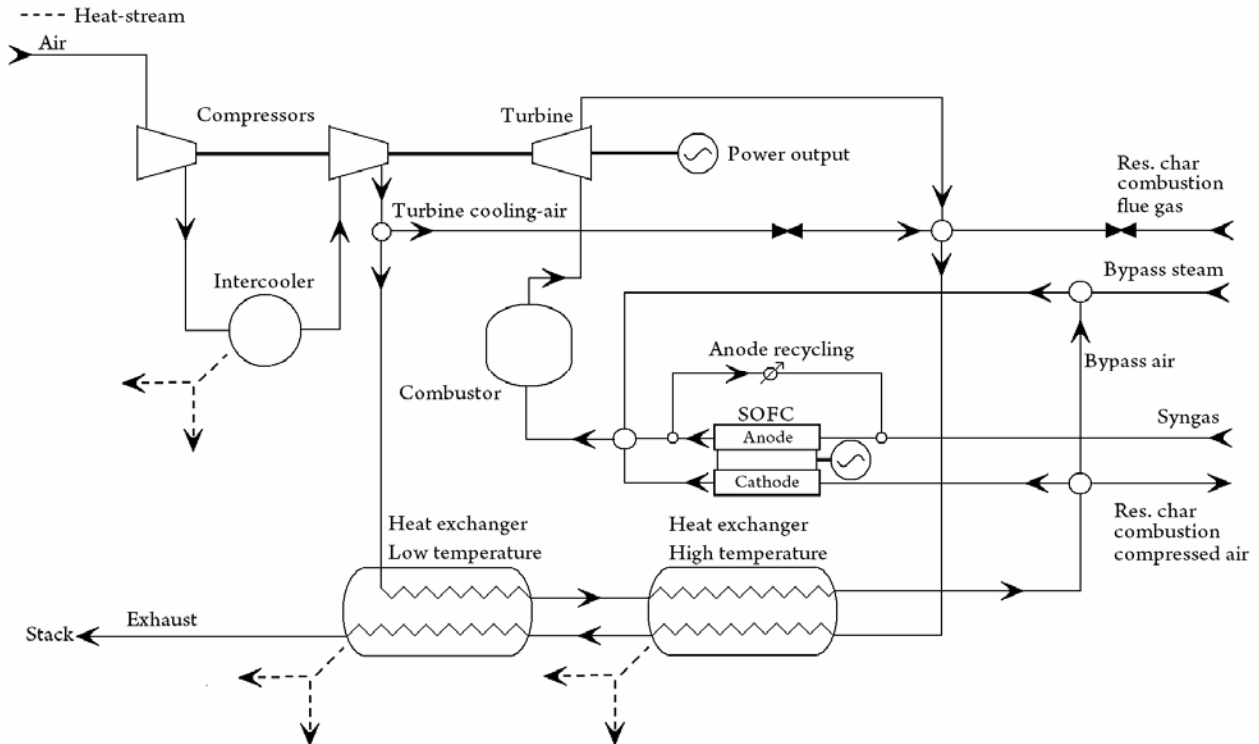

figure 11.1

integrated directly upstream of the combustor, without removing any of the units used in the gas turbine cycles. All units also present in the gas turbine cycle model remain as described for that model. In addition to the fuel cell, some streams have been added to

increase fuel cell performance. These are the anode recycling and bypass air, both physically representing stream splitters/valves. Anode recycling is a mean to adjust fuel partial pressure in the anode stream, for reasons that will be explained thoroughly in a subsequent chapter. Bypass air offers the possibility of letting a fraction of air directly to the combustor chamber, avoiding unnecessary cooling of the fuel cell. Fuel cell heating and energy balance will also be covered in a subsequent chapter.

11.2 Fuel cell model

AP does not contain built-in units for fuel cells, AP modeling must therefore be done by combining several built-in units and calculator scripts.

Fuel cell performance is fundamentally governed by comparatively simple physical/chemical relations. They are however complicated by mass and heat transfer considerations in and around their core-components. Simple fuel cell models, largely avoiding these considerations, can still be made with satisfactory predicting power. The fuel cell model used in this chapter is developed on the basis on a model by Zhang et. al. [15] for use in AP. The model is zero-dimensional and steady state. Its main principle is the assumption that although it is possible to oxidize both CO and H_2 in a SOFC, the shift reaction converting CO to H2 is much faster than the oxidization if CO. Consequently, only the oxidization of H2 is considered in calculating fuel cell voltage potential and power, and the anode is assumed to be in equilibrium.

The complete fuel cell model is presented as a flowsheet in figure 11.2. Note that units depicted here are not representing fuel cell parts or geometry, but fundamental processes in the fuel cell model. Where appropriate, the corresponding fuel cell part is given in parentheses.
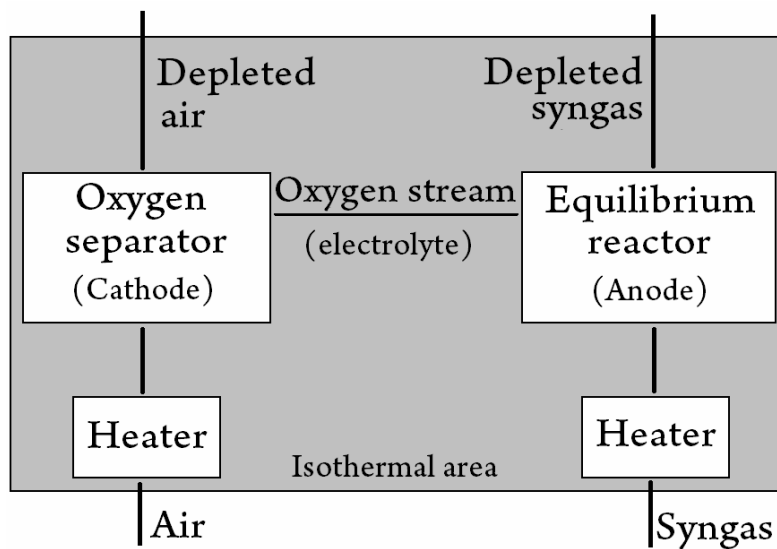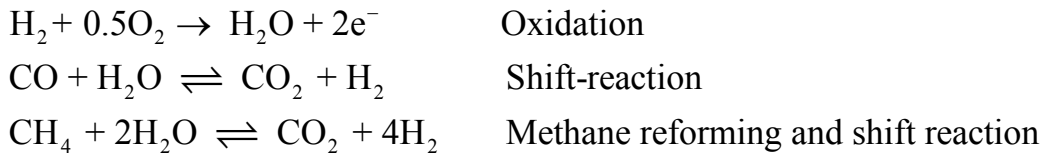

figure 11.2

Air and syngas are brought to fuel cell temperature by heaters as they enter. This represents the heating of air and syngas as they make contact with the fuel cell walls. At the "cathode", a given amount of oxygen is separated from the air stream to a separate stream, representing the migration of oxygen-ions through the electrolyte. Nitrogen and remaining oxygen in the air stream exits the cathode in the cathode exhaust stream.

Oxygen and syngas mixed at the "anode" reacts to form an equilibrium composition, before exiting in the anode exhaust stream. The heat of this reaction is calculated by the equilibrium reactor.

So far, the model is only describing an oxygen-fired combustion. The final properties enabling the model to describe a fuel cell must be added in calculator scripts. The central calculations in this regard are the amount of oxygen transferred to the anode, the cell voltage and power, and the energy balance.

The flow of oxygen to the equilibrium reactor, or anode, is given as a stochiometric relation to the amount of H_2 available at the anode. This value differs from the amount of H_2 in the inlet stream, as H_2 is produced at the anode by the shift reaction, and is termed "equivalent H_2". Considering the main reactions taking place at the anode:

$$H_2 + 0.5O_2 \rightarrow H_2O + 2e^- \qquad \text{Oxidation}$$
$$CO + H_2O \rightleftharpoons CO_2 + H_2 \qquad \text{Shift-reaction}$$
$$CH_4 + 2H_2O \rightleftharpoons CO_2 + 4H_2 \qquad \text{Methane reforming and shift reaction}$$

Equivalent H_2 is

$$\dot{n}\,H_{2,equiv.} = \dot{n}\,H_2 + \dot{n}\,CO + 4\dot{n}\,CH_4 \qquad (11.1)$$

The dotted "n" is the molar flow rate of the given component. Oxygen flow is then determined by

$$\dot{n}\,O_2 = U_f \frac{\dot{n}\,H_{2,equiv.}}{2} \qquad (11.2)$$

U_f is the fuel utilization ratio, a variable determining to which extent the fuel cell is to oxidize the fuel. Set to 1, all fuel including CO and CH_4 (through shift and reforming), is oxidized by the fuel cell.

Fuel cell voltage is equal to the reversible, open circuit voltage minus losses. The reversible voltage is given by the Nernst equation and is proportional to the change in Gibbs free energy for the oxidation reaction. Gibbs free energy is sensitive to temperature and partial pressure of the components concerned. The former is constant for all parts of the fuel cell, while the latter is changing as components are consumed and formed in

reactions at the anode and cathode, and thus has spatial variations. Partial pressures for the reactants in the oxidation reaction are at their lowest at the exit of the fuel cell, product partial pressure is simultaneously at its highest, resulting in a voltage minimum value. Since the fuel cell cathode and anode is modeled as equipotential plates, fuel cell voltage cannot be higher than the lowest value across the cell. Reversible fuel cell voltage is therefore calculated with partial pressures of O_2, H_2, and steam at the exit of the fuel cell.

$$V_{rev.} = \frac{\Delta G}{nF} \qquad\qquad V = V_{rev.} - V_{loss} \qquad\qquad (11.3)$$

Fuel cell current can readily be determined from the oxidation reaction, and the electrical output of the fuel cell can be established.

$$I = 4\dot{n}O_2 \qquad\qquad P = VI \qquad\qquad (11.4)$$

When calculating energy balance, basis is taken in the reactions in the equilibrium reactor. From a modeling point of view, this reaction is a combustion and the total and only energy supply to the fuel cell. In a fuel cell, a fraction of the fuels chemical energy is converted directly to electrical energy, while the rest is converted to heat. Electrical output of the fuel cell, as calculated, is therefore subtracted from the heat of reaction calculated for the equilibrium reactor. The resulting value is the net heat released in the fuel cell.

The fuel cell is set to operate at a fixed temperature, the heating balance must therefore be summed to zero to avoid heating or cooling. The fuel cell is assumed to be adiabatic, heating is however required by the incoming air and syngas streams. To aid the energy balance in AP simulations, an imaginary heat drain/source is added to make the energy balance as follows:

$$\Delta\dot{H}_{anode} + P_{electricity} + \dot{Q}_{heaters} = \dot{Q}_{drain/source} \qquad\qquad (11.5)$$

The energy balance is consequently always satisfied. An external regulation mechanism is then regulating the amount of heat required by the heaters by varying air flow, until heat to or from the heat drain/source is zero. This represents an air-cooled fuel cell, with the option of additional cooling (or heating, though unrealistic) streams other than the reactant streams if required.

12 Recuperator

The recuperator is already described in full in connection with both the thermochemical converter and the power cycle. Streams entering and exiting have however been divided between the two flowsheets, the complete recuperator with all streams is therefore reproduced for clearity. Direction of increasing temperature is from left to right for all streams.
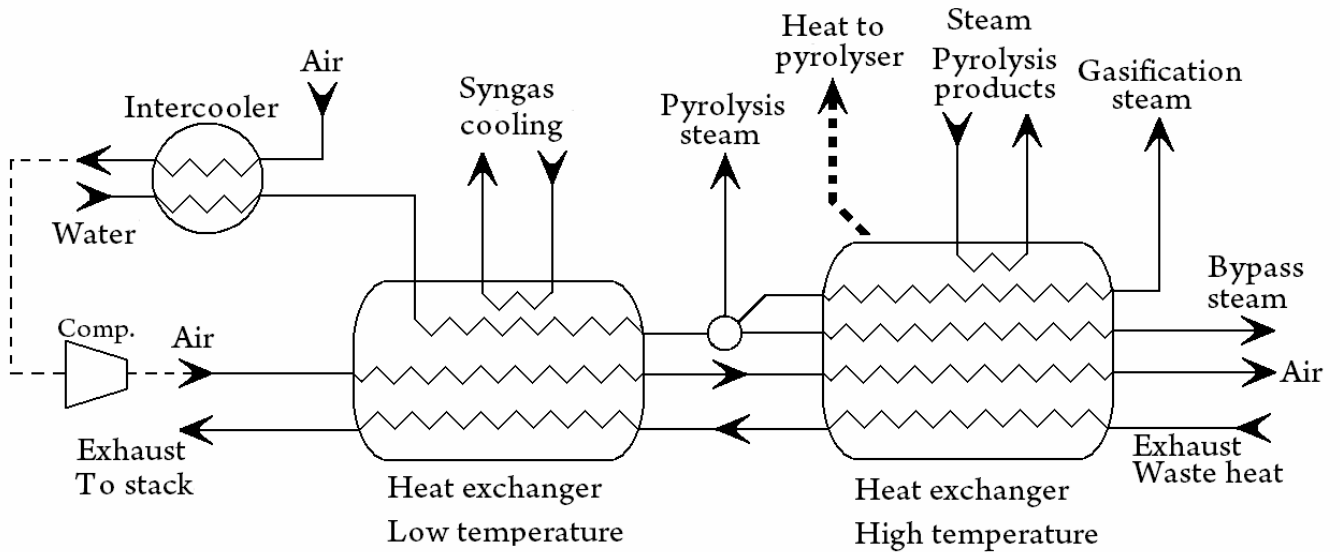
figure 12.1

13 Gas turbine power cycle simulation inputs

The integrated cycle of thermochemical converter and gas turbine cycle is simulated in AP. For reference, the gas turbine cycle is also integrated and simulated with the reference converter.

13.1 Input settings

The system is simulated with the following input settings

Inlet Streams				
Biomass	100 kg/h			
Steam	Optimized	Biomass moisture	7.4 %	
Air	Optimized	Exhaust temp. (to stack)	200 ºC	
Compressors		**Heat exchangers**		
Mech. eff.	0.95	LT pressure loss	0.1 bar hot side	
Isentropic eff.	0.90	LT heat loss	3% duty	
1.st stage pressure	Optimized	LT cold stream outlet temp.	550 ºC	
2.nd stage pressure	12 bar	HT pressure loss	0.1 bar hot side	
Turbine		HT heat loss	5% duty	
Mech. eff.	0.95	HT hot stream outlet temp.	580 ºC (minimum)	
Isentropic eff.	0.90	IC pressure loss	No pressure loss	
Outlet pressure	1.2 bar	IC heat loss	Adiabatic	
Turbine blade cooling air	12% inlet air	Syngas reheater	Adiabatic, no pressure loss	
El. generator eff.	0.97	IC/LT/HT min. pinch	30 K	
Pump outlet pressure	14 bar	Syngas reheater min. pinch	50 K	
Pyrolysis pressure loss	0 bar	Syngas cleaning press. loss	1 bar	
Gasifier press. loss	1 bar	Syngas cleaning temp.	400 ºC	
Tar cracker pressure loss	1 bar	Bed material flow rate	1000 kg/h	
Char combustor press. loss	1 bar	Inert carbon/residual char	10 % (biomass carbon)	
Gasifier inert methane	0.15 kmol/h	Tar cracker inert methane	0.25 kmol/h	

table 13.1

Mechanical efficiency for the compressors and turbine is comparatively low, reflecting the fact that the complete cycle represents a small-scale power plant; chemical energy-flow to the cycle in the form of biomass is 490 kW. Variables set as "optimized" in table 13.1 are values not given an explicit value. AP optimizes these values through an iterative algorithm to satisfy a criterion given by another input value.

Biomass has the same properties as specified in chapter 8. As the settings for the pyrolysis reactor is the same as in this chapter, pyrolysis results are equal too. Results from the complete converter in chapter 8 are not equal to simulation results for the integrated converter as steam feed temperature is a function of recuperator performance. The reactors of the converter and the gas cleaner are assumed to have pressure loss as given in table 13.1. Steam and biomass therefore enters the converter at 2 bar higher pressure than the power cycle pressure.

The low and high temperature heat exchangers (LT-HX/HT-HX) are arranged so that the temperature of the cold side stream exiting the LT-HX and entering the HT-HX is equal to the pyrolysis temperature. Heat loss is 3% and 5% of hot stream duty (including losses) for the LT-HX and HT-HX respectively, reflecting higher losses at high temperature.

The exhaust temperature is limited downwards to 200 ºC. This is well above dew-point at ambient pressure, and the exhaust gas could in this regard safely be cooled further. The exact temperature is still less important than the fact that all simulations are subjected to the same limitations and requirements, and 200 ºC is chosen to represent actual restrictions on exhaust temperature with a good margin.

13.2 Regulation mechanisms

AP provides iterative algorithms termed design specs which vary and calculate the value of one variable to achieve a preset value of another dependent variable. In the current simulation, four such algorithms are used to control the operation of the integrated cycle. These are:

1. Combustor Temperature/Turbine inlet temperature (TIT)

TIT is regulated to the preset value by varying airflow to the cycle. TIT tolerance (end of iteration) is 1 K.

2. Exhaust temperature (to stack)

Exhaust temperature is regulated by varying the outlet pressure, and consequently outlet temperature, of the first stage compressor. The temperature of the compressed air determines intercooler duty, and hence the temperature of the water entering the first heat exchanger. Exhaust temperature tolerance is 1 K.

3. Heat exchanger pinch point temperature difference.

Two iterative algorithms control and optimize the temperature difference at the pinch points so that it is equal to the minimum pinch temperature. The variables are steam feed and air preheating temperature. Tolerance is 0.5 K.

13.3 Reference cycle

The reference system is simulated with the additional inputs:

Gasifier temperature	850 ºC
Gasifier pressure loss	1 bar

table 13.2

Units present in both the proposed converter system and the reference converter have equal input settings. Due to the use of air in the gasifier, an additional compression step has to be added to increase the pressure from gas turbine cycle pressure (outlet pressure of the second stage compressor) to converter pressure. Settings for this compressor are equal to the main compressors. An iterative algorithm is used to vary the airstream to the gasifier to achieve the preset temperature. As with the proposed system, TIT, exhaust temperature, and pinch point temperature difference are regulated by such mechanism.

14 Gas turbine cycle simulation results

The integrated converter and gas turbine cycle as defined in chapter 10, is simulated in AP with the input settings of chapter 13. A reference system is simulated in the same manner for result comparison. The reference system and its input settings are defined in chapter 9 and 13.

Complete result flowsheets with temperature, pressure, and exergy and energy flow are given for the converter and gas turbine cycle in appendix 3.1 and 3.2 respectively. Corresponding flowsheets for the reference system are given in appendix 3.3 and 3.4.

14.1 Converter results

The results of simulation of the integrated converter are given table 14.1, with comparable results from the reference system.

Results	Proposed system	Reference system
Cold gas efficiency	105.7%	91.9%
Syngas HHV (wet/dry)	8.6/14.8 MJ/kg	5.9/9.3 MJ/kg
Char gasification temp	841 °C	850 °C
Tar cracking temp	893 °C	
Char combustion temp	927 °C	939 °C
Chem. energy combustion	-152 MJ/h	-152 MJ/h
Converter Δ HHV	101 MJ/h	-143 MJ/h
Converter Δ LHV	8 MJ	-210 MJ/h
Gasifier Δ LHV	82 MJ/h	-58 MJ/h
Tar cracker Δ LHV	32 MJ/h	
Steamflow (SC-ratio)	121.4 kg/h (2.44)	121.4 kg/h (2.44)
Syngas-flow	217 kg/h	275 kg/h
Syngas water content % feed / wt. % syngas	74.5% / 41.7%	83.3% / 36.7%

table 14.1

Cold gas efficiency is slightly lower than for the stand-alone simulation of the converter, despite higher reactor temperatures (gasifier and tar converter). This is apparent by decreased tar cracker change in LHV (58 MJ/h for stand-alone simulation), and caused by the introduction of inert methane in the equilibrium calculations. As a fraction of methane, or carbon and hydrogen more specifically, is not participating in equilibrium calculations, less extensive reforming reactions are occurring, and chemical recuperation is decreased.

Equal amounts of water are supplied to both the proposed and the reference converters for the purpose of result comparison. This amount is not equal to the total amount that is fed to the system, as additional water (steam) can be directed to the power cycle through a bypass stream.

The performance of the proposed converter is significantly higher than the reference converter, which has below unity cold gas efficiency and a negative value for net chemical recuperation. The values for change in converter HHV and LHV are including the combustion of residual char, the actual recuperation in the reactors is thus calculated by subtracting the chemical energy of the residual char. Syngas water content, as percentage of water fed to the converter, is higher for the reference converter, suggesting partial oxidation reduces chemical recuperation. Water in the reference cycle syngas is however also a product of partial oxidation. Even though syngas from the proposed converter contains less water, it is wetter (higher relative steam content) than the reference cycle syngas which contain nitrogen and additional CO_2 from partial combustion.

Clearly, the proposed conversion system is superior to the reference system, regarding its ability to conserve biomass chemical energy and perform chemical recuperation. As a direct consequence, and as will be discussed further in the recuperation section, the proposed system places a heavier load on the recuperator, decreasing other types of recuperation.

14.2 Power cycle result

Results for the power cycle are given in table 14.2

Results	Proposed system	Reference system
Thermal efficiency (% fuel HHV)	41.8%	40.7%
(% fuel LHV)	44.6%	43.4%
Electric output	737 MJ/h	720 MJ/h
Turbine / Compressor duty	1311 / 551 MJ/h	1241 / 501 MJ/h
Turbine vol. flow @ outlet	4810 m^3/h	4547 m^3/h
Exhaust vol.flow	2575 m^3/h	2427 m^3/h
Steamflow	152.72 kg/h	171.8 kg/h
Airflow	1559 kg/h	1420 kg/h
Specific work (electricity)	431 kJ/kg air+water	453 kJ/kg air+water

table 14.2

Given the comparatively large differences in converter performance, the performance of the proposed system is not a significant improvement on the reference system. Furthermore, mass and volumetric flow rate are larger for the proposed system, resulting in lower specific work, on an air- and water flow basis, than for the reference system.

Electricity required by the water pumps are neglible, and not included in the calculation of the performance.

14.3 Recuperator results

The recuperation configurations for the two systems differs in the way the recuperate energy. In figure 14.1, heating curves for the recuperators of both systems are presented. The intercooler is in this figure and later discussions not regarded as a part of the recuperator.
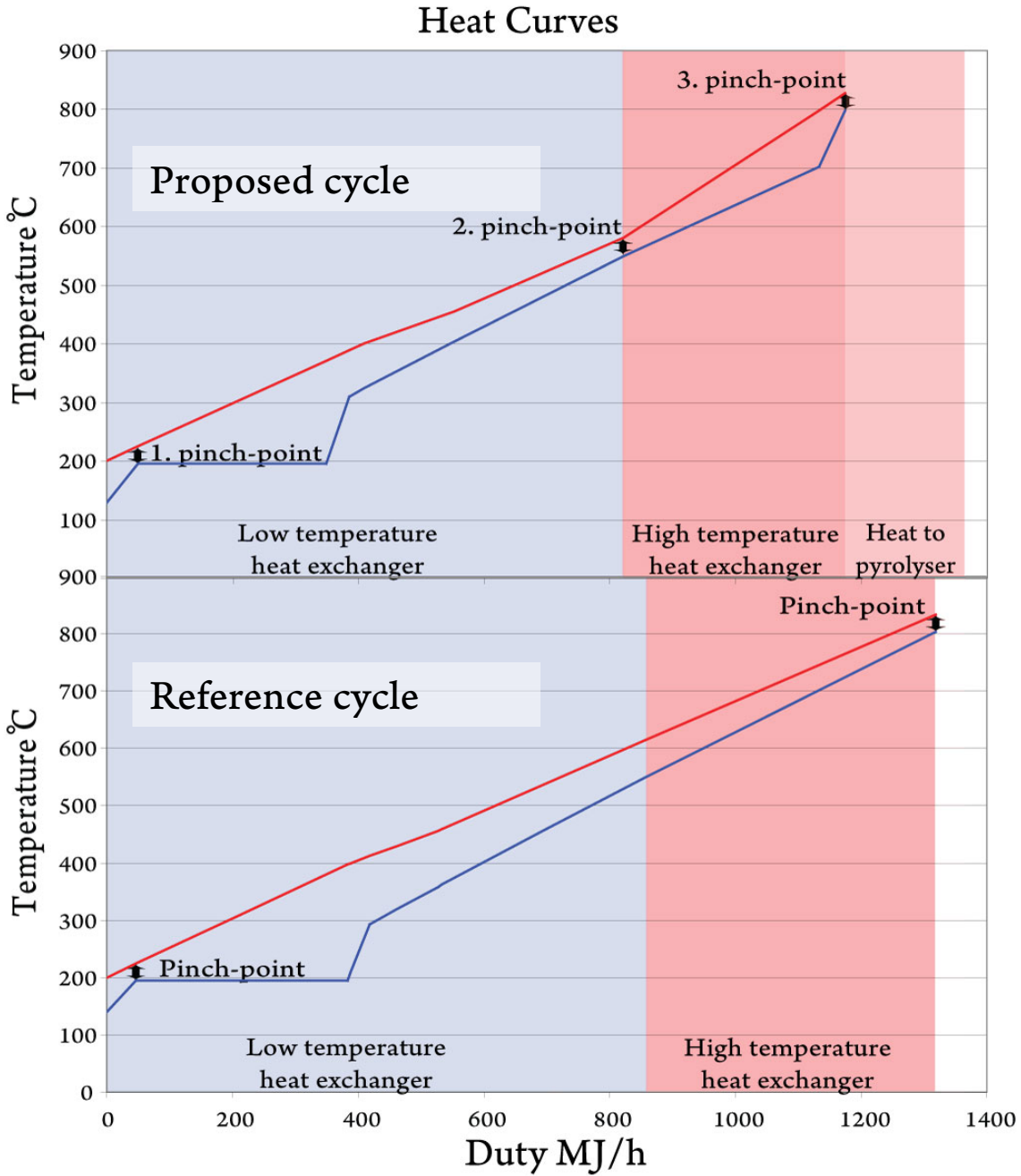

figure 14.1

Duties and heat curves are on cold side basis, e.g. not included heat loss or heat to pyrolyser. The hot side is made up of the exhaust stream, except between approximately 400 and 500 MJ/h where syngas cooling is also contributing. The cold side is a composite of air, water/steam, and syngas streams. The heat exchanger in which the heat transfer occurs is given by the transparent background colour, and the length on the x-axis of these blocks is proportional to the respective heat exchanger duty. For the proposed cycle a block is added for convection heat to the pyrolyser for correct representation of total recuperation duty.

The recuperator of the proposed system has three highlighted pinch points; at the water saturation point, between the two heat exchangers, and at the end of the high temperature heat exchanger. The change of slope of the hot side at the second pinch point is a result of convection heat to the pyrolyser. Heat is in the high temperature heat exchanger transferred to the pyrolyser, reducing its capacity to transfer heat to the cold stream per degree of cooling. The sharp change of slope of the cold side close to the hot end of the high temperature heat exchanger is the exit of the air stream.

The term pinch point is here a (spatial) point in the heat exchanger, or collection of heat exchangers, where the difference between the hot and cold stream is a global or local minima. These minimas may be made to approach a defined minimum temperature difference by optimizing the operating conditions of the heat exchanger(s).

By definition, all heat exchangers have at least one pinch point (with the hypothetical exception of equal temperature difference across the whole heat exchanger) and single-phase counter-current heat exchangers seldom have more than one. Additional pinch points may arise when the relationship between the temperature/heat slope (analogues and often equal to heat capacity) of the two sides is changed inside the heat exchanger (or collection of heat exchangers), by for example phase-change or addition or exit of streams.

The optimization of the pinch point temperature difference to a defined minimum is restricted by the variables available for manipulation. For a given number of manipulable variables, two or more pinch points may not approach their defined minimum simultaneously as they are dependent on the same variable.

For the proposed system, minimum pinch point temperature difference is approached at the highlighted points by controlling water flow, air preheating temperature, and steam preheating temperature. The first pinch point is highly dependent of water flow and only slightly dependent on air preheating temperature. This dependence is reversed for the second pinch point, while the third pinch point is dependent on steam preheating temperature only. The problem of approaching the defined minimum for the three points simultaneously could be described and solved mathematically with an equation-set with three unknowns, the problem is however solved with iteration in AP, resulting in the values for steam flow and air and steam preheating temperatures of table 14.3

Without convection heat to the pyrolyser, the reference system recuperator is lacking the second pinch point. Minimum pinch point temperature difference is approach by varying water flow and a common steam/air preheating temperature. The problem is solved in the same manner as the proposed system. The values are then the optimized values for water flow and steam/air preheating temperature in the two recuperators.

|	Proposed system	Reference system
Air preheat temp	701 °C	803 °C
Steam preheat temp	798 ℃	803 ℃
Net duty	1370 MJ/h	1319 MJ/h
Preheating	875 MJ/h	981 MJ/h
Pyrolysis heat	195 MJ/h	0 MJ/h
Recuperator heat recup.	1070 MJ/h	981 MJ/h
Recuperator steam recup.	300 MJ/h	338 MJ/h

table 14.3

Steam preheating temperatures are approximately equal. There is however a large difference in air preheating temperature, and as can be seen in figure 1 air preheating is terminated before the end of the heat exchanger in the proposed cycle. Alternatively, steam and air could be preheated to the same temperature, slightly higher than the current air preheating temperature. However, by using steam preheating temperature to approach the defined minimum temperature difference in the third pinch point, a design choice is made to maximize the steam preheating temperature, at the cost of slightly lower air preheating temperature, in turn maximizing reactor temperatures in the converter.

The duties of table 14.3 can be read directly from figure 14.1; steam generation is equal to the length of the cold side phase-change line, preheating is then found by difference. It is important to distinguish between the way energy is transferred in the recuperator and the distribution between the different recuperation methods for the complete cycle, as the actual chemical recuperation is taking place outside the reformer and consumes energy provided by heat and steam generated in the recuperator.

The duty of the recuperator differs little between the converter systems, there are however a slight shift toward heat recuperation for the proposed system. This is not a direct consequence of the extended energy transfer to the converter. The shift are indirectly caused by the heat load of pyrolysis convection heat transfer, making the heat capacity of the hot side smaller than the cold side in the high temperature heat exchanger. This makes for a better match with the cold side, compared to the diverging heat curves of the reference system, and less water is required for recuperation at the cold end of the low temperature heat exchanger. The shift is thus a matter of adapting to changes in heat exchanger conditions, and explains the increased mass flow and decreased specific work output (on an air and steam basis) of the proposed cycle, both inherent effects and drawbacks of heat recuperation.

The calculation of the distribution between the different recuperation methods in the entire cycle is more complex. Chemical recuperation is in this paper calculated as the difference in LHV between reactant and product streams (as the actual reactions are not detailed), and corresponds to the heat received by a reaction where liquid water is not a part of either product or reactant. Chemical recuperation in the converter must therefore be subtracted from the heat generated in the recuperator to calculate the correct amount of heat recuperation. A corresponding definition for chemical recuperation defined as change in HHV would include the heat received, as with the ΔLHV definition, plus the vaporization energy of steam consumed in the reaction.

Note that the value for chemical recuperation used in the calculation is not equal to the difference in LHV between biomass and syngas, as the combustion of residual char decreases the net effect of chemical recuperation in the converter. Correct chemical recuperation is found as the sum of chemical recuperation in the pyrolyser, tar cracker, and gasifier. The calculation is represented graphically in figure 14.2. Results where the HHV-definition is used for chemical recuperation are given in grey.
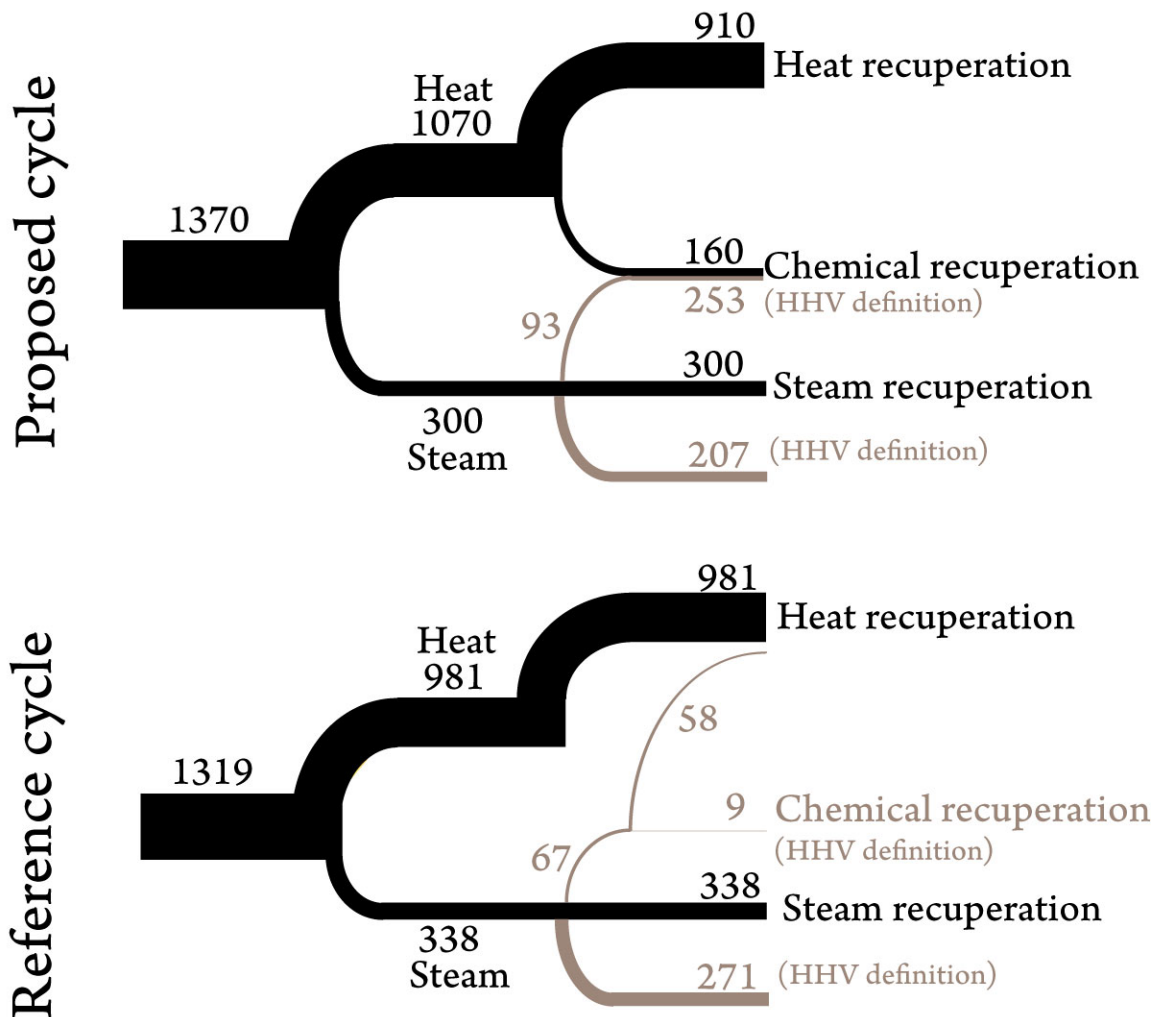
figure 14.2

All values are MJ/h

This stricter definition of recuperation corresponds to the recuperation "seen" from the power cycle. Heat and chemical recuperation is the increase in temperature and LHV respectively of the streams entering the power cycle, compared to a theoretical condition without recuperation. Steam recuperation is equal to the potential work accompanying the steam mass-flow. Steam consumed by reactions reappears as steam after combustion, making the form in which it entered the power cycle irrelevant for mass-flow.

From this point of view, heat recuperation is used to provide chemical recuperation in the proposed cycle, while there is no net chemical recuperation in the reference cycle (negative change in LHV). Alternatively, using the HHV definition for recuperation, steam recuperation is also used to provide chemical recuperation in the proposed cycle. In the reference cycle, chemical recuperation with the HHV definition is less than the vaporization energy in the consumed steam, and hence there is a net release of heat represented by the grey line from chemical recuperation to heat recuperation. This transfer of energy is however not considered recuperation, but combustion, although the effect is equal.

14.4 Exergy analysis

Complete exergy flow is presented in the flowsheets of appendix 3. See appendix 1 for further details on exergy calculations. In figure 14.3, exergy losses are organized in categories. "External" is the exergy lost in the discharge of the exhaust stream, "mech" is losses in mechanical manipulators like turbine and compressors, "HX" is exergy losses in all heat-exchange units including the recuperator, intercooler, and syngas reheater. "Combustion" is exergy losses in both the gas turbine and residual char combustor, "conversion" is the sum of exergy losses in the reactors of the converters, excluding the residual char combustor. Finally, "choke/mix" is the sum of exergy losses associated with throttling and mixing of streams.
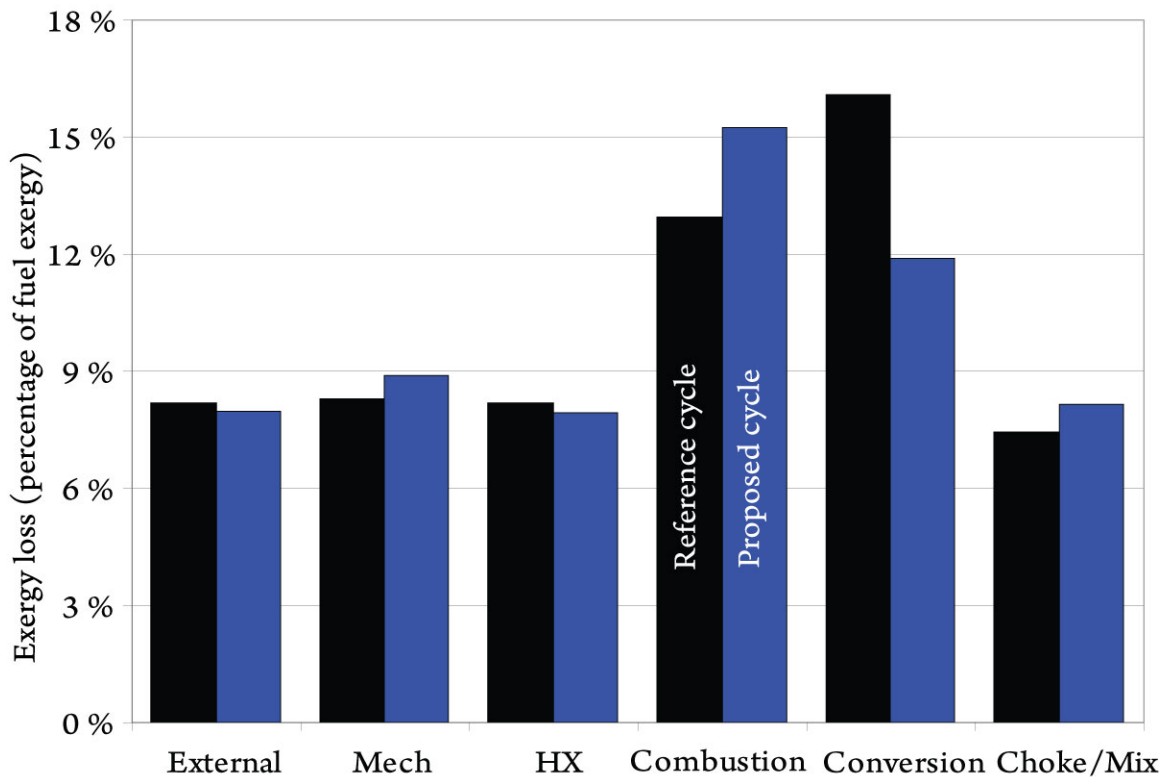
figure 14.3

With the exception of combustion and conversion exergy loss, there are small differences in exergy losses. The reference cycle has slightly higher losses in the external and HX category. This is an effect of higher water flow; steam has higher exergy than air at a given temperature and exergy losses associated with heat exchange is higher for single phase/phase change heat transfer than for single phase/single phase heat transfer. Conversely, the proposed cycle has higher losses in the mech and choke/mix category, because of higher air and mass flow. The significant differences in exergy losses are however in the combustion and conversion categories, the sum which are 27.1% and 29.0% for the proposed and reference cycle respectively. As expected, the proposed converter has far less exergy losses than the reference converter. This advantage is

however countered to a far extent by high exergy losses in combustion for the proposed cycle.

Exergy losses (% fuel exergy)	Proposed cycle	Reference cycle	Diff.
Converter loss	14.3%	18.6%	-4.3
Recuperation loss	7.8%	7.9%	-0.1
Power cycle loss	38.9%	35.4%	+3.5
Total	61.0%	61.9%	-0.9

table 14.4

In table 14.4, losses are further categorized into the three principle constituents of the integrated cycle. As suggested by table 4 there are small overall differences in exergy losses; differences in one category are countered by differences in another. The sum of exergy losses is in accordance with the difference in thermal efficiency for the cycles, both suggesting marginally higher efficiency for the proposed cycle. Total exergy loss summed with the thermal efficiency of the cycle is not 100% as exergy losses are in relation to biomass exergy, while thermal efficiency is in relation to biomass energy. Exergy efficiencies of the cycles are 39.0% and 38.1% for the proposed and reference cycle respectively.

14.5 Sensitivity

Sensitivity is calculated for the following variables; turbine inlet pressure (TPR), turbine inlet temperature (TIT), residual char (inert carbon), and pinch point temperature difference. Sensitivity to TPR is given in figure 14.4 and 14.5, with efficiency and reactor (converter reactors) temperatures respectively. The given TPR is the pressure at the gas
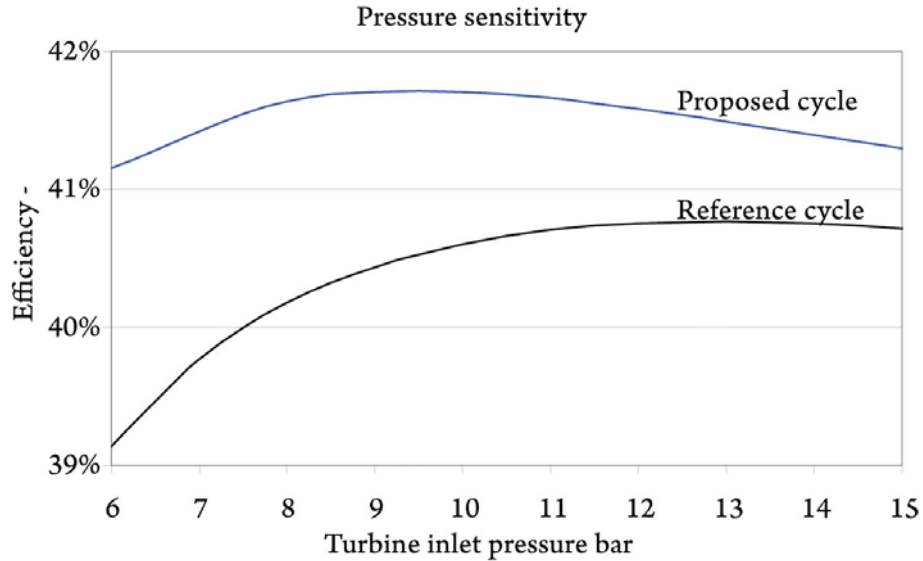

figure 14.4

turbine inlet; converter pressure is at 2 bars above the gas turbine inlet pressure at the inlet of the converter and decreases toward gas turbine inlet pressure through the converter. Optimal TPR for the proposed cycle is between 9 and 10 bar, the efficiency is however comparatively stabile over a wide range of pressures. The mechanisms responsible for the peak in efficiency around 9 bar are complex and not thoroughly investigated. On general basis, low TPR improves heat recuperation (higher turbine inlet temperature and less steam recuperation is required) which in turn increases mass flow. The former has positive effect on efficiency, while the latter has negative effect, depending on the operating conditions of the cycle the net result will be either positive or negative. For the power cycle integrated with the converter, additional complexities are added considering the increase in reactor temperatures as TPR is decreased and heat recuperation is improved. However, at peak efficiency only
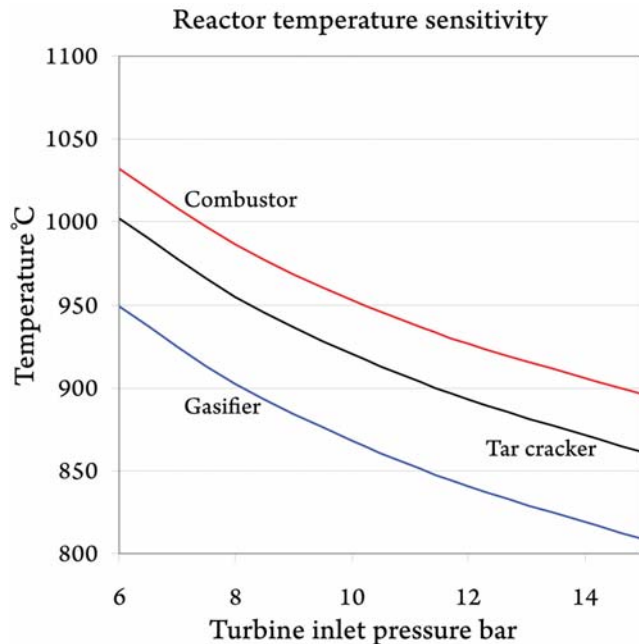

figure 14.5

modest temperature increases are experienced in the converter, making this an unlikely primary contributor to the peak in cycle efficiency. As can be seen in figure 14.4, converter operation is feasible in a wide range of TPRs, up to at least TPR 15.
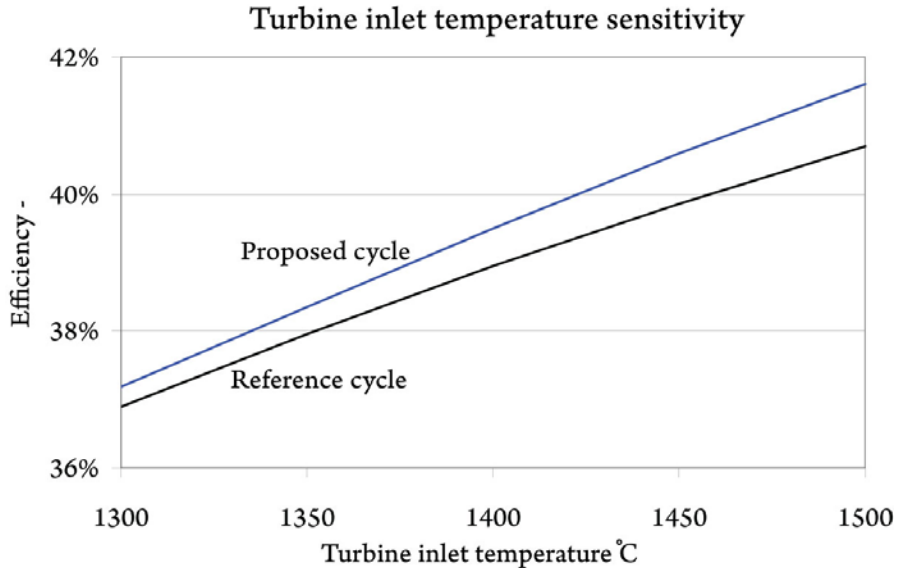
figure 14.6

In figure 14.6 and 14.7, sensitivities for changes in TIT are given. TIT is an indirectly controlled parameter, by regulation of air flow. In accordance with basic thermodynamic principles, efficiency increases with increasing TIT. Compared to the sensitivity to TPR, TIT sensitivity is large. At the in practice more common TIT of 1300 ºC, efficiency is down to 37.2% for the proposed cycle, compared to 41.8% at the simulation TIT of 1500 ºC.

Low TIT may also be problematic for reactor temperatures, although not critical in itself. Combined with other changes in operating conditions decreasing reactor temperatures however, critical temperatures may be approached.

Figure 14.8 and 14.9 show sensitivities to the amount of residual carbon that is combusted in the converter. This amount is equal to the amount of carbon set as inert in the gasifier (chapter 5). In the sensitivity analysis of the stand-alone converter, cold gas efficiency had a non-linear response to variations in inert char caused by a

figure 14.7

54
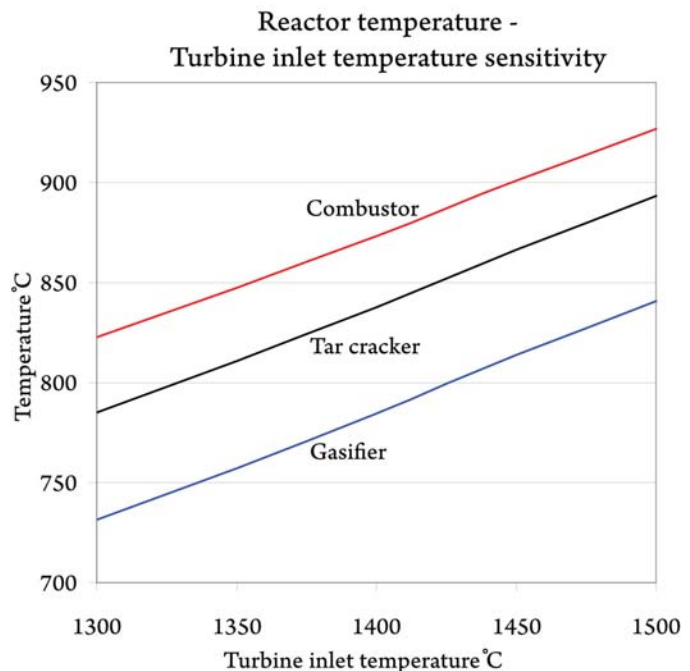
secondary effect of variations in chemical recuperation. Contrary to this, the integrated cycle's efficiency is close to linear, suggesting that heat production in the converters as char is combusted is utilized by the power cycle, countering the negative effect of decreased chemical recuperation. The decrease in flow of chemical energy to the power cycle is however not completely countered by increased heat flow; efficiency is decreasing with increasing amounts of residual char.
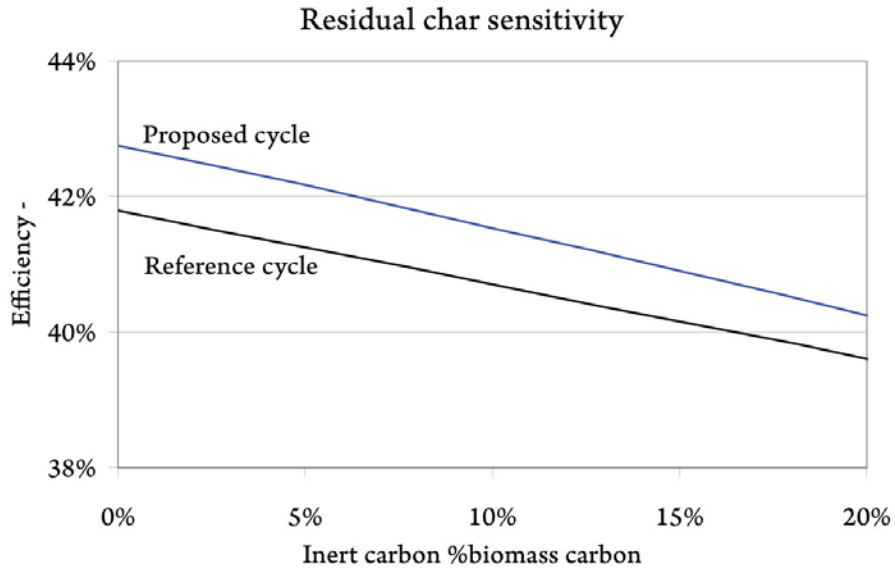
figure 14.8

Naturally, reactor temperatures are very sensitive to changes in residual char. At least 5% of biomass carbon must be combusted to achieve 700 ºC or more in all reactors. While the amount of residual carbon is not purely a design choice, but subject to limits in char chemistry and feasible converter size and conversion time, combusting more char than strictly necessary might be required if the possible char conversion ratio is very high (highly active char etc.), or if other variables are changed which decrease reactor temperatures (TIT etc.).

Finally, the sensitivity of pinch point temperature difference is calculated in figure 14.10. Graphs show efficiency and pinch point temperature
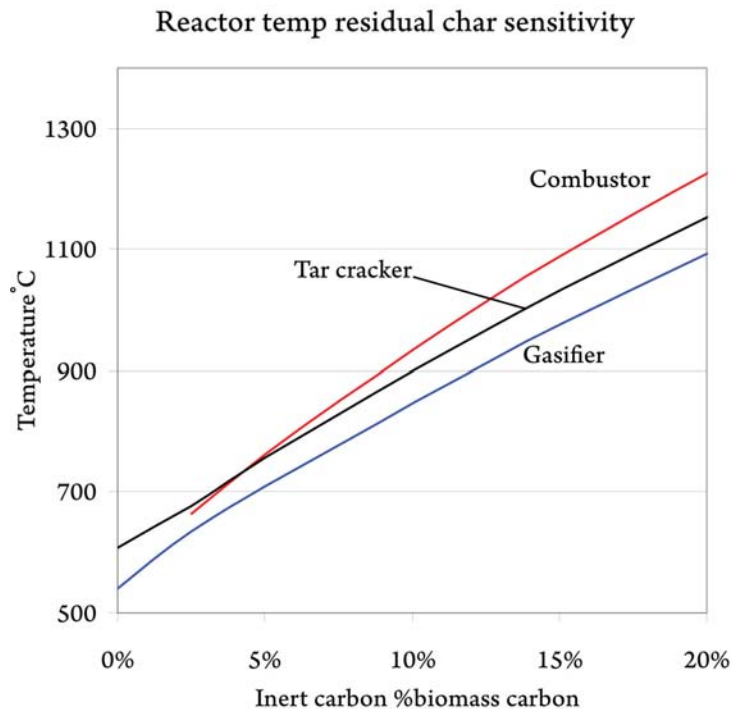
figure 14.9

difference as a function of water flow for the first pinch point (see figure 14.1), and air preheating temperature for the second pinch point. Effects of air preheating temperature on the first pinch point, and vice versa, is very small and not given in figure 14.10. The minimum temperature difference, 30 K, is represented by horizontal lines. The intersection of this line by the temperature difference line fixes the optimized value and corresponding efficiency. As the sensitivity in both graphs are large is evident that pinch point temperature difference, and hence recuperation, plays a significant role in achieving high cycle efficiency.

Pinch point temperature difference sensitivity
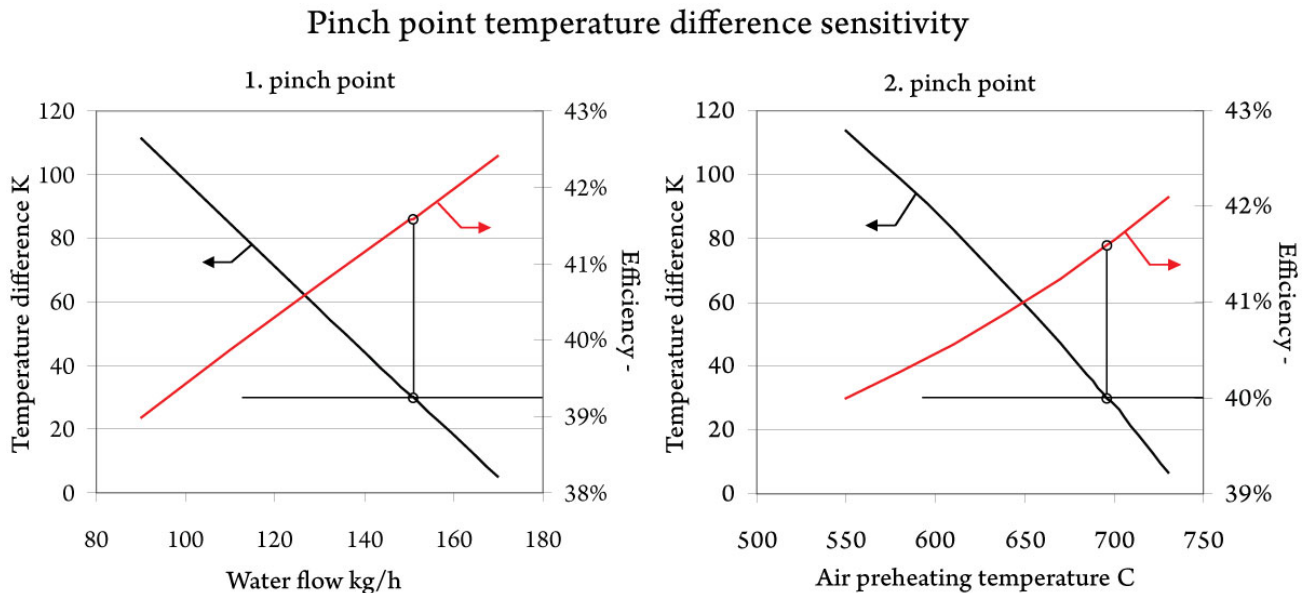
figure 14.10

To sum up, the cycle responds as thermodynamically expected to the changes in operating conditions, and with no abrupt change in cycle efficiency. The cumulative effect of change of several variables, each reducing converter reactor temperatures, might lead to too low converter reactor temperatures for feasible converter operation.

14.6 Conclusions on gas turbine cycle

Despite superior performance, the proposed converter fails to significantly increase thermal efficiency when integrated with a gas turbine cycle, compared to the simpler reference converter. Small changes in operating conditions are enough to produce differences in efficiency of the same order of magnitude. Furthermore, the proposed cycle is not offering any practical advantages in unit sizing etc. as mass flow is increased compared to the reference cycle

The reason for this is found in the principal gas turbine cycle, which essentially is a heat engine, dealing exclusively in heat energy. Chemical energy supplied to the gas turbine cycle is converted to heat energy in the combustor, making the form in which energy enters the cycle less significant. The advantage of the proposed converter is its ability to conserve and increase the chemical energy of the biomass, its net energy efficiency (all

forms of energy) is however equal to that of the reference converter. Consequently, the gas turbine cycle is unable to properly utilize the advantages of the proposed converter..

The marginal difference in efficiencies between the cycles can be said to have a primary and secondary cause. The secondary cause is the difference in the recuperator configurations of the cycles; optimum recuperation is achieved with less water flow for the proposed cycle, airflow is however higher. Steam recuperation, following water flow, is from an ideal point of view associated with more losses than heat recuperation, as the energy used for vaporizing water is not recoupable when water is leaving the cycle in the form of steam (no condensation is occurring in the cycle). As the cycle in question is not ideal, the increased airflow following heat recuperation is also associated with losses, making an optimum recuperation configuration more of a compromise. These considerations can be extended to the exergy analysis; steam recuperation increases recuperation exergy losses, while the increase in airflow following heat recuperation increases flow-related exergy losses. As seen in figure 14.3, exergy losses associated with steam and heat recuperation are largely counteracting each other, making the secondary cause a small contributor to overall cycle efficiency.

The primary cause is associated with irreversibilities or exergy losses in conversion from chemical to heat energy. These losses depend on the temperature of the conversion process, i.e. combustion temperature. Losses increase as the temperature decreases, and at all temperatures in the cycle the losses are substantial. The proposed converter allows for more of the chemical energy to be converted to heat at high temperature (combustion temperature 1500 ºC), as opposed to conversion at comparatively low temperature (converter temperature ~850 ºC) through partial oxidation. This is confirmed by the combustion and conversion exergy losses of figure 14.3. Both theses categories are essentially exergy losses from conversion of chemical energy to heat energy. The proposed converter shifts this process from the converter to the combustor, resulting in a net decrease in exergy loss responsible for the marginally better thermal efficiency of the proposed cycle.

15 Combined fuel cell / gas turbine cycle simulations inputs

The integrated cycle of thermochemical converter combined fuel cell /gas turbine cycle is simulated in AP. For reference, the gas turbine cycle is also integrated and simulated with the reference converter

15.1 Input settings

The system is simulated with the following input settings

Inlet Streams				
Biomass	100 kg/h			
Steam	Optimized	Biomass moisture	7.3 %	
Air	Optimized	Exhaust temp. (to stack)	200 ºC	
Compressors		**Heat exchangers**		
Mech. eff.	0.95	LT pressure loss	0.1 bar hot side	
Isentropic eff.	0.90	LT heat loss	3% duty	
1.st stage pressure	Optimized	LT cold stream outlet temp.	550 ºC	
2.nd stage pressure	12 bar	HT pressure loss	0.2 bar hot side	
Turbine		HT heat loss	5% duty	
Mech. eff.	0.95	HT hot stream outlet temp.	580 ºC (minimum)	
Isentropic eff.	0.90	IC pressure loss	No pressure loss	
Outlet pressure	1.2 bar	IC heat loss	Adiabatic	
Turbine blade cooling air	12% inlet air	Syngas reheater	Adiabatic, no pressure loss	
El. generator eff.	0.97	IC/LT/HT min. pinch	30 K	
Pump outlet pressure	14 bar	Syngas reheater min. pinch	50 K	
Pyrolysis pressure loss	0 bar	Syngas cleaning press. loss	1 bar	
Gasifier press. loss	1 bar	Syngas cleaning temp.	400 ºC	
Tar cracker pressure loss	1 bar	Bed material flow rate	1000 kg/h	
Char combustor press. loss	1 bar	Inert carbon/residual char	10 % (biomass carbon)	
Gasifier inert methane	0.15 kmol/h	Tar cracker inert methane	0.25 kmol/h	
Fuel cell				
Operating temperature	1000 ºC	Fuel utilization ratio	0.65	
Operating pressure	12 bar	Voltage loss	256 mV	

table 15.1

The fuel cell is assumed adiabatic and with no pressure loss. Voltage loss is the sum of resistive, activation, and overpotential losses taken from the simulation of Kuchonthara [100]. Input settings not directly associated with the fuel cell is equivalent to the input settings for the gas turbine cycle simulation (see chapter 13), with the exception of combustor temperature, or TIT, which is no longer a controlled variable, however limited to 1500 ºC.

15.2 Regulation mechanisms

Iterative algorithms are used to regulate four variables. The variables are regulated to preset values by varying other input variables

1. Fuel cell operating temperature

As detailed in chapter 11, the fuel cell is temperature controlled by varying airflow through it. This regulation mechanism replaces the TIT regulation of the gas turbine cycle simulation. Tolerance is 2 K

2. Exhaust temperature (to stack)

Exhaust temperature is regulated by varying the outlet pressure, and consequently outlet temperature, of the first stage compressor. The temperature of the compressed air determines intercooler duty, and hence the temperature of the water entering the first heat exchanger. Exhaust temperature tolerance is 1 K.

3&4. Heat exchanger pinch temperature difference

Two iterative algorithms control and optimize the temperature difference at the pinch points so that it is equal to the minimum pinch temperature. The variables are steam feed and air preheating temperature. Tolerance is 0.5 K.

15.3 Reference cycle

The reference system is simulated with the additional or changed inputs:

Gasifier temperature	850 ºC
Gasifier pressure loss	1 bar
Fuel cell – fuel cell utilization ratio	0.5

table 15.2

Units present in both the proposed converter system and the reference converter have equal input settings. Due to the use of air in the gasifier, an additional compression step has to be added to increase the pressure from gas turbine cycle pressure (outlet pressure of the second stage compressor) to converter pressure. Settings for this compressor are equal to the main compressors. An iterative algorithm is used to vary the airstream to the gasifier to achieve the preset temperature. As with the proposed system, TIT, exhaust temperature, and pinch point temperature difference are also regulated by such mechanism.

16 Combined fuel cell / gas turbine cycle simulation results

The integrated converter and combined fuel cell / gas turbine cycle, as defined in chapter 11, is simulated in AP with the input settings of chapter 15. A reference cycle is simulated in the same manner for result comparison. The reference cycle and its input settings are defined in chapter 9 and 15.

This chapter is paralleling the presentation of the gas turbine cycle simulation results of chapter 14. A more thorough explanation of central concepts in analysis of the cycle can be found there.

16.1 Converter results

Results for the integrated converters are given in table 16.1.

Results	Proposed converter	Reference converter
Cold gas efficicency	105.7%	91.5%
Syngas HHV (wet/dry)	8.9/14.7 MJ/h	5.8/9.8 MJ/h
Char gasification temp	791 ºC	850 ºC
Tar cracking temp	843 ºC	
Char combustion temp	877 ºC	938 ºC
Chem. energy combustion	-152 MJ/h	-152 MJ/h
Converter Δ HHV	101 MJ/h	-150 MJ/h
Converter Δ LHV	6 MJ/h	-217 MJ/h
Gasifier Δ LHV	82 MJ/h	-65 MJ/h
Tar cracker Δ LHV	32 MJ/h	
Steamflow (SC-ratio)	114.7 kg/h (2.34)	121.4 kg/h (2.44)
Syngas-flow	210 kg/h	277 kg/h
Syngas water content % feed / wt. % syngas	72.3%/39.5%	83.6%/36.6

table 16.1

Results are in qualitative agreement with the results from the gas turbine cycle simulations and stand-alone converter simulations. To aid comparison of the result from different simulations, steam flow to the converters is fixed at 121.4 kg/h for all simulations, additional steam needed for optimum recuperation in the cycles are sent directly to the power cycle through a bypass stream. The proposed cycle of the current simulation however, uses less than 121.4 kg/h steam for optimum recuperation, and an exception is made as additional steam feed would deteriorate performance.

Compared to the gas turbine cycle simulation, reactor temperatures are decreased for the proposed cycle, caused by a reduction in steam feed temperature to the reactors. Despite this and lower steam flow, performance is approximately equal to that of the gas turbine cycle simulation. According to the results of the stand-alone converter simulation, decreases in both steam flow and reactor temperature should result in a decrease in cold gas efficiency. Why this is not the result in the present simulation is not completely understood, the setting of a fraction of methane as inert (departure from equilibrium), which is not the case in the stand-alone simulation, might however a have limiting effect on the sensitivity to steam and reactor temperatures at certain operating conditions.

Even though the reactor temperature is kept constant in the reference converter, there is a slight decrease in performance compared to the results from the gas turbine cycle simulation. This is caused by decreased steam and air temperatures to the converter, requiring increased partial combustion to maintain reactor temperature.

16.2 Power cycle results

Results for the power cycle are given in table 16.2

Results	Proposed cycle	Reference cycle
Thermal efficiency (% fuel HHV)	56.0 %	51.2 %
(% fuel LHV)	59.8 %	54.6 %
Electric output	988 MJ/h	903 MJ/h
Turbine / Compressor mech. duty	870/378 MJ/h	946/381 MJ/h
Turbine inlet temperature	1395 ºC	1460 ºC
Fuel cell electric output	511 MJ/h	353 MJ/h
Fuel cell fraction of output	51.7 %	39.1 %
Fuel cell efficiency ($W_{el}/Q+ W_{el}$)	47.6 %	52.1 %
Oxygen utilization ratio	34.6 %	24.7 %
Turbine vol. flow @ outlet	3202 m^3/h	3471 m^3/h
Exhaust vol. flow	1828 m^3/h	1898 m^3/h
Steamflow	114.7 kg/h	141.6 kg/h
Airflow	1072 kg/h	1081 kg/h
Specific work (electricity)	833 kJ/kg air+water	739 kJ/kg air+water

table 16.2

Performance of the proposed cycle is significantly better than the reference system, both in absolute values and relative to its mass flow, and consequently size. As would be expected of a combined fuel cell /gas turbine cycle, the results are also a significant improvement on the gas turbine cycle, for both converters.

An apparent difference between the cycles is the fuel cell fraction of output. As detailed in chapter 15, fuel utilization ratio is an input variable set to 0.65 and 0.5 for the proposed

and the reference cycle respectively, and in this respect the fraction of output power supplied by the fuel cell is not an inherent quality of the respective cycles. The fuel utilization ratios used are however optimized values, found by preliminary simulations, suggesting that extended loading of the fuel cell *is* a quality of the proposed cycle.

Fuel cell efficiency is the electric output of the fuel cell divided by the chemical energy consumed by the fuel cell (as opposed to through-flow of chemical energy). This value is closely connected to the fuel and air utilization ratios; the more fuel and oxidant consumed by the fuel cell, the lower the partial pressure of these components at the exit of the cell, and the lower the voltage. As the fuel cell electrodes are modeled as equipotential plates, fuel cell voltage will be equal to the lowest voltage along (flow axis) the cell, e.g. the voltage at the exit of the cell. Consequently, fuel cell efficiency decreases as increasing fractions of fuel and oxidizer are consumed.

At the extremities, at no or full utilization of fuel and oxidizer, the electrical output of the fuel cell is zero; at no utilization because no chemical energy is consumed, at full utilization because the efficiency is zero. In both cases the fuel will be completely converted to heat in either the fuel cell or in a downstream combustor. In the former case, conversion temperature will be restricted by the fuel cell operating temperature, in the latter case by restrictions on TIT. Under normal circumstances, and certainly in this simulation, maximum TIT is higher than fuel cell operating temperature and the downstream combustor is thus the preferable place for conversion of chemical energy to heat energy. Optimal fuel utilization ratio is consequently at the value where the advantageous effect of converting a given fraction (equal to fuel cell efficiency) of chemical energy directly to electricity is exactly opposed by the deteriorating effect of converting the reminder of the chemical energy to heat at low temperature (fuel cell operating temperature).

The power cycle of the proposed cycle receives 2914 MJ/h of which 57.0% is chemical energy (LHV), corresponding values for the reference cycle are 3027 MJ/h of which 47.5% is chemical energy. The reference cycle consequently relies more heavily on the gas turbine cycle to convert incoming energy to power, and is more sensitive to the negative effects of converting chemical energy to heat energy at low temperature. Therefore, the fuel cell of the proposed cycle can be used more extensively by increasing the fuel utilization ratio and allowed to run at lower fuel cell efficiency before the negative effects become significant. The net result of this shift in load from gas turbine cycle to fuel cell is a substantial increase in cycle efficiency caused by the inherent efficiency of converting chemical energy directly to power.

16.3 Recuperator results

Heat curves of the proposed and reference cycles are given in figure 16.1. Central concepts for analysis of the heat curves are given in the corresponding treatment of the gas turbine cycle.

Recuperation duty is much reduced, especially for the proposed cycle, compared to the results from the gas turbine cycle simulation. The reduction is caused by both decrease in flow and hot side inlet temperature for the proposed cycle, and chiefly by reduced flow for the reference cycle. Convection heat to the pyrolyser now makes up approximately 2/3 of the duty of the high temperature heat exchanger, at the cost of comparatively low air preheating temperature.
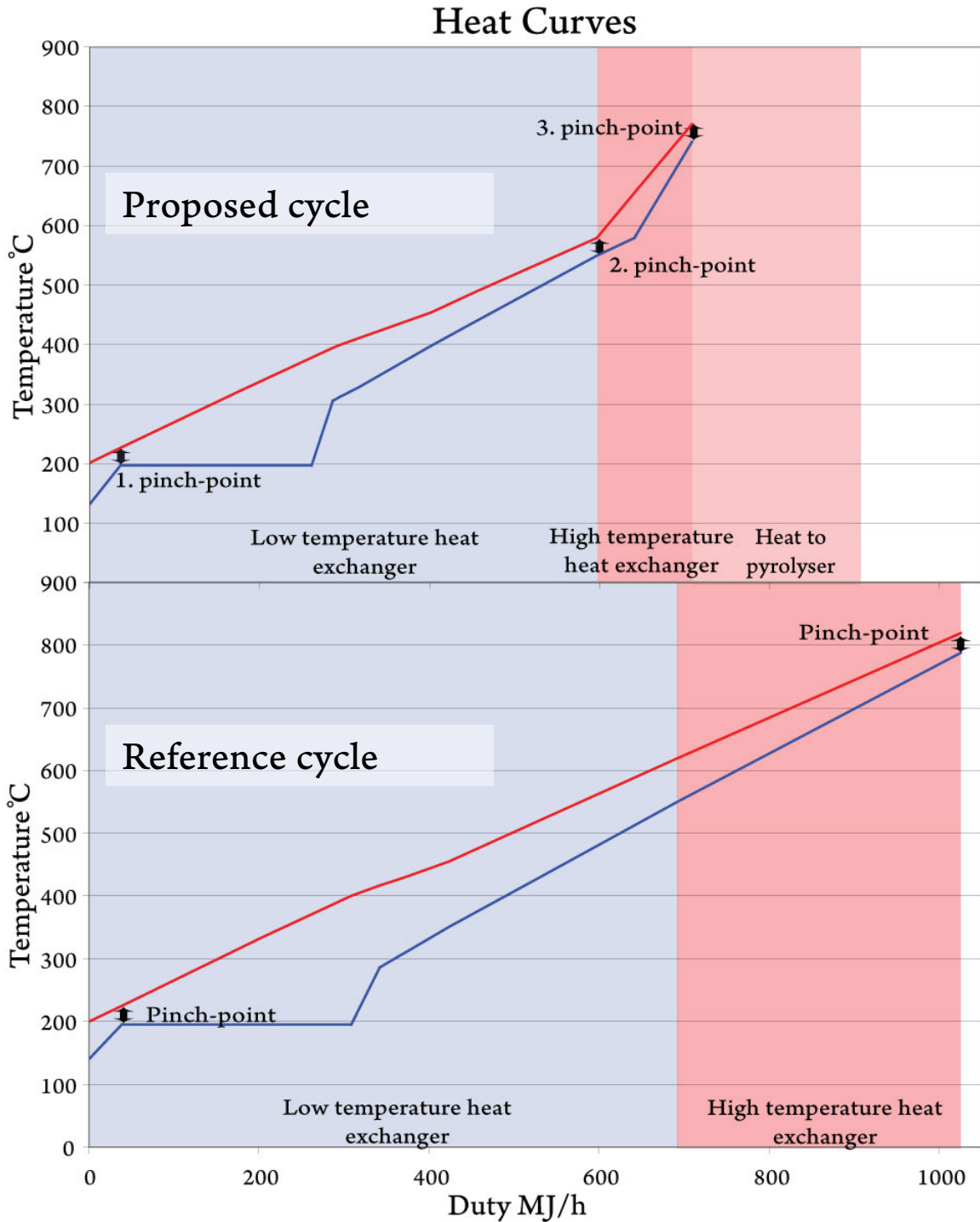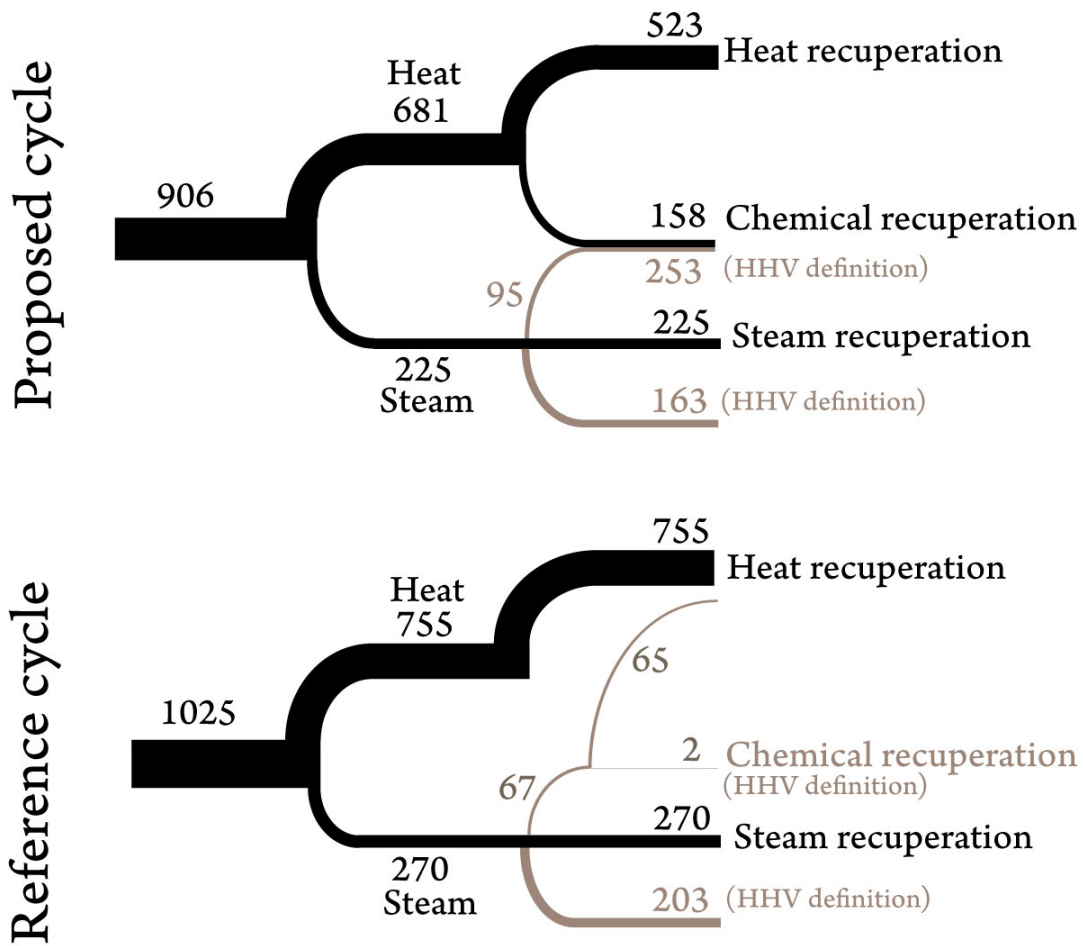

figure 16.1

As indicated by the steamflows of table 16.2, steam recuperation in the recuperator is also reduced for both cycles, approximately proportional to reduction in hot side mass flow (166 – 175 kJ of steam recuperation per kilo in the hot side stream for the proposed cycle, 200-204 kJ/kg for the reference cycle), the relative influence of syngas cooling (partly participating on the hot side) is the main source of error in this proportionality. Complete duties of the recuperators are summed in table 16.3.

	Proposed system	Reference system
Air preheat temp	581 ºC	788 ºC
Steam preheat temp	743 ºC	788 ºC
Net duty	906 MJ/h	1025 MJ/h
Preheating	486 MJ/h	755 MJ/h
Pyrolysis heat	195 MJ/h	-
Recuperator heat recup.	681 MJ/h	755 MJ/h
Recuperator steam recup.	225 MJ/h	270 MJ/h

table 16.3

figure 16.2

As explained further in chapter 14, the duties of the recuperator are not equal to the heat, steam and chemical recuperation of the cycle. Outside the recuperator, there are transfers between heat, steam and chemical energy also parts of the recuperation process. For example, all chemical recuperation is occurring outside the recuperator, consuming energy obtained by heat recuperation. Figure 16.2 shows the recuperation of the cycle, as well as the transfer-paths of the recuperated energy. Results where the HHV definition is used are given in grey. See chapter 6 for further details on chemical recuperation definition.

Compared to the results from the gas turbine cycle simulations, chemical recuperation is equal in the proposed cycle, and still absent in the reference cycle, heat and steam recuperation are however reduced for both cycles. Using the HHV definition for chemical recuperation, there is only slight chemical recuperation in the reference cycle, and as with the gas turbine cycle simulation chemical recuperation is less than the vaporization energy in the steam consumed by the reactions. The grey line from chemical recuperation to heat recuperation thus represents the release of heat in partial oxidation. For the gas turbine cycle simulation this value is 58 MJ/h, confirming that partial oxidation is increased in the combined fuel cell /gas turbine cycle.

16.4 Exergy analysis

See appendix 1 for details on exergy calculations. The result of the exergy analysis is coherent with the already presented results. The proposed cycle has less exergy losses in all categories, except for fuel cell exergy losses. The comparatively high losses in this category follow naturally from the extended use and somewhat lower efficiency of the fuel cell in the proposed cycle.

To parallel the exergy analysis of the gas turbine cycle simulations, combustion, conversion, and fuel cell losses are predominantly exergy losses associated with the conversion of chemical energy to heat energy (fuel cell losses are also derived from the heating of incoming streams). Combining these three categories, the proposed cycle has far less exergy loss, 22.5% compared to 25.4% for the reference cycle, caused by the direct and more efficient conversion of chemical energy to electricity featured by the fuel cell.

The direct conversion of chemical energy to electricity omits the use of heat energy, and thereby causes the secondary beneficial effect of reduced requirement for recuperation. In a sense, recuperation is a mean to *reduce* the losses associated with energy in the form of heat, good recuperation is therefore beneficial for the cycle, better still is the reduction of need for recuperation. Recuperation will always cause losses, both in the exergy analysis sense of the word and in the more concrete sense with heat loss, mechanical loss etc.

Consequently, due to less recuperation in the proposed cycle, exergy losses are smaller than for the reference cycle in all categories associated with mass flow and heat transfer, giving raise to additional difference in the thermal efficiency of cycle.
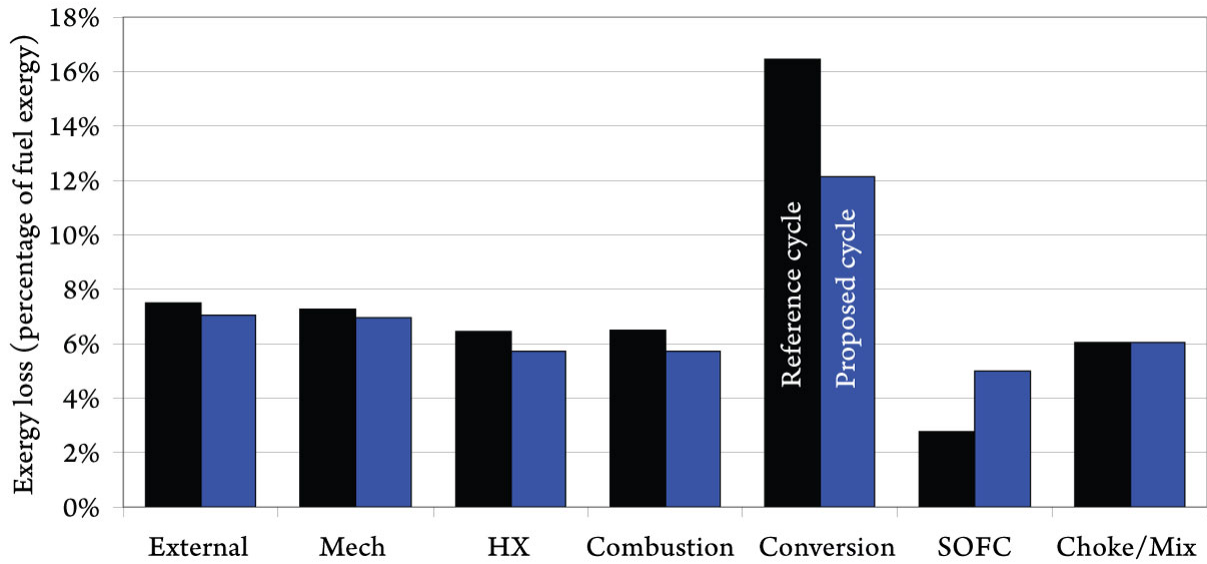
figure 16.3

Exergy losses (% fuel exergy)	Proposed cycle	Reference cycle	Diff.
Converter loss	14.4%	18.7%	-4.3
Recuperation loss	5.4%	6.4%	-1.0
Power cycle loss	27.9%	27.0%	+0.9
Total	47.7%	52.1%	-4.4

table 16.4

Exergy losses categorized by the three principle constituents of the cycles are given table 16.4, and corresponds to the exergic efficiencies of 52.2% and 47.8% for the proposed and reference cycle respectively (calculated by dividing electrical output by the exergy content of the biomass).

16.5 Sensitivity analysis

Sensitivity to turbine inlet pressure (TPR), residual char (unreacted carbon), and fuel utilization ratio is calculated.

figure 16.4

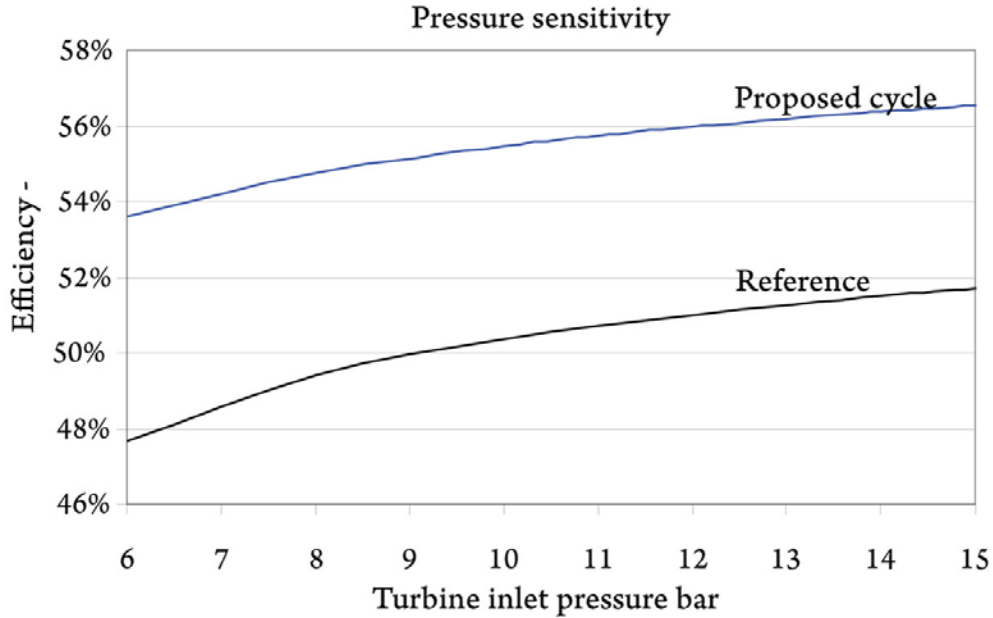In figure 16.4, efficiency as a function of TPR is given. Converter pressure is at 2 bars above this pressure at the inlet of the converter, decreasing through the converter towards TPR. Sensitivity is comparatively large and equal for both cycles. In addition to being an important parameter for the gas turbine and the flow of the cycle, TPR is also an important parameter for fuel cell efficiency.

Reactor temperature TPR sensitivity for the proposed cycle is given in figure 16.5. Due to increased heat recuperation at low pressures, reactor temperatures are also higher. Temperatures beyond 14 bars are with a dashed line, indicating slight uncertainties of the results due to convergence problems in simulation. At low TPR, exhaust temperature is low, necessitating heat transfer from the fuel cell to the gas turbine exhaust for sufficient preheating temperatures. This is a "quick-fix" to aid
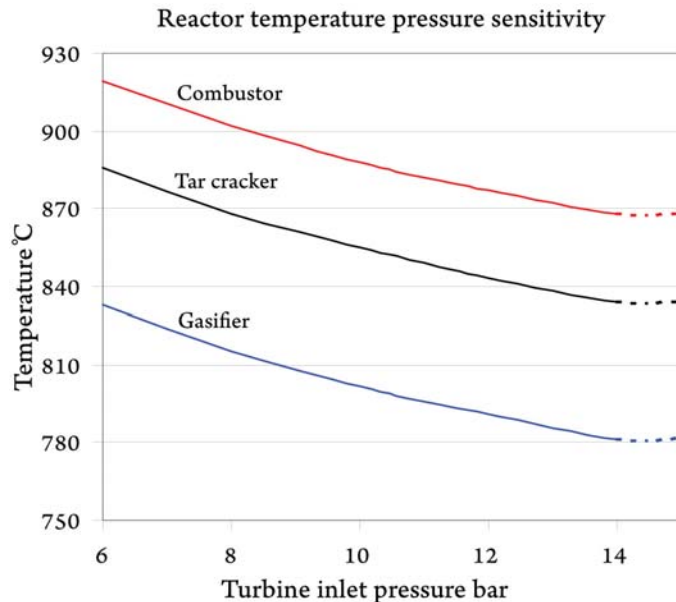

figure 16.5

convergence; a heat exchanger redesign would also solve the problem. Except for this anomaly, the sensitivity analysis shows that reactor temperatures are sufficient for feasible operation for all tested pressures.

Sensitivity to the amount of residual char combusted in the converter is shown in figure 16.6 and 16.7. Efficiency is very sensitive to this variable, especially for the proposed cycle. Varying residual char, or inert carbon, from 0 to 25% results in a decrease in efficiency of 10 pp., corresponding values for the gas turbine cycle simulation are approximately 2 pp. with variations from 0 to 20% in residual char. This is closely connected to the fuel cell's principle of converting chemical energy directly to electricity. In the gas turbine cycle, combustion of residual char in the converter is merely conversion of chemical energy to heat energy in unfavorable conditions, in the combined
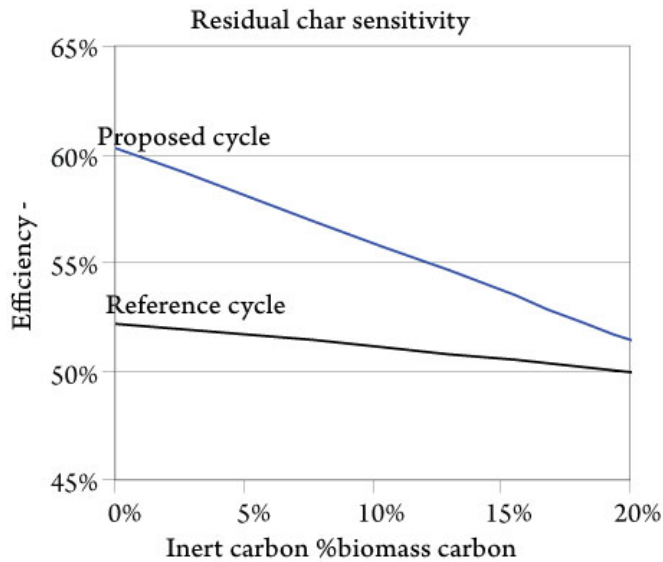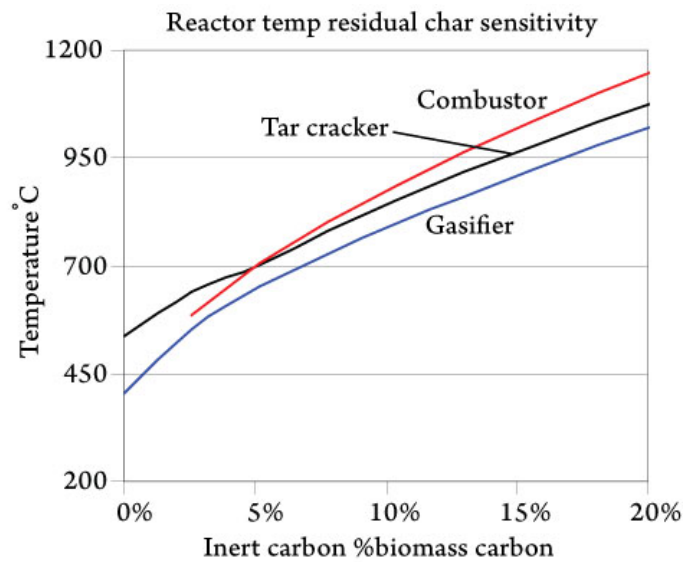

figure 16.6

figure 16.7

fuel cell / gas turbine cycle it is the shift from direct conversion to electricity to combustion at in unfavorable conditions. As the proposed cycle utilizes the fuel cell to a further extent, it is also more sensitive to combustion of residual char.

In figure 16.6, efficiency of the reference cycle may seem to exceed the efficiency of the proposed cycle if combustion of residual char is increased. At 22% inert carbon however, partial oxidation is no longer necessary to achieve the preset reactor temperature of 850 ºC, and the reactor temperature starts rising above this temperature at more than 22% inert carbon. Operating conditions are thus changed and the linear relationship between residual char / inert carbon is discontinued. Behavior of the cycle beyond this point is not investigated. Also note that the fuel utilization ratio is not optimized for other than the base case (10% inert carbon) for either cycle.

 From figure 16.7, it is clear that reactor temperatures also are very sensitive to the amount of combusted residual char; temperatures are critically low for less than 5% inert carbon. The proposed cycle is consequently forced to combust at least 5% of the carbon present in the biomass to maintain operation. As mentioned in chapter 1 however, more

than 95% carbon conversion is not probable in any practicable cycle operation. At very low amounts of inert carbon, tar cracker temperature is higher than combustor temperature. This is caused by the comparatively low reaction duty of the tar cracker allowing the steam feed to the reactor heat up the circulating bed material. Both the tar cracker and combustor is thus heat sources supplying the high reaction duty of the gasifier with heat.

Figure 16.8 shows sensitivity to fuel utilization ratio, as discussed previously. Dashed lines are fuel cell efficiency. The fuel cell of the reference cycle is more efficient at all fuel utilization ratios, as the relative difference between outlet and inlet partial pressures
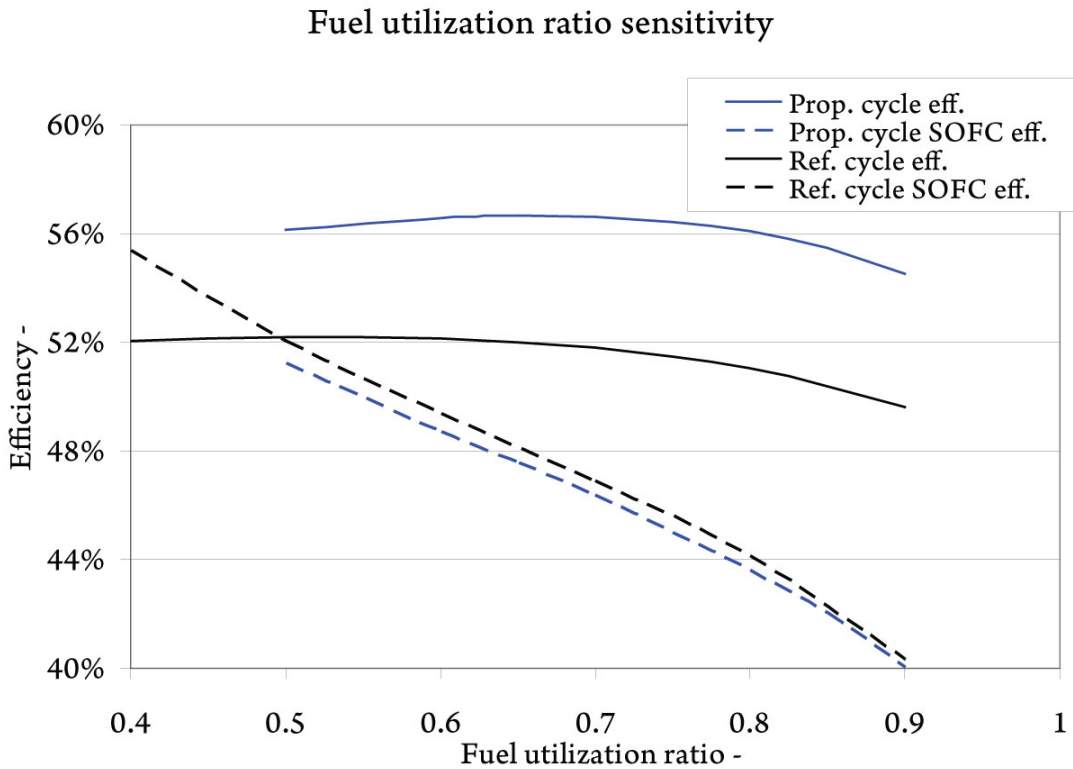
Fuel utilization ratio sensitivity

figure 16.8

of the fuel gases is smaller for the reference cycle. The difference between fuel cell voltage and the theoretical voltage at the inlet of the cell where partial pressures of the fuel gases are highest is thus smaller for the reference cycle, resulting in higher efficiency.

16.6 Conclusions on the fuel cell / gas turbine cycle

The proposed converter significantly increases the performance of the combined fuel cell / gas turbine cycle, by conserving and increasing the chemical energy of the biomass in the conversion process.

The direct conversion of chemical energy to electricity in a fuel cell is more efficient than conversion of chemical energy to power/electricity through heat energy by the means of a gas turbine. Increasing the ratio of chemical energy in the energy available to the combined fuel cell / gas turbine cycle, as seen in the proposed cycle, is therefore beneficial for cycle efficiency.

Recuperation is a technique to abate the lacking efficiency of a heat engine in converting heat energy to power and is not beneficial in its own right, e.g. high degree of recuperation is not necessary indicative of a highly efficient cycle. Furthermore, recuperation is associated with losses, both 2.nd law irreversibilities and conventional energy losses. A reduction in the demand for recuperation, as seen in the proposed cycle, is therefore also beneficial for cycle efficiency.

The two above mentioned causes for improvements in efficiency are closely related. As less heat energy exits the power cycle due to the first cause, there is less heat energy requiring recuperation, giving rise to the second cause.

In the sensitivity analysis, it is shown that cycle efficiency is stable for a wide range of pressure settings. Although reactor temperatures are critically low at high char/carbon conversion (~95% - 100%), operation is feasible at char conversion ratios expected in practice.

17 Conclusion

When integrated with a power cycle, the proposed waste-heat driven biomass converter is able to improve the thermal efficiency of the cycle, compared to a conventional air blown converter (reference converter, gasifier with partial oxidation). The increase in efficiency is marginal when integrated with a gas turbine cycle, and significant when integrated with a combined fuel cell/gas turbine cycle.

The advantage of the proposed converter lies in its ability to conserve and increase the chemical energy of the biomass by utilizing waste heat in the conversion process. As the gas turbine cycle is a heat engine, relying on conversion of chemical energy to heat energy, the advantage of the proposed converter is not fully exploited. With the proposed converter, a higher fraction of chemical energy entering the cycle is converted to heat at high temperature (combustion chamber, 1500 ºC) as opposed to converter temperature (~850 ºC), and the marginal increase in cycle thermal efficiency is mainly caused by reduced 2.nd law irreversibilities associated with this conversion of chemical energy to heat energy. The waste heat recuperated and converted to chemical energy in the proposed converter can alternatively be recuperated by heat or steam recuperation, recuperation is thus not a distinct advantage of the proposed converter.

Integrated with the gas turbine cycle, the proposed converter is not able to reduce mass and volumetric flow and consequently unit sizing, compared to the reference cycle. Mass- and volumetric flow is actually increasing due to increased heat recuperation. Adding to that the increased complexity of the proposed converter, it is arguably unsuitable for integration with a gas turbine cycle.

As the fuel cell can utilize and convert chemical energy directly to electricity, the advantages of the proposed cycle can be exploited more extensively. Optimum performance is therefore obtained with higher fuel cell loading (through the fuel utilization parameter of the fuel cell) and lower gas turbine load, compared to the reference cycle, resulting in better thermal efficiency.

The decrease in conversion of chemical energy to heat energy reduces the need for recuperating waste-heat from the gas turbine exhaust. With less to recuperate, less mass-flow is required and losses and irreversibilities associated with flow and heat exchange is reduced, further improving the thermal efficiency of the cycle. The combination of improved thermal efficiency and reduced mass flow makes the proposed converter a promising and interesting candidate for integration with a combined fuel cell/ gas turbine cycle.

Although inseparable from a source of waste heat, the proposed converter is as a stand-alone unit far superior to the reference converter in producing high quality gaseous fuel. In applications where only chemical energy from the conversion could be used, i.e. fuel

for large area distribution, the proposed cycle shows promise if sufficient waste heat at sufficiently high temperatures can be provided.

Sensitivity analyses suggest that the proposed converter achieves sufficiently high reactor temperatures to sustain operation at a wide range of operating conditions. An exception to this is for very high char conversion ratios, especially in the combined fuel cell/gas turbine cycle.

18 Literature comparison

Thermochemical conversion of biomass is a much investigated topic in literature. A large number of articles describe results of bench-scale experiments of pyrolysis and gasification under a wide range of operating conditions. Other articles focus on the mathematical modeling of such processes. These articles make up the basis for the thermochemical conversion model developed in this paper.

On the subject of integration of a thermochemical converter with a power cycle, there are naturally few articles describing experimental results. Modeling and simulation is however performed in a number of articles, producing results more or less suitable for comparison with the results of this paper.

Kuchonthara [8] has in his doctoral thesis simulated the integration of a waste-heat driven thermochemical converter with several power gas turbine power cycles. The thermochemical converter is modeled as a single reactor with equilibrium conditions at the outlet. Carbon conversion is consequently 100%. Waste heat is transferred to the converter from the waste heat stream by the means of heating coils. In the gas turbine cycle most resembling the gas turbine cycle simulated in this paper, TIT is 1579 ºC, conversion temperature is 700 ºC, turbine pressure ratio is 15, and steam to carbon ratio is 2.5. Thermal efficiency is calculated to 38.2%. Kuchonthara also compares the waste-heat driven converter with a conventional converter with partial oxidation, both integrated with a gas turbine cycle. Operating conditions are different from those described above, and thermal efficiencies are calculated to 33.79% and 32.39% for the waste-heat driven and the conventional converter respectively. This is in accordance with the differences found in this paper between the proposed and reference cycle.

In another article, Schuster et al.[16] has simulated an autothermal converter where combustion of residual char (15% of biomass carbon) ,and if necessary syngas, supply the required heat. Equilibrium is used to describe the syngas composition at the outlet of the converter. The converter is integrated with a gas turbine cycle and a district heating system. As heat is utilized for district heating, recuperation is performed only to a very limited degree. Overall electric efficiency is calculated to 18.4% on LHV basis. The lack of proper recuperation is likely to be the reason for the low efficiency.

Rodrigues et al. [17] have simulated an air gasifier (no steam feed) integrated with a gas/steam turbine combined cycle, with special and detailed attention to gas turbine specifications. Thermal efficiency is calculated to between 40.0% and 43.4%.

Sucipta et al.[20] have simulated a combined fuel cell/micro gas turbine cycle with both air- and steam-blown biomass gasification, however with less recuperation than featured in this paper. Thermal efficiency is approximately 50%, depending on operating conditions for steam-blown gasification, and approximately 46% for air-blown gasification.

Appendix 1 Exergy calculations

In Aspen Plus™ (AP), components are divided in two distinct categories; conventional and non-conventional. Exergy calculation method depends on which category a given component belongs. The components are divided in three sub-streams, se chapter 2 for details, stream exergy is then the sum of exergy in these sub-streams.

Ambient pressure is 1 bar., ambient temperature is 25 ºC.

Conventional components

Exergy for conventional components is calculated largely with AP values. Thermomechanical exergy for the mixture is calculated as:

$$\varepsilon_{tm} = h(T) - h(T_0) - T_0 \left(s(p,T) - s(p_0,T_0) \right)$$

with enthalpies and entropies from AP. T_0, p_0 are the ambient temperature and pressure. Chemical energy is calculated as:

$$\varepsilon_{ch} = \sum_i x_i (\varepsilon_{ch,i} - RT_0 \ln x_i)$$

where x_i is the mole fraction of each component and $\varepsilon_{ch,i}$ is standard chemical exergy taken from Moran & Shapiro[18], model 2. The ideal gas law is used for this correlation. In this paper, p_{ref} for standard chemical exergy is equal to p_0. Total exergy for the conventional components is then:

$$E = n \left(\varepsilon_{tm} + \varepsilon_{ch} \right)$$

n is the mass or molar flow of the mixture.

Non-conventional components

Non-conventional components lack complete thermodynamical and chemical definition and do not necessarily correspond to chemical components in nature, rather they represent a lumped product group or pseudo component, i.e. tar and char.

To calculate exergy, data must be found and associated with the components. Since the components themselves are not real components, these data will not be exact. Empirical correlation or data of related real components are used for the purpose. See appendix 2 for details.

By supplying AP with enthalpy of formation and heat capacity, enthalpies can be calculated. Entropy must however be calculated outside of AP, along with chemical exergy. The exact calculation method differs depending on if the non-conventional component is a permanent gas, a condensable gas/liquid (liquid at ambient conditions), or a solid.

For a permanent gas, thermomechanical exergy is calculated as:

$$\Delta h = \int_{T_{sat}}^{T} C_p(T) dT$$

$$\Delta s = \int_{T_0}^{T} \frac{C_p(T)}{T} dT - \int_{p_0}^{p} \frac{R}{p} dp$$

$$\varepsilon_{tm} = \Delta h + T_0 \Delta s$$

Change in enthalpy is calculated directly by AP. Chemical exergy is calculated as with conventional components, with standard chemical exergy as detailed in appendix 2.

For condensable gas/liquids, thermomechanical exergy is calculated as

$$\Delta h = \int_{T_0}^{T_{sat}} C_{p,liq}(T) dT + \Delta h_{vap(p_{sat})} + \int_{T_{sat}}^{T} C_{p.gas}(T) dT$$

$$\Delta s = \int_{T_0}^{T_{sat}} \frac{C_{p,liq}(T)}{T} dT + \frac{\Delta h_{vap(T_{sat}, p_{sat})}}{T_{sat}} + \int_{T_{sat}}^{T} \frac{C_{p.gas}(T)}{T} dT - \int_{p_{sat}}^{p} \frac{R}{p} dp$$

$$\varepsilon_{tm} = \Delta h + T_0 \Delta s$$

Change in enthalpy is calculate by AP. AP does however not handle phase-change for the non-conventional components, enthalpy must therefore be corrected for this outside AP.

As these components are liquid at ambient conditions, chemical exergy is equal to the standard chemical exergy given in appendix 2.

For solids, thermomechanical exergy is calculated as

$$\Delta h = \int_{T_0}^{T} C_p(T)\, dT$$

$$\Delta s = \int_{T_0}^{T} \frac{C_p(T)}{T}\, dT$$

$$\varepsilon_{tm} = \Delta h + T_0 \Delta s$$

Change in enthalpy is calculated by AP. Chemical exergy is equal to the standard chemical exergy as given in appendix 2. As with conventional components, total exergy for all non-conventional components is.

$$\mathrm{E} = n\left(\varepsilon_{tm} + \varepsilon_{ch}\right)$$

Total stream exergy is the sum of exergy of the conventional and non-conventional components (in separate sub-streams).

Sub-stream interactions

Although exergy is the sum of exergy of all sub-streams, exergy for one sub-stream can not be calculated without knowledge of conditions in other sub-streams. This is because components from different sub-streams share phase, e.g. conventional gas components are in the same mixture as non-conventional gas and vaporized gas/liquid components. Partial pressures of components in gas phase must therefore be corrected outside AP. Furthermore, the whole stream must be evaluated outside AP to determine the phase of different components at T, p, and T_0, p_0. A schematic overview of the complete exergy calculation algorithm is given in figure A1.
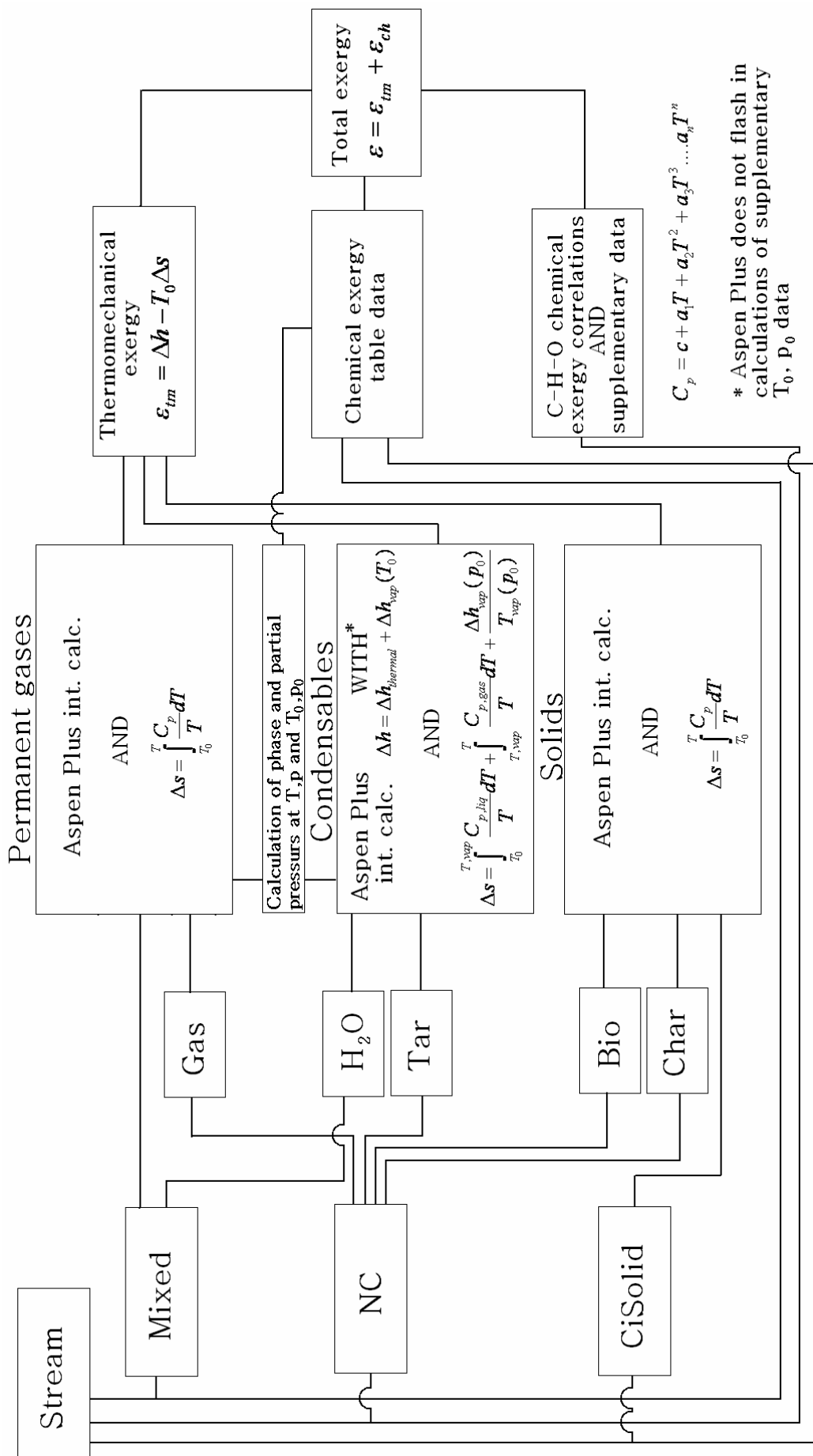
Stream

Mixed

NC

CiSolid

Gas

H_2O

Tar

Bio

Char

Permanent gases

Aspen Plus int. calc.

AND

$$\Delta s = \int_{T_0}^{T} \frac{C_p}{T} dT$$

Calculation of phase and partial pressurs at T,p and T_0,p_0

Condensables

Aspen Plus int. calc.

WITH*

$$\Delta h = \Delta h_{thermal} + \Delta h_{vap}(T_0)$$

AND

$$\Delta s = \int_{T_0}^{T,vap} \frac{C_{p,liq}}{T} dT + \int_{T,vap}^{T} \frac{C_{p,gas}}{T} dT + \frac{\Delta h_{vap}(p_0)}{T_{vap}(p_0)}$$

Solids

Aspen Plus int. calc.

AND

$$\Delta s = \int_{T_0}^{T} \frac{C_p}{T} dT$$

Thermomechanical exergy

$$\varepsilon_{tm} = \Delta h - T_0 \Delta s$$

Chemical exergy table data

C–H–O chemical exergy correlations AND supplementary data

Total exergy

$$\varepsilon = \varepsilon_{tm} + \varepsilon_{ch}$$

$$C_p = c + a_1 T + a_2 T^2 + a_3 T^3 \dots a_n T^n$$

* Aspen Plus does not flash in calculations of supplementary T_0, p_0 data

figure A1

78

Appendix 2 Non-conventional component data

Sources and values for non-conventional component data:

Component	Data type	Value	Source
Biomass			
	HHV	19.06/17.64 MJ/kg (db/wb)	Boie HHV correlation [12]
	LHV	16.63/15.21 MJ/kg (db/wb)	Calculated
	Heat capacity	$1.5 + 10^{-3}\,T$ kJ/kg K	Grønli, Melaaen [13]
	St. chem. exergy	$1.143 \cdot LHV$ MJ/kg	Szargut, Styrylska [19]
Pyrolytic gas			
	HHV	$3.226 + 4.12 \cdot 10^{-12}\,T$ kJ/kg	Di Blasi et. al. [9]
	Heat capacity	$0.77 + 6.29 \cdot 10^{-4}\,T - 1.91 \cdot 10^{-7}\,T^2$ kJ/kg K	Grønli, Melaaen [13]
	Chem. Exergy	$-6.5 \cdot 10^6 + 2.5 \cdot 10^4\,T$ kJ/kg	Di Blasi et. al. [9]
Tar			
	HHV	25/15 MJ/kg (db/wb)	Meier, Faix [10]
	LHV	23.5 db MJ/h	Calculated
	Heat capacity	$-0.1 + 4.4 \cdot 10^{-3}\,T - 1.57 \cdot 10^{-6}\,T^2$ kJ/kg K	Grønli, Melaaen [13]
	St. chem. exergy	$1.091 \cdot LHV$ MJ/h	Szargut, Styrylska [19]
	Vap. $\Delta h, p, T$	Toluen chemical data	
Char			
	HHV	-	Boie HHV correlation [12]
	Heat capacity	$0.42 + 2.09 \cdot 10^{-3}\,T - 6.85 \cdot 10^{-6}\,T^2$ kJ/kg K	Grønli, Melaaen [13]
	St. chem. exergy	$1.059 \cdot LHV$ MJ/h	Szargut, Styrylska [19]

Enthalpy of formation is calculated from HHV for all components.

Pyrolytic gas is the non-condensable product of pyrolysis. Chemical energy and exergy is calculated with table data from Moran&Shapiro[18] directly from the experimental results of pyrolysis presented by Di Blasi et. al.[9]. Temperature-dependent functions are curve-fitted functions developed for the purposes of this paper. See chapter 4 for details.

For data regarding vaporization of tar, toluene is used as a model component. This includes vaporization temperature and vaporization energy at ambient pressure (1 bar.). All other data for tar are taken from the sources given above (different from toluene).
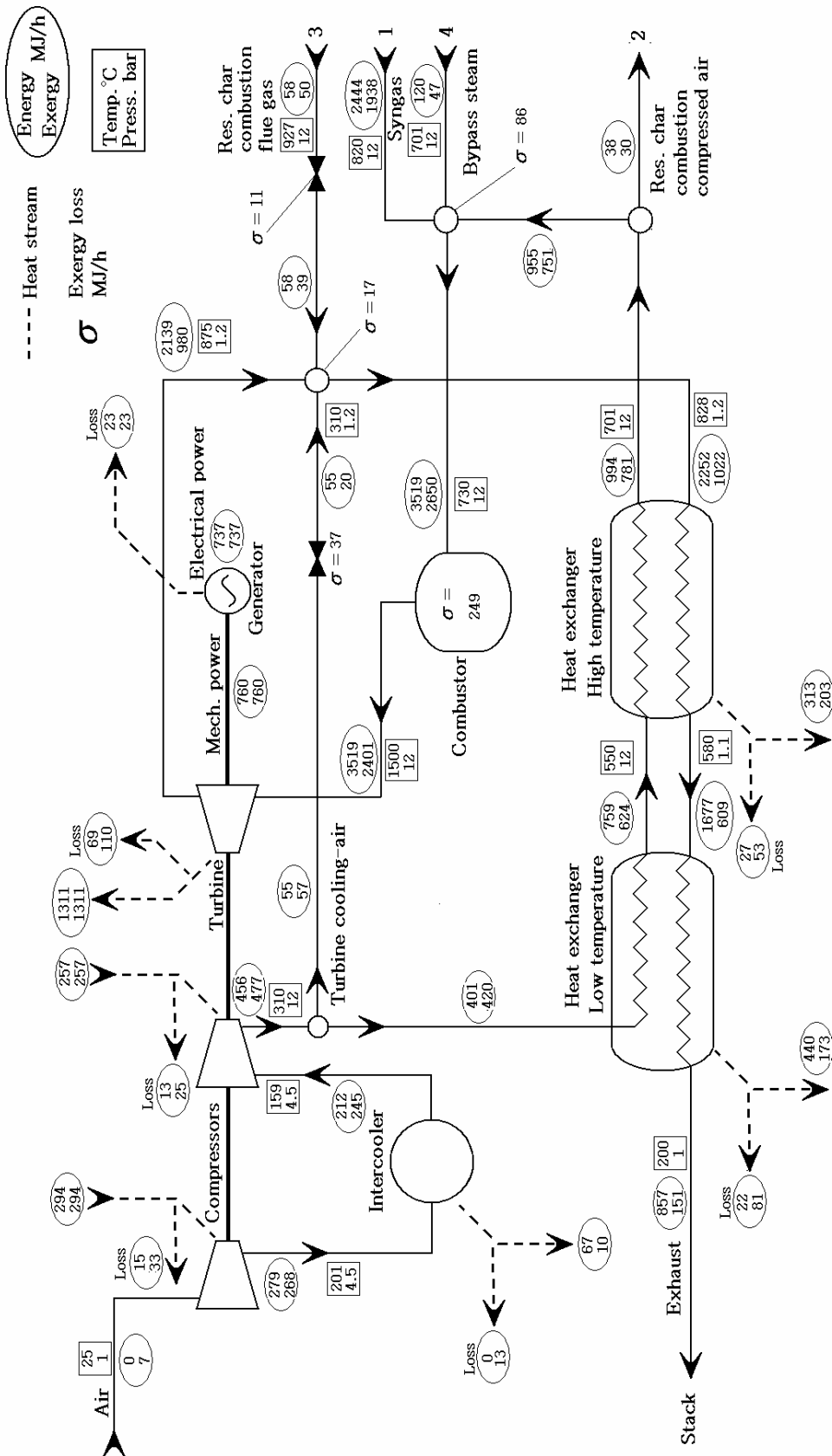
Values for LHV not stated in the table are calculated from HHV values.
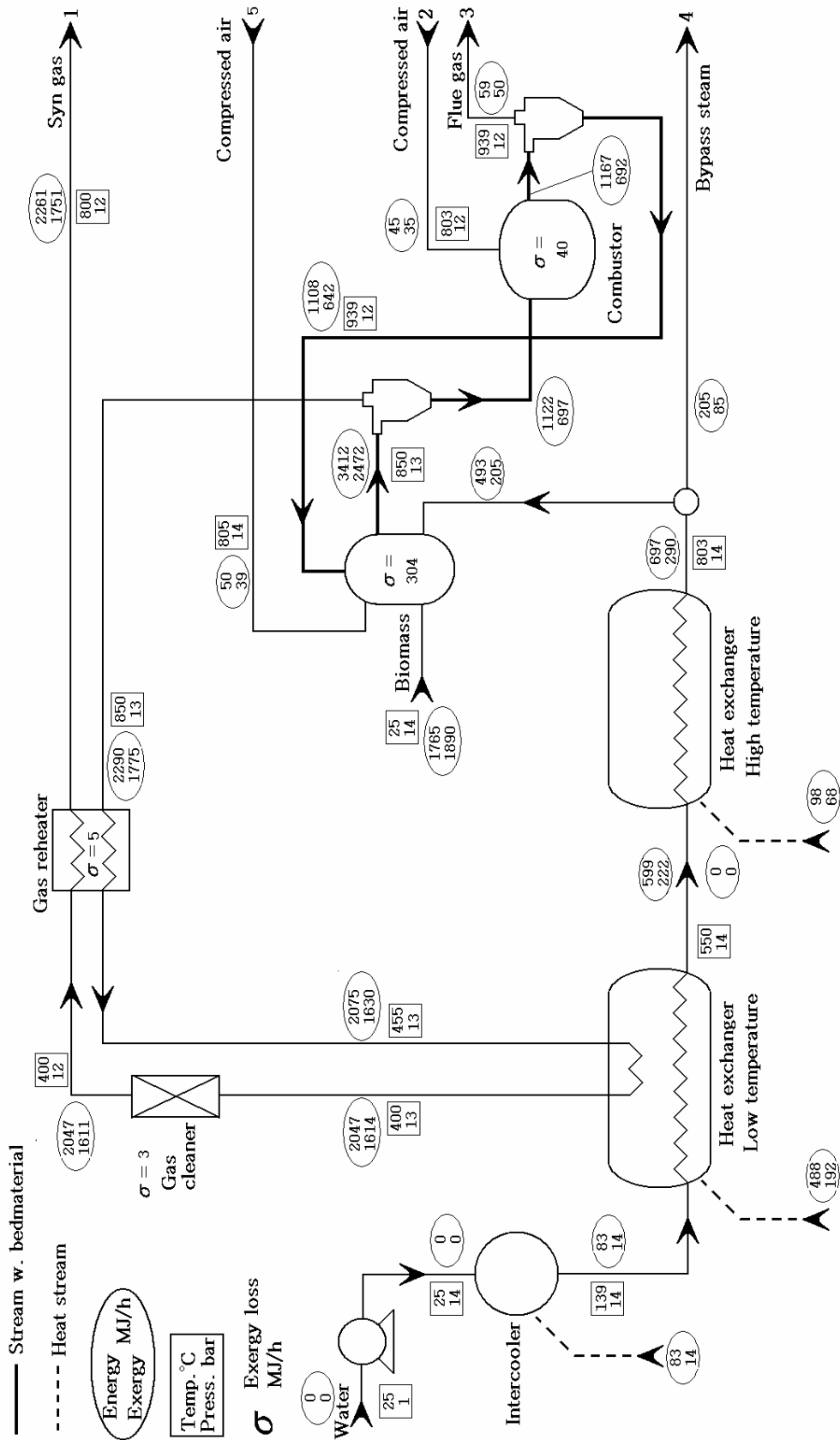
Appendix 3 Flowsheets

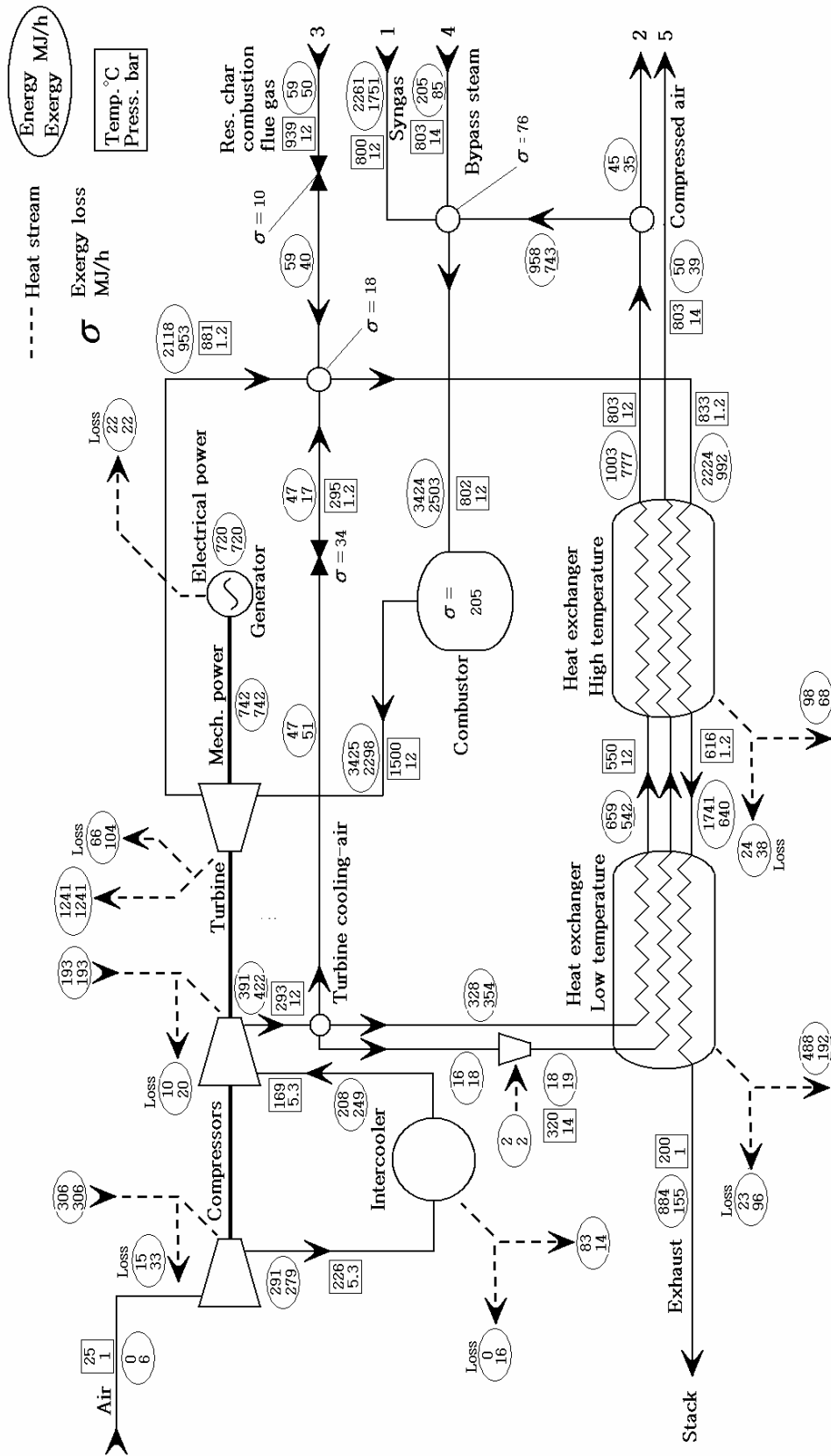## Appendix 3.1 Converter, proposed cycle, gas turbine simulation.
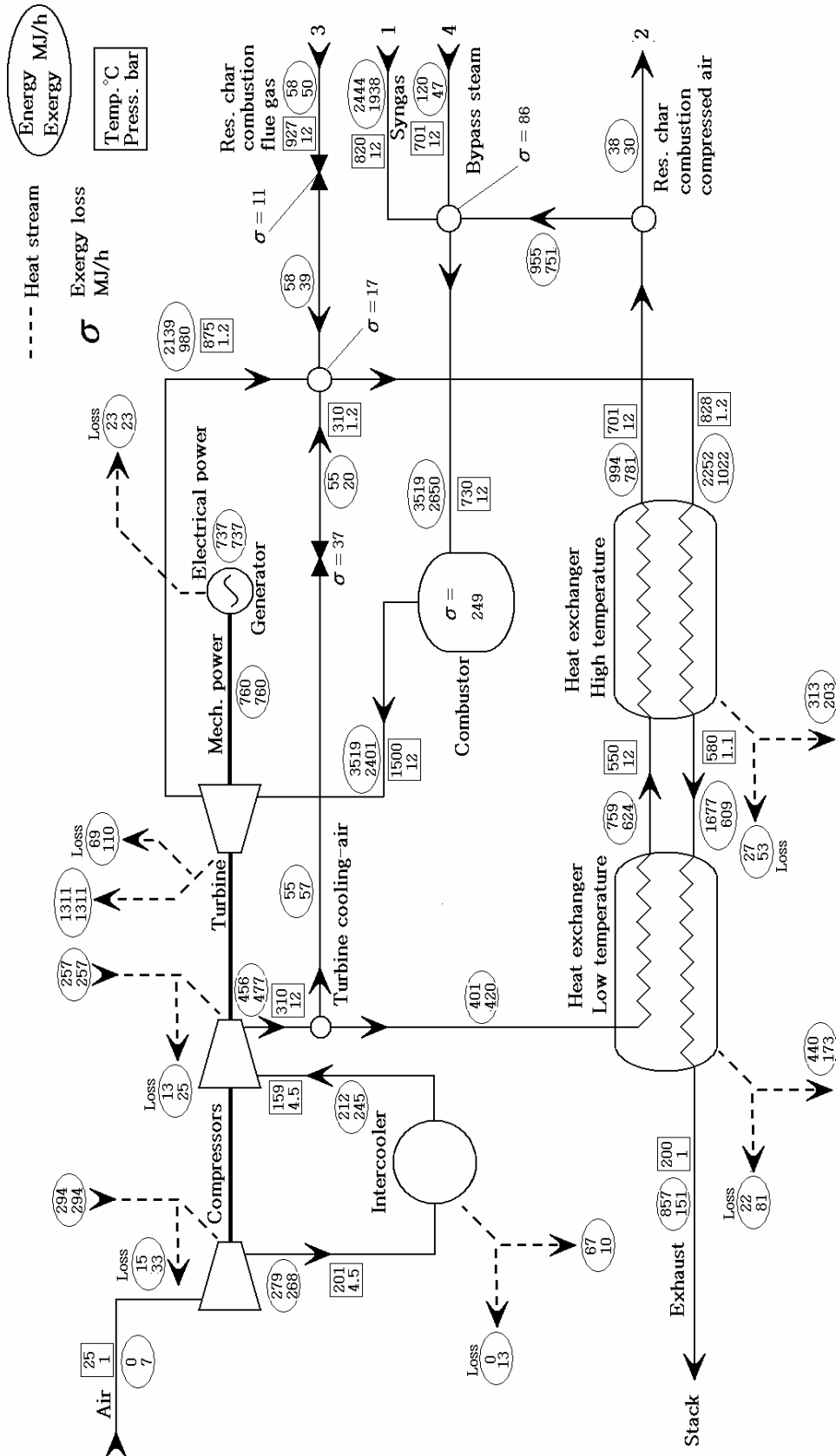
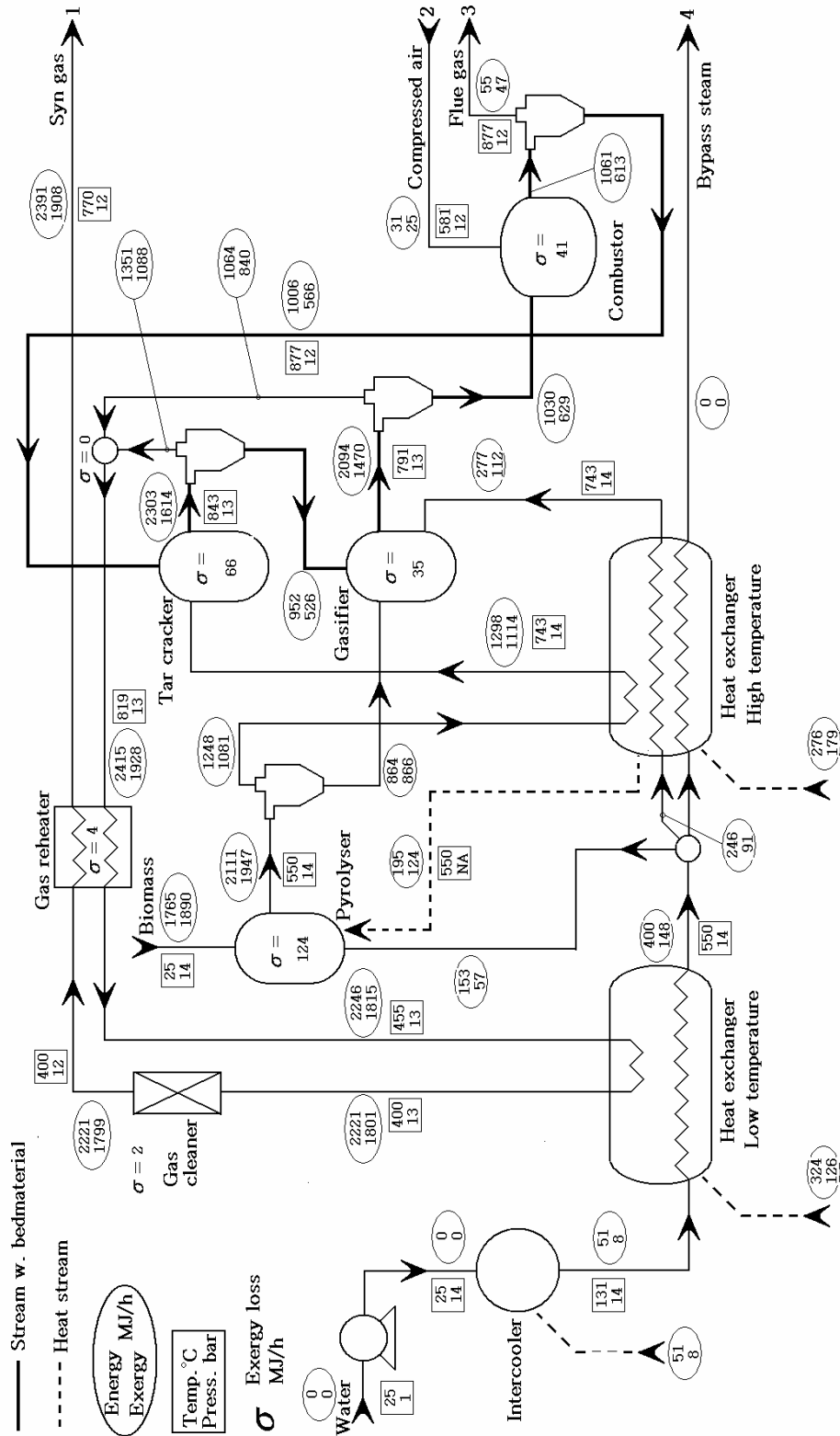## Appendix 3.2 Power cycle, proposed cycle, gas turbine simulation.

Appendix 3.3 Converter, reference cycle, gas turbine simulation.

Syn gas 1

Compressed air 5

Compressed air 2

Flue gas 3

Bypass steam 4

Gas reheater

$\sigma = 5$

Combustor

$\sigma = 40$

$\sigma = 304$

Biomass

Heat exchanger
High temperature

Heat exchanger
Low temperature

$\sigma = 3$
Gas cleaner

Intercooler

Water

Stream w. bedmaterial
— Stream
- - - - Heat stream

Energy MJ/h
Exergy

Temp. °C
Press. bar

σ Exergy loss
MJ/h

2261 1751
800 12

1108 642
939 12

45 35
803 12

59 50
939 12

1167 692

803 12

205 85

3412 2472

850 13

493 205

50 39
805 14

25 14
1765 1890

697 290
803 14

2290 1775
850 13

599 222
0 0

98 68

550 14

2075 1630
455 13

2047 1611
400 12

2047 1614
400 13

83 14

0 0
25 14

139 14
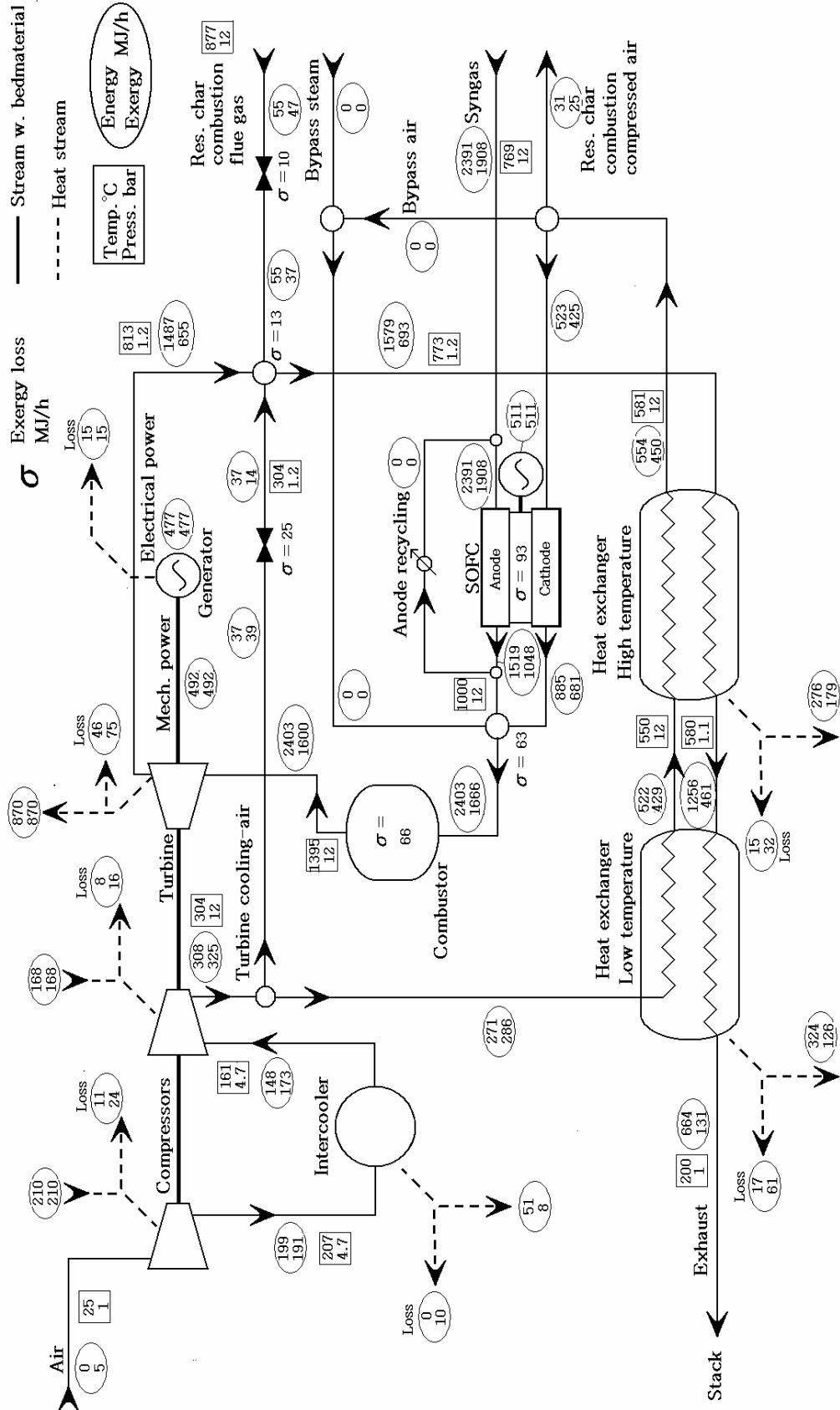
83 14

488 192

0 0
25 1

83

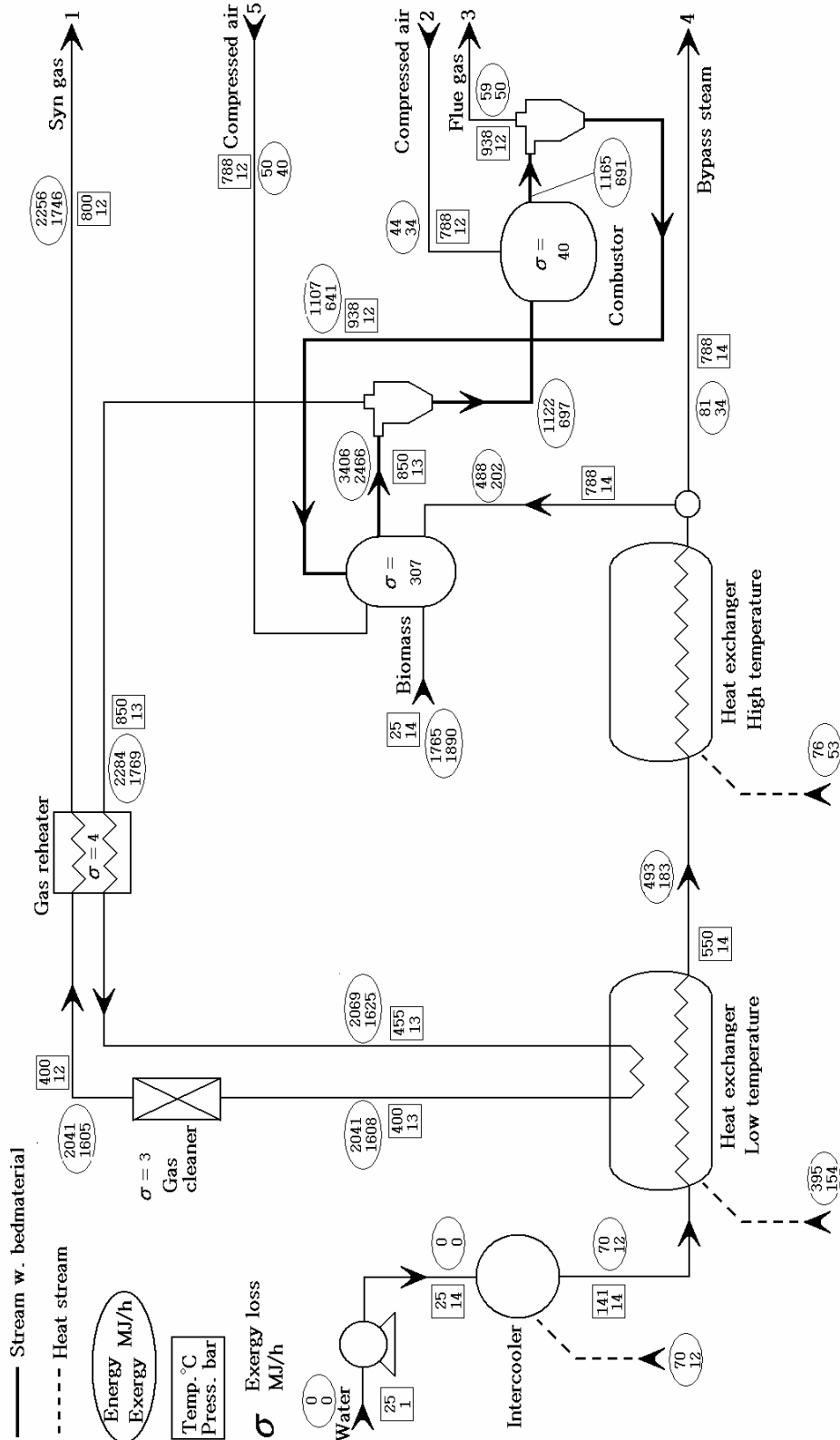# Appendix 3.4 Power cycle, reference cycle, gas turbine simulation.

Appendix 3.5 Converter, proposed cycle, combined fuel cell/gas turbine cycle simulation
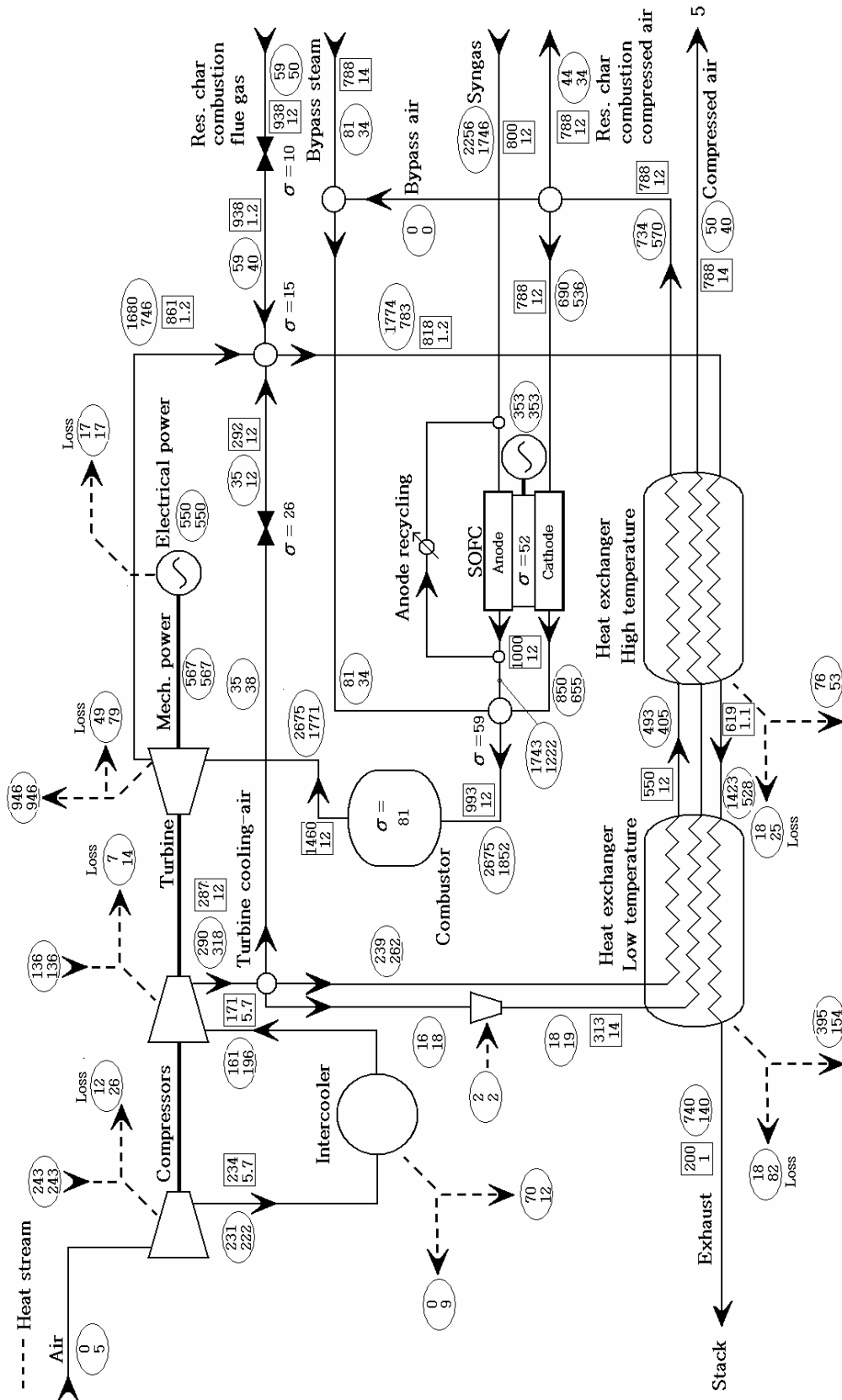
Appendix 3.6 Power cycle, proposed cycle, combined fuel cell/gas turbine cycle simulation

Appendix 3.7 Converter, reference cycle, combined fuel cell/gas turbine cycle simulation

Appendix 3.8 Power cycle, reference cycle, combined fuel cell/gas turbine cycle simulation

Appendix 4 Settings for Aspen Plus

An overview of settings and properties used with the Aspen Plus Simulation Tool

Software version	Aspen Plus 2004.1
Solver method	Sequential Modular
Property method	UNIFAC
Equation of state property method	Redlich – Kwong - ASPEN
Considered conventional components	H_2, O_2, H_2O, N_2, CH_4, CO, CO_2 , $C(s)$, SiO_2
Trace component convergence setting	"Gradual"
Trace component mole fraction threshold	0.00001
Tear stream convergence tolerance	0.001
Tear stream convergence variables	Total mole flow All component mole flow* Pressure Enthalpy

*) Components with mole fraction below the threshold is not subjected to the convergence criteria.

Tear stream convergence criteria [7]:

$$-tol \le \frac{X_{calculated} - X_{assumed}}{X_{assumed}} \le tol$$

Trace component convergence setting "gradual" relaxes the convergence criteria for trace components [7]:

$$-tol \le \frac{X_{calculated} - X_{assumed}}{X_{assumed} + tol} \le tol$$

References

[1]   Ragnar Warnecke, "Gasification of biomass: comparison of fixed bed and
        fluidized bed gasifier" Biomass and Bioenergy 18 (2000) 489-497

[2]   Fushimi et al. "Effect of heating rate on steam gasification of biomass. 1.
        Reactivity of char" Ind. eng. chem. res. 2003, 42, 3922-3928

[3]   Christoph Pfeifer, Hermann Hofbauer, "Development of catalytic tar
        decomposition downstream from a dual fluidized bed biomass steam
        gasifier", Powder Technology 2007 (Article in press)

[4]   Kazuhiro Sato, Kaoru Fujimoto, "Development of new nickel based catalyst
        for tar reforming with superior resistance to sulfur poisoning and coking in
        biomass gasification", Catalysis Communications 8 (2007) 1697–1701

[5]   F. Mermoud et al. "Influence of the pyrolysis heating rate on the steam
        gasification rate of large wood char particles", Fuel 85 (2006) 1473–1482

[6]   S. T. Chaudhari et al "Steam gasification of biomass-derived char for the
        production of carbon monoxide-rich synthesis gas". Energy & Fuels 2001,
        15, 736-742

[7]   Aspen Technology, Aspen Plus reference manuals
        http://www.aspentech.com

[8]   Prapan Kuchonthara, " Process Integration and Design of High
        Efficiency Power Generation Systems Based on Energy Recuperation
        Technology",   Doctoral thesis 2004, The university of Tokyo, Department of
        chemical engineering

[9]   Colomba Di Blasi et al., "Product Distribution from Pyrolysis of Wood and
        Agricultural Residues" Ind. Eng. Chem. Res. 1999, 38, 2216-2224

[10]   D. Meier, O. Faix, "State of the art of applied fast pyrolysis of lignocellulosic
        materials - a review" Bioresource Technology 68 (1999) 71-77

[11]   X. Wang et al., "Biomass Pyrolysis in a Fluidized Bed Reactor. Part 2:
        Experimental Validation of Model Results", Ind. Eng. Chem. Res. 2005, 44,
        8786-8795

[12]   Changdong Sheng, J.L.T. Azevedo, "Estimating the higher heating value of
        biomass fuels from basic analysis data" Biomass and Bioenergy 28 (2005)
        499–507

[13]   M.G. Grønli, M.C. Melaaen, "Mathematical Model for Wood Pyrolysiss - Comparison of Experimental Measurements with Model Predictions" Energy & Fuels 2000, 14, 791-800

[14]   Daren E. Daugaard and Robert C. Brown, "Enthalpy for Pyrolysis for Several Types of Biomass", Energy & Fuels 2003, 17, 934-939

[15]   W. Zhang et al, "Simulation of a tubular solid oxide fuel cell stack using AspenPlus™ unit operation models" ., Energy and conversion management 46 (2005) 181-196

[16]   G. Schuster et al., "Biomass steam gasification – an extensive parametric study", Bioresource Technology 77 (2001) 71-79

[17]   Monica Rodrigues et al. "Performance evaluation of atmospheric biomass integrated gasifier combined cycle systems under different strategies for the use of low calorific gases" Energy Conversion and Management 48 (2007) 1289–1301

[18]   M.J. Moran & H.N. Shapiro: Fundamentals of Engineering Thermodynamics, 3. edition, John Wiley & Sons

[19]   J. Szargut, T Styrylska, "Angenäherte Bestimmung der Exergie von Brennstoffen". Zeitsschrift für energietechnik und energiewirtschaft – Brennstoff – Wärme – Kraft Bd. 16 Nr. 12 S. 589 bis 636. Dezember 1964

[20]   Made Sucipta et al., "Performance analysis of the SOFC–MGT hybrid system with gasified biomass fuel", Journal of Power Sources 174 (2007) 124–135

[21]   W.S.L Mok and M.J.Antal, "Effects of pressure on biomass pyrolysis. II. Heats of reaction of cellulose pyrolysis", Thermochrmrca Actu, 68 (1983) 165 186

[22]   Masayoshi Sadakata, "Production of fuel gas and char from wood, lignin and holocellulose by carbonization", Fuel 1987, Vol 66, December

[23]   Zheng Ji-lu, "Bio-oil from fast pyrolysis of rice husk: Yields and related properties and improvement of the pyrolysis system", J. Anal. Appl. pyrolysis 80 (2007) 30–35